Tu-Pos227 A SINGLE COMPONENT, NON-PHOSPHOLIPID, pH-SENSITIVE LIPOSOME. Ana Tari, David Collins and Leaf Huang (Intr. by Jorge Churchich) Department of Biochemistry, University of Tennessee, Knoxville, TN 37996-0840.

A synthetic amphiphile, 1,2-dioleyl-3-succinylglycerol (DOSG) had been found to form stable bilayer liposomes by itself at pH 7 or above. Sonicated unilamellar vesicles of DOSG entrapping calcein were prepared at pH 7.4. Release of calcein from liposomes was measured spectrofluorometrically at different acidic pH. DOSG liposomes were pH-sensitive with 50% calcein release when acidified to pH 6.5. Destabilization of DOSG liposomes at acidic pH was also confirmed with a lipid mixing experiment using N-NBD-PE and N-Rhodamine-PE as fluorescent probes. Half maximal lipid mixing occurred when the liposomes were acidified to pH 5.5. DOSG liposomes were stable in the tissue culture medium containing 10% fetal calf serum. However, exposure to medium had modified the pH-sensitivity of the liposomes in that the 50% calcein release occurred at pH 5.5. The cytoplasmic delivery activity of the DOSG immunoliposomes was demonstrated in mouse L929 cells using the diphtheria toxin A fragment (DTA) as an entrapped cytotoxic agent. Empty immunoliposomes, DTA-liposomes without antibody were not cytotoxic. The specific cell killing by the immunoliposomes containing DTA could be blocked by excess antibody, excess empty immunoliposomes, NH_4Cl or chloroquine. These results indicate that the cytoplasmic delivery activity of the DOSG immunoliposomes was mediated by a receptor-mediated endocytosis mechanism and possibly via liposome fusion with the endocytic vesicle membranes. (Supported by NIH grants CA 24553 and AI 25843).

Tu-Pos228 pH-SENSITIVE LIPOSOMES PREPARED FROM PHOSPHATIDYLETHANOLAMINE AND SYNTHETIC DOUBLE CHAIN AMPHIPHILES: PLASMA STABILITY AND DELIVERY OF DIPHTHERIA TOXIN A FRAGMENT TO CULTURED CELLS. D. Collins and L. Huang, Department of Biochemistry, University of Tennessee, Knoxville, TN 37996-0840.

The synthetic double chain amphiphiles, 1,2-dioleoyl-3-succinyl-glycerol (DOSG) and 1,2-dipalmitoyl-3-succinylglycerol (DPSG) have been used in combination with dioleoylphosphatidylethanolamine (DOPE) to prepare pH-sensitive liposomes. These liposomes undergo leakage and lipid mixing as the pH of the media is decreased below neutrality. In comparison with previous formulations of pH-sensitive liposomes prepared from DOPE: oleic acid or DOPE: palmitoyl-N-homocysteine, DOPE:DOSG and DOPE:DPSG liposomes require more acidic conditions to achieve the same level of destabilization. In plasma, DOPE: oleic acid liposomes have been shown to be very unstable. By contrast, pH-sensitive liposomes prepared from DOPE and either DOSG or DPSG are quite stable in plasma for up to 3 hr. at 37° C. Liposomes prepared with either DOPE:DOSG or DOPE:DPSG remain acid-sensitive after 3 hr. incubation in plasma although the extent of release and the pH required for release are decreased. This suggests the possiblility that plasma proteins may be inserting into or coating the liposomes and inhibiting leakage. We have also incorporated acylated antibody into the membranes of DOPE:DOSG and DOPE:DPSG liposomes and evaluated the ability of the immunoliposomes to deliver diphtheria toxin A fragment (DTA) to the cytoplasm of cultured cells. Encapsulated DTA, which requires liposome-cell fusion in order to reach the cell cytoplasm is delivered efficiently by DOPE:DOSG and DOPE:DPSG liposomes in a process which requires specific binding and endocytosis of the immunoliposomes. Supported by NIH grants CA 24553 and AI 25834.

Tu-Pos229 PHOTOINDUCED POLYMORPHISM OF PHOSPHOLIPIDS DETECTED BY ^{31}P NMR SPECTROSCOPY. Judith A. Barry, Ulrich Liman, Michael F. Brown, and David F. O'Brien, Department of Chemistry, University of Arizona, Tucson, AZ 85721.

Phospholipid polymorphism has attracted considerable interest because of possible implications in the function of biological membranes. A new means of modulating the phase behavior in membranes is by the photoinduced polymerization of phospholipids. Photopolymerization of homogeneous, two-component liposomes of dioleoylphosphatidylethanolamine (DOPE) and the polymerizable 1,2-bis[10-(2',4'-hexadienoyloxy)decanoyloxy]phosphatidylcholine (Sorb-PC) causes a significant increase in membrane permeability to hydrophilic molecules (Liman, et al., 1988, Biophys. J. 53, 325a). In order to probe the molecular basis for the photodestabilization of these membranes, we have used ^{31}P NMR spectroscopy because of its ability to distinquish between the lamellar, cubic and inverted hexagonal lipid phases. Proton coupled ^{31}P NMR spectra were determined as a function of the extent of photopolymerization of a lipid membrane of DOPE and Sorb-PC (2:1) at 25 °C in excess buffer. The spectra show a progressive change from a lamellar powder pattern for the unexposed membranes to an isotropic signal superimposed on a residual lamellar signal for the photopolymerized membranes. No evidence for the inverted hexagonal phase was found. It is possible that the appearance of the isotropic signal may represent a transition from the lamellar to the inverted cubic phase. The experiments show that ^{31}P NMR is an especially sensitive method to observe light-induced phospholipid polymorphism.

Tu-Pos230 PHOTOINDUCED FUSION OF LIPOSOMES. Ulrich Liman, David A. Frankel, and David F. O'Brien, Department of Chemistry, University of Arizona, Tucson, AZ 85721.

Photoinduced polymerization of phospholipids can modulate the phase behavior of model membranes. The photopolymerization of homogeneous, stable, two-component liposomes of dioleoylphosphatidylethanolamine (DOPE) and the polymerizable 1,2-bis[10-(2',4'-hexadienoyloxy)decanoyloxy]phosphatidylcholine (Sorb-PC) causes a significant increase in membrane permeability to hydrophilic fluorescent molecules (Liman, et al., 1988, Biophys. J. 53, 325a). In the previous poster it is shown that UV light exposure of DOPE/Sorb-PC (2/1) membranes, which causes the liposome destabilization, also initiates a change in the ^{31}P NMR spectrum of the membranes from a lamellar powder pattern to an isotropic signal. Here we show that photopolymerization of DOPE/Sorb-PC (2/1) liposomes results in the mixing of the aqueous contents of two populations of the liposomes, one with entrapped terbium citrate, and the second with dipicolinic acid (Wilschut et al., 1980, Biochemistry 19, 6011). The efficiency of liposome contents mixing ranged from 8 to 30%, whereas control membranes of DOPC/Sorb-PC (2/1) did not show evidence of mixing.

The photoinduced perturbations of DOPE/Sorb-PC membranes appear to involve photopolymerization initiated phase separation of polymerized PC from PE, which allows the enriched PE domains to assume a nonlamellar isotropic structure. This new membrane morphology favors liposome-liposome fusion.

Tu-Pos231 TRIGGERING OF MEMBRANE FUSION BY HYDROPHOBIC PROTEIN-TARGET MEMBRANE INTERACTIONS DURING SENDAI VIRUS FUSION WITH ARTIFICIAL AND BIOLOGICAL MEMBRANES. Steven L. Novick[1], John D. Baldeschwieler[1], and Dick Hoekstra[2], [1]Division of Chemistry, 127-72, California Institute of Technology, Pasadena, CA, 91125 and [2]Laboratory of Physiological Chemistry, University of Groningen, Bloemsingel 10, 9712KZ Groningen, The Netherlands.

The hydrophobic photoaffinity label 3-(trifluoromethyl)-3-(m-^{125}I-iodophenyl)diazirine (TID) was used to probe protein-lipid interactions in the target membrane during initiation of fusion between Sendai virus and erythrocyte membranes or liposomes composed of cardiolipin and phosphatidylserine. Labeling was conducted as a function of time, temperature, and pH, yielding a mechanistic profile of the protein-lipid interactions involved in membrane fusion. Using a high photon flux during photolysis allows analysis of this process on a shorter timescale than was previously possible. Comparison of the kinetics of labeling with independently monitored fusion kinetics indicates that hydrophobic penetration of the fusion peptide into the target membrane precedes membrane fusion (lipid mixing), and that the hydrophobic penetration of the fusion protein into the target membrane is the trigger of viral protein-mediated fusion. Label distribution within the fusion peptide and labeling with a membrane-bound probe will also be discussed. This work was supported by ARO grant DAAG29-83-K-0128 and NIH grant RR07003 administered by the Division of Research Resources. One of us (S.L.N.) is the recipient of an NSF Graduate Research Fellowship.

Tu-Pos232 A POSITIVELY CHARGED LIPOSOME USED FOR THE EFFICIENT DELIVERY OF DNA TO MOUSE L-CELLS, AN ALTERNATIVE TO LIPOFECTIN. P. Pinnaduwage, L. Schmitt, and L. Huang (Intr. by P.P. Constantinides) Department of Biochemistry, University of Tennessee, Knoxville, TN 37996-0840.

Sonicated liposomes composed of dioleoyl phosphatidylethanolamine (DOPE) and a quaternary ammonium detergent (dodecyl, tetradecyl, or cetyl trimethyl ammonium bromide) were able to mediate functional transfer of pSV2 CAT plasmid DNA to mouse L929 fibroblasts. Successful transfection was determined by assaying for chloramphenicol acetyl transferase activity in cell lysates collected 40 hours after exposure to the lipid/DNA complexes. In spite of various degrees of toxicity toward the cells, it was seen that liposomes prepared with the quaternary ammonium detergents were much less toxic than the free detergents in solution and were more efficient in their delivery of the plasmid DNA. Analysis of the three detergents in combination with the lipid showed that cetyl trimethyl ammonium bromide was least toxic toward the cells, hence it was used throughout the rest of the project. This detergent, at a minimal concentration of 20 mole % in DOPE, allowed for stable liposome preparations and efficient transfection. Optimal efficiency of transfection occurred with 30 µg of DNA. Further increases in the DNA concentration caused a decrease in the transfection efficiency, perhaps due to charge repulsions between the liposomes now saturated with negatively charged DNA and the negatively charged cell surface. It was also shown that the transfection activity of the liposome was limited by its cytotoxicity at high liposome concentrations. Although the overall transfection activity of these liposomes was somewhat lower than that of the lipofectin, another positively charged liposome preparation, which is commercially available, it may serve as an inexpensive and convenient alternative. Support by NIH grants CA 24553 and AI 25834.

Tu-Pos233 COMPARATIVE STUDY OF FLUORESCENT ASSAYS FOR CONTENTS MIXING AND LEAKAGE IN LIPID VESICLES. Dennis Alford[a] Nejat Düzgünes[b,c] and Joe Bentz[a,b]. Depts. of [a]Pharmacy and [b]Pharmaceutical Chemistry, and [c]Cancer Research Institute, University of California, San Francisco, CA 94143

Membrane fusion, involving the intermixing of two aqueous compartments previously enclosed by separate membranes, can be monitored by sensitive fluorescence assays[1]. The usefulness of these assays depends on a) a thorough understanding of the assay reaction, b) testing the assays in well-defined fusion systems, and c) assay components not affecting the fusion characteristics of the membrane. Constituents of the Co^{2+}/ calcein/ EDTA assay[2] bind strongly to PS SUV. The lytic event reported by this assay is most likely the release of membrane-associated Co^{2+}/ calcein upon Ca^{2+} binding to the membrane. ANTS bound considerably to PS SUV, hence the ANTS/DPX assay cannot be used to monitor the fusion of SUV. None of the constituents of these assays, nor those associated with the Tb^{3+}/DPA assay bind significantly to PS LUV. The ANTS/DPX and Tb^{3+}/DPA assays were in close agreement at the early stages of fusion of PS and cardiolipin/DOPC (1:1) LUV; however, the Co^{2+}/calcein assay disagreed completely with the other two assays. Here, we investigated whether these assay components of the affect the fusion kinetics, by co-encapsulating the components of two assays in the same vesicles and monitoring the Ca^{2+} induced fusion/leakage in sequential runs. Also, the extent of contents mixing could be dramatically increased by reducing the ionic strength of the external medium, even when iso-osmotic conditions were maintained with sucrose. This observation suggests that contents leakage from LUV is primarily due to collapse of higher order aggregation/fusion products, since the lower ionic strength enhances electrostatic repulsion and inhibits aggregation. (Supported by NIH grants GM31506, GM28117 and AI25534.)

[1] Düzgünes, N. and Bentz, J. (1988) In: Spectroscopic Membrane Probes, Vol. 1 (L.M. Loew, ed.) pp. 117-159, CRC Press, Boca Raton, Florida.
[2] Kendall, D.A. and Macdonald, R.C. (1982) J. Biol. Chem. 257, 13892-13895.

Tu-Pos234 INTERMEDIATES IN MEMBRANE FUSION AND $L_\alpha/I_{II}/H_{II}$ PHASE TRANSITIONS IMAGED BY TIME-RESOLVED CRYO-TRANSMISSION ELECTRON MICROSCOPY

D. P. Siegel, J. L. Burns, M. H. Chestnut[1], and Y. Talmon[2], [1]Procter & Gamble Co., P.O. Box 398707, Cincinnati, OH 45239-8707, [2]Dept. of Chem. Engn., Technion-Israel Institute of Technology, Haifa 32000, Israel

Using Time-Resolved Cryo-Transmission Electron Microscopy (TRC-TEM) [1], we studied the microstructure of liposomal aggregates undergoing $L_\alpha/I_{II}/H_{II}$ phase transitions. TRC-TEM has several advantages over conventional EM. We have shown that these transitions proceed via interbilayer structures, and we have imaged one of the proposed [2] intermediates, interlamellar attachments (ILAs). ILAs have the predicted structure and dimensions and form in large numbers only in systems with the predicted range of interfacial curvature [2,3]. ILAs were observed to mediate membrane fusion [2] and form the inverted cubic (I_{II}) phase via the predicted ILA lattice [3]. Intermediate formation was induced in LUV samples by a $[H^+]$ or $[Mg^{2+}]$ jump applied seconds before cryofixation. ILAs were imaged in DOPE-ME samples at 10°C below T_H but not in DOPE ($T \approx T_H$) or egg PE (10°C below T_H). LUV fusion via ILAs and ILA aggregation into regions of I_{II} phase precursor were observed in DOPE-Me, but not DOPE or egg PE. Comparison with freeze-fracture EM shows that "lipidic particles" are ILAs. These data are in accord with both the observation of fusion in DOPE-ME under the same conditions [4] and the observation of "lipidic particles" and I_{II} phases in DOPE-ME [4,5], but not DOPE or egg PE. Together with results of earlier studies of fusion kinetics [4], these data represent the first unambiguous characterization of a fusion intermediate. [1] Talmon et al., J. Elect. Micros. Tech. (in press); [2] Biophys. J. 49:1155 & 1171; [3] Chem. Phys. Lipids 42:279; [4]Ellens et al., Biochemistry 25:4141 and Biochemistry (in press); [5]Biochemistry 27:2853.

Tu-Pos235 CORRELATION OF FUSION AND PHASE BEHAVIOR FOR GLYCEROLMONO-OLEATE/1,2-DIOLEOYLGLYCERO-3-PHOSPHO-N,N' DIMETHYLETHANOLAMINE (GMO/DOPE-ME_2) LIPOSOMES

J. Bentz[1], D. P. Siegel[2], D. Alford[1], J. Banschbach[2], G. Orädd[3], and G. Lindblom[3], [1]Dept. of Parmacy, UCSF, San Francisco, CA 94143, [2]Procter & Gamble Co., P.O. Box 398707, Cincinnati, OH 45239-8707; [3]Dept. of Physical Chemistry, University of Umeå, 901 87 Umeå, Sweden

DOPE/DOPC mixtures and mono-methylated DOPE (DOPE-ME) share a common set of intermembrane intermediates for the processes of fusion (aqueous contents mixing) and the lamellar/inverted cubic (I_{II}) phase transition [1,2]. The L_α/I_{II} phase transition can be quite hysteretic and is characterized by isotropic ^{31}P-NMR resonances, lipidic particles in electron micrographs, and slow evolution of X-ray diffraction patterns [3]. Gutman et al. [4] showed that the phase diagram of GMO/DOPC contains a region where isotropic ^{31}P-NMR resonances and lipidic particles are evident. We were unable to determine the fusion kinetics in GMO/DOPC because stable liposomes do not form. We overcame this problem by using an analog of DOPC, DOPE-ME_2. At neutral pH, the phase behavior of DOPE-ME_2 is quite similar to that of DOPC, but it is negatively charged at pH 9.5. GMO/DOPE-ME_2 liposomes at pH 9.5 retain their contents for up to 2 weeks at 4°C. At pH 4.5, these liposomes fuse at low temperatures and undergo contact-mediated lysis at temperatures where the fluorometric NBD-PE assay predicts a transition to the inverted hexagonal phase. ^{31}P-NMR, DSC, and X-ray diffraction will be used to determine the phase behavior of this lipid system. We will then determine the extent to which the fusion mechanism for these liposomes can be predicted from this lipid phase behavior. [1] Ellens et al., Biochem. 25:4141 (1986); and Biochemistry (in press); [2] Siegel et al., Biochemistry (in press); [3] Siegel et al., (this meeting); [4] Gutman et al., pp. 143-152 in: Surfactants in Solution, Vol. 1, (Mittal & Lindman, eds.), Plenum (1984).

Tu-Pos236 EFFECT OF A VIRAL FUSION INHIBITORY PEPTIDE ON LIPID PHASE BEHAVIOR AND FUSION IN A MODEL SYSTEM. Daniel Kelsey, Thomas Flanagan* and Philip L. Yeagle. Department of Biochemistry and *Department of Microbiology, University at Buffalo, (SUNY), Buffalo, NY 14214.

The effect of the viral fusion inhibitory peptide, Z-D-Phe-Phe-Gly, on the phase behavior and fusion characteristics of N-methyl phosphatidylethanolamine vesicles has been examined. The temperature at which the isotropic phase appeared in the P-31 NMR spectra was reduced in the presence of concentrations of Z-D-Phe-Phe-Gly (peptide/phospholipid ratio) that inhibit viral fusion. In addition, initial rates of fusion and leakage of vesicle contents were measured by fluorescence assays. The effect of the presence of Z-D-Phe-Phe-Gly on fusion and leakage of N-methyl phosphatidylethanolamine vesicles will be presented.

Tu-Pos237 PEG INDUCED AGGREGATION: LIPID EXCHANGE BUT NOT FUSION IN DIPALMITOYL PHOSPHATIDYLCHOLINE LARGE VESICLES. Stephen W. Burgess, Gail F. McIntyre, Julie Yates, Donald Massenburg, and Barry R. Lentz. Department of Biochemistry, University of North Carolina- Chapel Hill, Chapel Hill, NC 27599.

There has been a great deal of work done in recent years examining the mechanism of fusion induced by poly(ethylene glycol) (PEG). Most studies have involved inherently fusogenic small, unilamellar vesicles (SUV). Recently, we have found that more stable large, unilamellar vesicles (LUV) formed by a rapid extrusion technique (LUVET) and composed of 1,2-dipalmitoyl-3-*sn*-phosphatidylcholine (DPPC) do not fuse in the presence of PEG at any concentration (3.8-35 wt. %). We used the ANTS/DPX assay to monitor leakage and mixing of internal aqueous contents, and the 1-palmitoyl-2-[[[2-[4-(6-phenyl-*trans*-1,3,5-hexatrienyl)phenyl]ethyl]oxy]carbonyl]-3-*sn*-phosphatidylcholine (DPHpPC) lifetime assay to monitor exchange of membrane components. In agreement with our previous studies of reverse-evaporation LUV's (Parente & Lentz, *Biochemistry* 25, 6678), PEG did induce lipid exchange between large vesicles and extensive leakage of internal contents at PEG concentrations >27 wt. %. However, in contrast to our previous work, we could detect no mixing of internal contents. This discrepancy has been identified as being due to photobleaching of ANTS at the very high concentrations existing within a vesicle exposed to PEG. We are now able to correct for this anomaly. In agreement with the lack of contents mixing, trapped volume and dynamic light scattering experiments showed no size increase in vesicles incubated in PEG. We conclude that large vesicles composed of DPPC do not fuse in the presence of even high concentrations of PEG. The observation of lipid mixing in the absence of fusion has been of particular interest to us as it implies intimate vesicle contact but without the additional bilayer perturbation necessary to cause fusion. We found that approximately 15-20% of the bilayer lipids mix at all concentrations of PEG examined. The observed lipid mixing was immediate and did not require dilution of the PEG solution as was suggested by MacDonald (*Biochemistry* 24, 4058). We are presently exploring possible mechanisms for this lipid exchange. Since we have shown in this work that lipid mixing is not a reliable indicator of membrane fusion, we question the validity of some previous reports of PEG-induced vesicle fusion. Supported by GM32707 to BRL.

Tu-Pos238 PH DEPENDENT FUSION OF AGGREGATED LARGE VESICLES BY GALA, A SYNTHETIC AMPHIPATHIC PEPTIDE. Roberta A. Parente, Christine Ring, & Francis C. Szoka Jr. Departments of Pharmacy and Pharmaceutical Chemistry, School of Pharmacy, University of California, San Francisco, CA 94143-0446

A model peptide and various lipid vesicle systems have been employed to study the aggregation and destabilization steps required for protein induced fusion. Aggregation of large unilamellar vesicles (LUV) was mediated by : 1. lectin binding 2. electrostatic interactions or 3. Ca^{++}. Destabilization was induced by GALA, a synthetic, amphipathic, pH dependent peptide (*J.Biol.Chem. 263*, 4724-4730, 1988). LUV composed of palmitoyl-oleoyl phosphatidylcholine with 10mol% lactosyl ceramide can be reversibly aggregated by the ricin B chain, independent of pH. Addition of a ricin-GALA covalent conjugate to the lactosyl ceramide LUV caused a pH dependent increase in lipid mixing, as determined by fluorescence energy transfer of the lipid probes NBD-PE and Rh-PE. Dynamic light scattering also indicated an irreversible increase in vesicle size. Moreover, neither the addition of ricin B chain to LUV or GALA to LUV aggregated by the ricin B chain induced lipid mixing or caused an irreversible increase in LUV size under any conditions studied. Egg phosphatidylcholine LUV containing 15mol% dioleoyl trimethylammonium propane (DOTAP), a positively charged lipid, aggregated as a result of electrostatic interactions when mixed with GALA at neutral pH. A drop in pH enabled GALA to destabilize the vesicles and induce lipid mixing. In these two systems a lipid to peptide ratio below 50:1 was necessary to induce the changes observed. Egg phosphatidylglycerol vesicles aggregated with Ca^{++} (up to 15 mM) could also be induced to fuse in the presence of GALA even at a 500:1 mole ratio as determined by lipid mixing and dynamic light scattering. Fusion was most efficient at low pH but could also occur to a limited extent at pH 7. Fusion at higher pH can occur in this particular system because Ca^{++} is able to induce a helical conformation in GALA. Partially supported by NIH-GM30163 and by the Biotechnology Resources & Education Program.

Tu-Pos239 THE KINETICS OF FUSION BETWEEN INTACT HUMAN ERYTHROCYTES INDUCED BY POLY(ETHYLENE GLYCOL)
Shi Kun Huang and Sek Wen Hui; Membrane Biophysics Lab., Biophysics Department, Roswell Park Memorial Institute, Buffalo, NY 14263

The kinetics of Poly(ethylene flycol) (PEG)-induced fusion between intact human erythrocytes was continuously monitored with a fluorescence dequenching method. The Fluorescence probe, 1-Oleoyl-2-[12-[(7-nitro-2,1,3-benzoxadiazol-4-yl)amino]dodecanoyl]phosphatidylcholine (C_{12}-NBD-PC) was employed in this lipid mixing assay. The steady-state fluorescence intensity was detected from the surface of cells in a monolayer. The kinetics of relief of fluorescence self-quenching, after fusion occurred between C_{12}-NBD-PC labeled and unlabeled intact erythrocytes (at 1:1 ratio), was monitored. A mathematical formula was developed to take into account the dequenching due to fusion and to lipid flip-flop.

There was no significant lipid mixing during PEG treatment for 5 minutes, in 4°C, nor spontaneous flip-flop between bilayer leaflets within 30 minutes of dilution. The fluorescence intensity increased with time following the dilution of PEG. The efficiency of fusion increased with increasing concentrations of PEG. Flip-flop was monitored in a parallel experiment. The fusion-induced flip-flop was found to account for approximately 30% of the fluorescence dequenching. The kinetics of dequenching is therefore dependent not only upon the fusion rate, but also upon the rates of flip-flop and the lateral diffusion of dyes after fusion. The latter was monitored by video-enhanced fluorescence microscopy.

Tu-Pos240 CONDITIONS UNDER WHICH FUSION ASSAYS AGREE WHEN THE FUSOGEN IS AN ELECTRIC PULSE.
Arthur E. Sowers, American Red Cross - Jerome H. Holland Laboratory, Rockville, MD 20855.

Individual FITC-dextran-based contents mixing events and DiI-based membrane mixing events in erythrocyte ghosts were followed with fluorescence optics in separate but otherwise identical experiments. Dielectrophoresis was used to hold membranes in close contact while an electric pulse was used as a fusogen. However, over a range of variables, the contents mixing events were usually much higher than the number of membrane mixing events. However, when the dielectrophoretic force was removed by shutting off the alternating current after the pulse, then a fraction of the membranes which showed contents mixing separated by Brownian motion, thus showing that they were not fused (Sowers, BJ 54,619-626). When the number of contents mixing events which do not represent fusion are subtracted from the total number of contents mixing events (to obtain a corrected contents mixing fusion yield), and the experiments are conducted at 20 mM NaPi (pH 8.5), then close agreement is obtained with the number of membrane mixing events. An increase in the ionic strength caused: i) a large decrease in the number of non-fusion contents mixing events, suggesting that they are due to some combination of electropore induction and electroosmosis, and ii) a small decrease in corrected contents mixing fusion yield and a small increase in DiI-based fusion yield. Supported by ONR Contract N00014-87-K-0199.

Tu-Pos241 MICROMANIPULATION OF ELECTROFUSED RED BLOOD CELLS.
D. Miles, Dept. of Biomedical Engrg. and R. Hochmuth, Dept. of Mechanical Engrg. and Materials Science, Duke University, Durham, NC 27706.

A system developed for the fusion and micromanipulation of red blood cells has been modified to allow a more "gentle" fusion process and a variation of conditions for cellular manipulation. Cells are suspended in a 200mOsm salt-sucrose solution, aligned in an AC field and fused with 4 DC pulses of 3-5kV/cm height and 20-25μs width. Several types of fusion products are obtained depending upon the extent of fusion. The most gently fused cells are attached by a tether (<0.1μm dia.) while other pairs of fused cells are joined by a larger lumen. The fused cells are flushed into a manipulation chamber with a 295mOsm solution to counteract cell swelling. Micromanipulation is used to characterize the mechanical properties of the fusion site. The application of large membrane tensions (1-2.5 dyn/cm) may cause the tether connection to suddenly open to a larger tunnel structure (0.5-1μm dia.). Moderate tensions of 0.5 dyn/cm cause the tunnel structure to expand to the diameter required to sphere the doublet. Upon release of the pressure the lumen area of the doublet quickly returns to its original tunnel configuration. The tether represents the least amount of membrane involved in the fursion process, the "gentlest" of fusion conditions and the earliest stable state of lumen formation in untreated, electrofused red cells. The spectrin network is left across the ends of the tether in its original configuration. The applied tension breaks down enough of the network to allow the formation of a tunnel that is able to stretch 3-4x its size to sphere the doublet. The tension required to open the doublet is that required to stretch the remaining spectrin network from its native configuration. The elastic response of the tunnel is due to the return of the network to its unstretched state. An elastic modulus for the spectrin network is estimated to be somewhat higher than the elastic shear modulus of normal red cell membrane. Supported by NIH-HL-23728.

Tu-Pos242 **USING MUTANT AND CHEMICALLY-MODIFIED HEMOGLOBINS TO PROBE THE MOLECULAR MECHANISM OF COOPERATIVITY.** George J. Turner and Gary K. Ackers, Department of Biology, The Johns Hopkins University, Baltimore, MD 21218

The strategy of mapping by structure-function perturbation (1) has been employed to determine the structural location of cooperative free energy in human hemoglobin: Gibbs free energies of cooperativity (ΔG_c) were determined for a series of hemoglobins possessing single-site amino acid substitutions or chemical modifications. The perturbations in ΔG_c brought about by the local-site modifications are mapped against their structural locations. This analysis (2) has now been extended to include 55 human hemoglobins, yielding the conclusion that the $\alpha_1\beta_2$ intersubunit contact is the structural location of ligand-linked interactions that generate the cooperative free energy ΔG_c.

Many of the hemoglobins studied may be grouped in clusters of sites previously implicated as critical to cooperative oxygenation and the Bohr Effect. It is now possible to selectively assess the energetic consequences of altering non-covalent bonding interactions in these clusters. Cooperative enthalpies and entropies have been determined for a series of hemoglobins where putatively critical proton-linked salt bridge partners, and interchain hydrogen bonds, are perturbed. Hemoglobins investigated include Cowtown (β146 His-Leu), Barcelona (β94 Asp-His), Bunbury (β94 Asp-Asn), Kariya (α40 Lys-Glu), Ypsilanti (β99 Asp-Tyr), and Des Arg (α141 deleted). The temperature dependence of these mutant hemoglobins at pH7.4 (1M NaCl, .1M Tris-base, 1mM EDTA) suggest that the dominant non-covalent bonding interactions responsible for their cooperative mechanisms are identical to those of hemoglobin A_0. Results of these mutant Hb studies are inconsistent with a mechanism that is energetically dependent on a set of oxygenation-sensitive salt bridges. Consistent with prior work from this laboratory (2) these data support a molecular mechanism of cooperativity whose major energetic contributions originate from hydrogen bonding, proton release and van der Waals interactions.

1. Ackers, G.K. and Smith, F.R., (1985) Ann, Rev. Biochem. 54, 597. 2. Pettigrew et al., (1982) PNAS 79, 1849.

Tu-Pos243 **COOPERATIVE INTERACTIONS OF HUMAN HEMOGLOBIN - PARTIALLY LIGATED SPECIES RESPOND DIFFERENTIALLY TO PROTONS.** Madeline A. Shea & Gary K. Ackers, Department of Biology, The Johns Hopkins University, Baltimore, MD 21218

Recent work in our laboratory has generated an approach to studying energetics of the eight intermediate species in the cooperative ligation of human hemoglobin. Experimental resolution of the distribution of these intermediates define constraints that must be satisfied by any mechanistic model proposed for hemoglobin cooperativity. We have shown at pH 7.4, 21.5C that the intermediate species are distributed in at least three cooperative free energy levels. This finding has proven to be independent of the ligand used; however, the species populations vary quantitatively with heme-site ligand. Cooperative free energy distributions are inconsistent with a two-state (MWC-type) model for cooperativity and require a minimum of three tetrameric structures with distinctly different free energies of heme-heme interaction.

Protons are known to be a significant physiological effector of hemoglobin function, accounting for up to 50% of cooperative free energy. While their effect on average oxygen binding properties at each stage has been rigorously examined, we wish to know more than the average effect of protons on each of the four binding steps. Thus, kinetic and thermodynamic studies are underway to characterize the response to changes in chemical potential of protons manifested by individual intermediate ligation species. Studies of CN-met hemoglobins at pH 8.5, 21.5C indicate that the doubly-ligated species differ in their cooperative free energy depending on the configuration of ligated sites within the tetramer. This finding rules out any two-state mechanism for hemoglobin function. These results permit us to predict the pertinent average properties for comparison with those determined by oxygen binding studies.

Tu-Pos244 EFFICIENT THERMODYNAMIC TREATMENT OF PROTEIN LINKAGE SYSTEMS. Roger Gregory, Kent State University, Kent, OH 44242 and Rufus Lumry, University of Minnesota.

The ligand–binding sites of hemoglobin are mutually coupled through protein conformation but weakly so. Were the coupling strong, there would be only two species: free and completely liganded. Nevertheless such weakly–coupled reaction systems are invariable treated in the same way as chemical reactions in which the atom composition of products is different from that of reactants. This is inefficient because it conceals quantitative details of linkage implicit in the data. The original "weak–coupling" treatment (The Fluctuating Enzyme, Wiley,1986,p.86) was based on two approximations: the species partition function could be factored into site partition functions and interaction factors (e.g.,for the hemoglobin species HbL(1) $q_{A\beta_1\alpha_2\alpha_3\alpha_4} \rightarrow q_A q_{\beta_1} q_{\alpha_2} q_{\alpha_3} q_{\alpha_4} \gamma_{A\beta_1} \gamma_{A\alpha_2} \gamma_{A\alpha_3} \gamma_{A\alpha_4}$) and the probabilities of the species could be approximated by products of unconditional site probabilities ($P_{A\beta_1\alpha_2\alpha_3\alpha_4} \rightarrow \pi_A \pi_{\beta_1} \pi_{\alpha_2} \pi_{\alpha_3} \pi_{\alpha_4}$). The latter assumption is obviously poor but it is consistent with a large number of experimental data from protein systems and in particular with the appearance of linear enthalpy–entropy compensation behavior from which the correct linkage diagram and the distribution of gross thermodynamic quantities among sites and coupling can be determined. Compensation behavior requires linear–free–energy behavior so both are invarient consequences of the weak–coupling approximation. However removal of the second approximation in general destroys linearity for both in disagreement with the data. The resolution of this paradox appears to lie in the validity of mean–field approximations for hemoglobin, enzymes, residue exchange in proteins,etc. since mean–field treatments give the same qualitative behavior as the "weak–field"approximation as we shall show. Fortunately for proteins the loss in precision in the dissection of the thermodynamic changes is not severe. The validity of mean–field treatments is probably due to the fact that the coupling free energies are small relative to total conformational free energies.

Tu-Pos245 SELF DIFFUSION AND EQUATIONS OF STATE FOR BIOMOLECULES.
Timothy J. O'Leary, Department of Cellular Pathology, Armed Forces Institute of Pathology, Washington, DC 20306.

The concentration dependence of macromolecular self diffusion may play a role in such diverse processes as enzymatic catalysis and photosynthetic electron transfer. We have previously shown that "hopping models", in which the probability of a molecule making a diffusive motion is given by the probability of forming an adjacent hole of molecular size , describe this concentration dependence quite well. In the present work we derive an expression for the concentration depsndence based upon a model which allows diffusion to take place in steps much smaller than a molecular diameter. We point out the relationships between the equation for the concentration dependence of self diffusion and such properties as protein partial osmotic pressure and solution structure factors, and we postulate that the concentration dependence of self diffusion may be universally described by the equation $D = D_o \exp(-PV^*/kT)$ where P is a partial osmotic pressure (or partial surface pressure), V* is an activation volume, k is Boltzmann's constant and T is the absolute temperature. We show that this equation aproximatley describes the concentration dependence of hemoglobin diffusion using several different equations of state, and explore the advantages and disadvantages of its use when compared to other theoretical expressions which have been proposed.

Tu-Pos246 Photophysics of Tryptophan Fluorescence Emission in Mutants of T4 Phage Lysozyme: Dan Harris, Bruce Hudson, Lawrence McIntosh, and Cynthia Phillips. Institute of Mol. Biology, University of Oregon, Eugene, Oregon, 97403

The excited state fluorescence lifetime descriptions of tryptophan in several mutants of T4 phage lysozyme are correlated with environment. The discussion is cast in terms of the amino acid neighbors of the tryptophans, their quenching efficiency, and proxmity to the tryptophan in question. The role of fluctuations in mediating the environment is inferred from molecular dynamics studies on WT T4L and associated mutants. Special emphasis is placed upon the analysis of single tryptophan containing mutants of T4 phage lysozyme. For one of these single trp mutants, W158, we shall present analysis in terms of the theory of Tanaka and Mataga describing the effects of tryptophan reorientation upon dynamic quenching and a resultant non-exponential decay. Data will be presented for W138, the most buried of the three tryptophans occurring in WT T4L, which illustrate the role of neighboring amino acids in determining its lifetime description. Finally, we present KI quenching data on W138 as a function of ionic strength which sheds light on the local electrostatic potential in the vicinity of this fluorophore.

Tu-Pos247 CHARACTERIZATION OF THE TRYPTOPHAN ENVIRONMENTS OF INTERLEUKINS 1α AND β BY FLUORESCENCE QUENCHING AND LIFETIME MEASUREMENTS. Dennis E. Epps, Anthony W. Yem, and Martin R. Deibel, Jr.

The tryptophan environments of interleukins 1α and β, two immunomodulatory proteins with similar biological activities but only 25% sequence homology, were characterized by steady state and dynamic fluorescence measurements. Both proteins exhibited similar emission maxima, but the emission intensity of IL-1β was greatly increased by increasing the ionic strength of the medium, whereas, IL-1α was unaffected. Both proteins were similarly quenched by acrylamide but not by the ionic quenchers iodide and cesium. The fluorescence intensity decays of both cytokines were characterized by two (long and short) component lifetimes. However, the average lifetimes of IL-1β (4.4 ns) was much longer than that for IL-1α(1.93 ns). Taken with the results of steady state measurements, we suggest that the single tryptophan of IL-1β is statically quenched by neighboring charged residues, whereas the tryptophan environments of IL-1α are unaffected by ionic strength. The results are discussed in terms of similarities and differences in the tryptophan environments of the two proteins.

Tu-Pos248 SPECTROSCOPIC STUDIES OF METAL-ION COMPLEXES OF HUMAN LACTOFERRIN AND TRANSFERRIN.
John P. Harrington, Department of Chemistry, University of South Alabama, Mobile, Alabama, 36688.

Several transition metal-ion complexes Fe(III), Cu(II), Mn(III), Co(III) of human lactoferrin (LF) and transferrin(TF) were investigated by direct visible and fluorescence spectroscopy. These methods are effective in assessing the conformational stability of these metal-protein complexes as well as providing evidence for different events leading to unfolding and the loss of each of these metal ions. Analysis of these metal-protein complexes in the presence of urea and several alkyl ureas demonstrated the uniqueness of each of these metal ion interactions with LF and TF. Observed transitions evident by direct visible spectroscopy are different in each case than those obtained by fluorescence spectroscopy. Higher midpoint transitions occurred for all direct spectral measurements. Fluorescence excitation at 290nm produced wavelength changes in fluorescence emission maximum(Δnm) resulting in spectral shifts from 330 to 356nm indicating exposure of tryptophan residues. Fluorescence transition midpoints($D_{\frac{1}{2}}$) for apo-LF and Fe(III)-LF in urea were 3.25 and 7.6M, respectively. Exposure of tryptophan in apo-TF required a higher urea concentration(3.70M) compared to apo-LF(3.25M) possibly reflecting a greater number of disulfide bonds in TF. For most metal-protein complexes studied, the metal-LF complexes had a higher midpoint transition than the metal-TF complexes indicating greater resistance to unfolding when these specific metal ions are associated with the corresponding proteins.

Tu-Pos249 INTRAMOLECULAR CHARGE TRANSFER IN MODEL PEPTIDES AND LYSOZYME INVOLVING TRYPTOPHAN AND TYROSINE

K. BOBROWSKI , J. HOLCMAN AND K. L. WIERZCHOWSKI,
Institute of Biochemistry and Biophysics, Polish Academy of Sciences, Warszawa, POLAND ;
Accelerator Department, Riso National Laboratory, DENMARK,

A series of Trp(Pro)nTyr (n=0-3) peptides and hen egg-white lysozyme were selectively oxidized at Trp with pulse radiolytically generated azide radicals in neutral aqueous solution.The rate of subsequent intramolecular charge transfer (k) between Trp/Tyr redox pair(s) was determined over the temperature range 278-338 K. From the plot of log k versus Trp-Tyr separation distance in peptides the parameter β=0.43 $Å^{-1}$, while from the Arrhenius plot low activation energy (17-23 kJ/mol) and large negative entropy (90-134.5 J/deg x mol) were obtained. These parameters seem to indicate involvement of electron tunnelling between strictly oriented aromatic moieties, observable up to $\sim$12.5 Å separation distance. The data for lysozyme indicated occurence of single intramolecular electron transfer characterized by non-linear Arrhenius plot. Using the distance limit of practical observability of electron transfer in polyproline peptides and crystallographic data for lysozyme, potentially effective Trp/Tyr redox pairs were selected. Selective oxidation by ozone of Trp-62 and/or Trp-63,belonging to this set, led to complete disappearance of the transfer process. In intact lysozyme it occurs most probably between Trp-62/Trp-63 radicals and Trp-53, located within one of the substrate binding lobes of the enzyme. Nonlinearity of the Arrhenius plot can thus be interpreted in terms of local intralobe fluctuations of the protein matrix.

Tu-Pos250 **PICOSECOND FLUORESCENCE DYNAMICS OF PLASTOCYANIN.**
D.P. Millar, and G.G. Dupuy, Department of Molecular Biology, Research Institute of Scripps Clinic, La Jolla, CA 92037; R. Powls, Department of Biochemistry, University of Liverpool, Liverpool, England.

The plastocyanins are type 1 "blue copper" proteins which function in chloroplast electron transport as carriers between cyt f and P700 in photosynthetic organisms ranging from algae to higher plants. In order to examine the structure and dynamics of plastocyanin (Pc) in solution, we have performed time- and frequency-resolved fluorescence measurements on the Pc obtained from the green algae Scenedesmus obliquus. This Pc has M_r 10,000 and contains a single tryptophyl (trp) residue at position 29. The protein was excited at 295 nm with the frequency doubled output of a hybrid mode-locked dye laser and the emission, which was exclusively due to the trp residue, was detected with a microchannel plate photomultiplier operated in single-photon-counting mode. The instrument response width was 30 ps. To investigate the role of the copper atom in the photophysics and dynamics of this protein, we have examined the oxidized, reduced and apo forms of the protein. All protein forms exhibit a lifetime heterogeneity which can be represented by a sum of three exponential decay components, with lifetimes ranging from 230 ps to 3.5 ns. The decay kinetics also vary with the emission wavelength. Removal of the copper atom leads to a substantial increase in the long-lifetime components. The role of protein conformational heterogeneity and tryptophyl rotamers in conjunction with energy and/or electron transfer to the copper atom or other nearby quenching groups will be discussed in relation to the fluorescence decay kinetics. The correlation times for trp motion have been determined from the fluorescence anisotropy decay and indicate that the trp-29 residue has limited internal mobility consistent with the solution structure of scenedesmus Pc recently determined by NMR methods (Moore et al., 1988, Science 240, 314-317) which shows that trp-29 is buried in the protein interior.

Tu-Pos251 LIFETIME AND ANISOTROPY DECAYS OF STAPHYLOCOCCAL NUCLEASE AND THE PA56 MUTANT. Ignacy Gryczynski, Gabor Laczko, Wieslaw Wiczk and Joseph R. Lakowicz, University of Maryland, Department of Biochemistry, Baltimore, MD, and Maurice Eftink, University of Mississippi, Department of Chemistry, University, MS.

Frequency-domain fluorescence spectroscopy was used to investigate the effects of temperature on S. Nuclease and its PA56 mutant. The intensity decays were analyzed in terms of a sum of exponentials and using Lorentzian distributions of decay times. Both the intensity and anisotropy decays indicate significant differences in the temperature stability of S. Nuclease and the mutant, which show characteristic temperatures of 50 and 30° C, respectively. For both proteins, the longer correlation time decreases dramatically at the transition temperature, indicating increased segmental mobility around the single tryptophan residue. The widths of the lifetime distribution, as observed using the bimodal Lorentzian model, decrease significantly over this same temperature range. For both proteins, a rigid environment for the single tryptophan residue results in a broad distribution of decay times. Thermal unfolding of the proteins results in more narrow Lorentzian widths, or equivalently, an intensity decay closer to the double exponential model. It appears that the folded protein structure is the origin of the distribution of decay times in these proteins.

Tu-Pos252 ULTRACENTRIFUGE STUDIES ON DISSOCIATION OF FIBRIN AGGREGATES AT ELEVATED TEMPERATURES. **Josiah I. Mega and John R. Shainoff. Res. Institute of The Cleveland Clinic Foundation. Cleveland, OH 44195.**

Fibrin monomer of type lacking fibrinopeptide A alone (alpha-fibrin) coagulates fully at physiologic pH and temperature, but has high solubility exceeding 1 mg/ml at elevated temperatures (40-43°C). Ultracentrifuge studies at 40-42° indicate that the dissolved fibrin consists principally of three components, 8S monomer and aggregates sedimenting bimodally at 16S and 24S ($S^{\circ}_{w,20}$). The 16S aggregates had not been observed before except with a weakly aggregating type of monomer (beta-fibrin, lacking fibrinopeptide B) which did not form 24S aggregates under the conditions studied. The resolution of two distinct and seemingly stable sedimenting forms of aggregates suggests disaggregation proceeds slowly compared to sedimentation. The 16S component consists of trimers which had been shown with beta-fibrin to have greater stability than dimers, while the 24S component corresponds to the large, double stranded oligomers described long ago by Shulman and Ferry. The principal mode of aggregation may involve assembly of monomers into trimers, and assembly of the trimers into oligomers, rather than stepwise accretion of monomers. The weak interaction favoring monomer aggregation into trimers rather than dimers would be duplicated and function as coupled bonding in trimer/trimer interactions, but not in monomer/trimer interactions. **(Support: NIH grant HL-16361).**

Tu-Pos253 DIFFERENTIAL SCANNING CALORIMETRIC STUDIES OF WILD-TYPE AND MUTANT THIOREDOXINS M. Santoro and W. Bolen, Department of Chemistry and Biochemistry; Southern Illinois University; Carbondale, IL 62901-4409.

Using differential scanning calorimetry (DSC), reversible thermal unfolding of oxidized and reduced forms of wild-type (wt) E. coli thioredoxins (TRX) has been established over two narrow pH ranges (2.0-3.0 and 6.5-7.0). Within these pH ranges the oxidized and reduced TRX species appear to exhibit two-state behavior with $\Delta H_{cal}/\Delta H_{vant\ Hoff}$ ratios very close to unity. These pH conditions were used to evaluate the thermal unfolding characteristics of reduced and oxidized forms (where possible) of several site-directed mutants of TRX. These mutants include replacement of cysteine 32 with serine (C32S) abolishing the single intramolecular disulfide bond functioning in oxidation/reduction, replacement of both cysteines with serines (C32, 35S), insertion of arginine within the disulfide loop between residues 33 and 34 (33R34), and substitution of proline 76 with alanine (P76A). In all cases, reduced wt TRX and reduced and oxidized forms (where possible) of mutant TRXs were found to be less stable than oxidized wt TRX. In some cases near neutral pH, consecutive DSC scans exhibit endotherms with broadened peaks and decreased Tms. Such changes in DSC behavior may be linked to a transformation of the protein to another as yet unidentified form of the folded protein.

Tu-Pos254 CHANGES IN THE APPARENT PARTIAL SPECIFIC VOLUME AND COMPRESSIBILITY ASSOCIATED WITH THE THERMAL DENATURATION OF LYSOZYME. Ling X. Shen and Don Eden, Dept. of Chemistry and Biochemistry, San Francisco State Univ., San Francisco, CA 94132.

Several changes have been made to our differential scanning density and sound velocity instrumentation in order to obtain more reproducible and accurate measurements. Experiments with lysozyme (~9 mg/ml) in a pH 2.0 glycine buffer have been performed over a temperature range of 25 to 82 C. The apparent partial specific volume of lysozyme increases by 0.017±0.001 ml/g over this temperature range. The temperature of denaturation, T_d, is determined to be 59±2 C, which agrees with the T_d determined from our absorbance measurements at 256 nm over the same temperature range. We have determined that the increase in the apparent partial specific volume at T_d of the transition from the native to the denatured protein is $(1.7\pm0.3)\times10^{-3}$ ml/g. This corresponds to a volume change of 24 ml/mol. This positive volume change associated with the thermal denaturation of lysozyme is in agreement with Lee and Timasheff's (Biochemistry 13, 257 (1974)) determination of the volume increase associated with the transfer of lysozyme from the native to a denatured state in 6 M Gdn-HCl. However, the consistent volume increase observed from our density measurements is in contradiction with the results of Velicelebi and Sturtevant (Biochemistry 18, 1180 (1979)) who observed a large volume decrease associated with thermal denaturation in the same buffer. The apparent partial specific compressibility of lysozyme increases in roughly a linear fashion over the temperature range of 25 to 82 C. No pronounced change in compressibility has been observed in the transition region. Its value determined at 25 C is in good agreement with previous measurements by Gekko and Hasegawa (Biochemistry 25, 6563 (1986)).

Tu-Pos255 VOLUME CHANGE REFLECTS METAL-ION COORDINATION TO PROTEIN BINDING LOOPS. D. W. Kupke, Department of Biochemistry, Sch. of Med., University of Virginia, Charlottesville, VA 22908.

The characteristic metal-binding sequences in many of the calcium-binding proteins bear similarities to the microenvironment of the common tetracarboxylate sequestrants. Indeed, the expansions in volume (ΔV) have been found to be similar upon Ca^{2+} coordination to the EGTA class of sequestrants and to the tested calcium-binding proteins. Moreover, synthetic peptide analogues of the 12-residue binding loop sequences in calmodulin show comparable expansions to that of the total protein when treated with lanthanide ions. (Ca^{2+} binds poorly to these loop peptides whereas the lanthanides bind strongly to both the peptides and to the proteins.) These results suggest 1) that factors other than the coordination event, such as void-space changes in proteins, do not contribute substantially to ΔV during metal-ion uptake, and 2) that the preformed binding-loop structures in the apoproteins are frozen in for accepting easily the relatively soft calcium ion. More significantly, clear differences in ΔV were observed during peptide-lanthanide interactions when the composition of the peptide was varied at single coordinating residues. This finding supports the hypothesis that each of the compositionally distinct binding loops in this class of proteins generate distinctive volume increases upon coordination with a metal ion. Hence, the variation in ΔV observed previously upon sequential addition of Ca^{2+} to some of these proteins apparently reflects an ordered type of metal-ion uptake.

(Supported by NIH Grant, GM-34938, from the U. S. Public Health Service.)

Tu-Pos256 MECHANISM OF INTERACTION OF STABILIZING CARBOHYDRATES WITH FREEZE-DRIED PROTEINS J.F.Carpenter[1,2] and J.H.Crowe[2], [1]CryoLife, Inc., Marietta, GA and [2]Univ. of Calif-Davis

Fourier transform infrared spectroscopy was used to characterize the interaction of carbohydrates with dried proteins. Freeze-drying of trehalose, lactose or inositol with lysozyme resulted in substantial alterations of the infrared spectra of the dried carbohydrates. In the finger print region (900-1500 cm^{-1}), there were large shifts in the frequencies of bands, a decrease in absorbance, and a loss of band splitting. These effects mimic those of water on hydrated trehalose. Bands assigned to hydroxyl stretching modes (around 3350 cm^{-1}) were decreased in intensity and shifted to higher frequency in the presence of the protein. In complimentary experiments, it was found that dehydration-induced shifts in the positions of amide I and amide II bands for lysozyme could be partially and fully reversed, respectively, when the protein was freeze-dried in the presence of either trehalose or lactose. In addition, the carboxylate band, which was not detectable in the protein dried without the sugar, was apparent when these sugars were present. Inositol was less effective at shifting the amide bands, and the carboxylate band was not detected in the presence of this carbohydrate. Also tested was the concentration dependency of the carbohydrates' influence on the position of the amide II band for dried lysozyme. The results showed that the ability of a given concentration of carbohydrate to shift this band back towards the position noted with the hydrated protein coincided with the capacity of that same level of carbohydrate to preserve the activity of rabbit skeletal muscle phosphofructokinase during freeze-drying. Taken together, these results suggest that hydrogen bonding occurs between dried proteins and carbohydrates, and that such binding is requisite for carbohydrate-induced stabilization of freeze-dried proteins.

Tu-Pos257 PROTEIN CONFORMATION SQUEEZE-DOWN VIA C_4-C_6 COSOLVENTS PROBABLY PROVIDES THE BEST BASIS FOR IMPROVING SEPARATIONS. Rex Lovrien and Constance Bergstedt; Biochemistry Dept., Univ. of Minnesota, St. Paul, MN 55108.

Protein separations are much more expensive problems in process technology than production of them. People are working hard on 'downstream' methods, especially chromatography. However they are mostly expensive, often tricky, don't scale up well. 'Upstream' means dealing with crudes. Crudes are unpopular for R and D, but actually most in need. We designed a Three Phase Partitioning (TPP)/t-butanol technique. TPP is increasingly used but the main gap now is understanding molecular basics in separation, both up- and downstream. Neat water as 'the biological solvent' is one problem; water has been oversold. It is not the in vivo solvent, mixtures are. Neat water is a powerfully leveling solvent that enhances conformation fluctuations, partly unfolds. Many proteins have a more compact but not disheveled conformation in in vivo-like mixtures of C_4-C_6 cosolvents with some water, but C_1-C_2 cosolvents help unfolding at 25°. There is need to impose protein protection by ligand tightening in separations, enhanced by C_4-C_6 cosolvents. This facilitates denaturation/precipitation of unwanted proteins that can't bind ligands, in crudes. Graded ligand tightening and cosolvent squeezing probably afford paths for pushing proteins into uniform, native, tightened states to get them to crystallize. Probably such means are best choices for getting refolding. Using some of these principles, we present TPP-DE (Differential Floatation) for separations from crudes. TPP-DF needs only simple settling to get phase separation. The DF part originates from C_4-C_6 cosolvent binding to proteins, tightening conformation, inducing phase separation, and giving buoyancy so they float up when they pop out as separate phases.

Tu-Pos258 **PROTEIN CONFORMATIONS IN SOLVENT PERTURBED MEDIA: A MODEL STUDY BY POLYETHYLENE GLYCOL-WATER SYSTEM.** **Kingman Ng and Andreas Rosenberg, Department of Laboratory Medicine and Pathology, University of Minnesota, Minneapolis, USA. Ingemar Wadso, Thermochemistry Division, Chemical Center, University of Lund, Lund, Sweden.**

There has been an increased interest in studying protein dynamics in mixed cosolvent systems. The usefulness of these studies is based on our considerable knowledge of the thermodynamic properties of the time averaged solvent structures present in the cosolvent systems. Polyethylene glycol (PEG), well known to be a powerful precipitant and crystallizing solvent for macromolecules, strongly influences water activity. Water activity is crucial in defining the hydration shell, and thus the protein conformation. We intend to define thermodynamically the type of structural changes taking place in water in the presence of PEG in the hope to use them as the model of changes taking place during the so-called hydrophobic hydration of protein sidechains. Heat capacity measurements of the PEG-water system have been carried out over the full range of composition at 25°C using a drop calorimeter. The linear heat capacity function between 0 and 40% (w/w) of PEG indicates that the change in heat capacity of the system simply reflects the addition of bulk water to fully hydrated PEG molecules. At higher PEG content, phase separation occurs leading to qualitatively different interactions between water and the polymer structure.
(Supported by NIH 5RO1-GM 35384)

Tu-Pos259 A CAVITY FORMATION METHOD FOR CALCULATING FREE ENERGY OF HYDRATION. Chyuan-Yih Lee, Chemical Dynamics Corp., 9560 Pennsylvania Avenue, Upper Marlboro, MD 20772.

The free energy of hydration for an ion can be approximated as the free energy change in replacing a water molecule by the ion. Migliore et al. [J. Chem. Phys., 88, 7766 (1988)] used the thermodynamic cycle-perturbation method where the physical property in the ensemble average involves configurations of two different systems, thus inefficient when the two systems differ dramatically. Let V_i be the interaction potential between the ion and the surrounding water molecules, and V_w be that between the water molecule to be replaced by the ion and the rest of water molecules. Then, the free energy of hydration can be evaluated by using a reference system with a cavity,

$$A_i - A_w = (A_c - A_w) - (A_c - A_i)$$

$$A_c - A_x = -k_B T \Sigma_i \ln \langle \exp [-(\lambda_{i+1} - \lambda_i) V_x] / k_B T \rangle_{\lambda_i}$$

where the subscript x is either i or w, A_w is the free energy of bulk water, A_i is the free energy of bulk water with one water molecule replaced by an ion, A_c is the free energy of bulk water with a cavity created by removing one water molecule or the ion, and λ is a coupling parameter (1 --> 0) which slowly transforms the ion or the water molecule into a cavity. In this cavity formation method, the physical property in the ensemble average over a system (i or w) is expressed in terms of the configurations of the system alone. This method can be applied to more complicated systems, provided that the cavity reference system is properly defined.

Tu-Pos260 MODULATION OF HUMAN α-THROMBIN ACTIVITY BY ORGANIC PHOSPHATES

Raimondo De Cristofaro*, Massimo Castagnola+, Raffaele Landolfi*, Enrico Di Cera#. Istituto di Semeiotica Medica (*), Chimica (+), Fisica (#), Università Cattolica S. Cuore, Largo F. Vito 1, 00168 Roma, Italy.

The effect of AMP, ADP and ATP on amidase activity of human α-thrombin is studied by using a synthetic chromogenic peptide as substrate. These organic phosphates enhance α-thrombin activity at low concentrations, but inhibit the catalytic rate at high concentrations. A phenomenological description of the modulation of α-thrombin activity by adenine nucleotides is suggested. Two binding sites are assumed to be responsible for the effect of AMP, ADP and ATP. The first site allosterically enhances the catalytic rate. The second site has lower affinity and sterically hinders the binding of the substrate at the catalytic site. The detailed free-energy levels of α-thrombin in its various configurations with respect to substrate and organic phosphate binding are resolved by a global analysis of the experimental data.

Tu-Pos261 CYTOPLASMIC LIQUID-LIQUID PHASE SEPARATIONS INDICATED BY THERMOMECHANICAL ANALYSIS OF DEEPLY FROZEN LIVING WOOD. Allen Hirsh, American Red Cross R&D Laboratories, Rockville MD 20855; Thomas Bent, Comsat Corp., Clarksburg, MD; Eric Erbe, USDA BARC, Plant Stress Lab, Beltsville, MD; and Robert J. Williams, American Red Cross R&D Laboratories, Rockville, MD 20855. (Intr. by H.T. Meryman)

The dormant woody tissue of Populus balsamifera, balsam poplar, is uninjured by freezing at 5° C/hr rates or less to the temperature of liquid nitrogen, -196°C. We have established that there are multiple glass transitions in this tissue using differential scanning calorimetry (DSC) and electron microscopy (EM). We report here correlative studies of model solutions examined by DSC and living twigs examined by dynamic mechanical analysis (DMA) and EM. These comparative studies support the hypothesis that the cytoplasmic fluids of the Populus undergo liquid-liquid phase separations during cooling slow enough to be non-injurious. These domains appear to contain varying ratios of protein to the storage polysaccharides raffinose and stachyose. These ratios explain the variation in the observed glass transition behavior of these solutions.

Supported by Grants GM 17959 and BSRG 2 507 RR05737 from NIH and the American Red Cross.

Tu-Pos262 THE INTERACTION OF RABBIT MUSCLE GLYCERALDEHYDE-3-PHOSPHATE DEHYDROGENASE WITH ALDOLASE.

Aydin Örstan and Ari Gafni (Intr. by Geneva M. Omann) Institute of Gerontology, The University of Michigan, Ann Arbor, Michigan 48109-2007

The interaction of rabbit muscle aldolase with glyceraldehyde-3-phosphate dehydrogenase (GPDH) labeled with fluorescein-5-isothiocyanate (FITC) has been investigated at 25°C in 10 mM Tris buffer, pH 7.5. The addition of at least 10 fold excess of aldolase to 0.4 μM labeled GPDH (GPDH-FITC) increases the fluorescence emission and polarization of FITC over a period of several hours. If 0.4 M GPDH-FITC is incubated with either 1 mM NAD or ADP, the fluorescence of FITC increases while the polarization, initially at a value of 0.17-0.19, decreases to a final value of 0.09-0.11. Since ADP is known to induce the dissociation of GPDH tetramers, at high concentrations NAD appears to have a similar effect on the tetrameric structure of GPDH-FITC. The subsequent addition of aldolase to a solution of GPDH-FITC incubated with either NAD or ADP increases the polarization with no significant effect on the fluorescence. The second order rate constant obtained under these conditions is larger than that obtained in the absence of the nucleotides. These results indicate that the mechanism of the interaction of the enzymes is complex, possibly involving the dissociation of GPDH into dimers. Fluorescence quenching experiments indicate that the availability of FITC to the quencher tryptophan increases during the first 20 minutes of the interaction of aldolase with GPDH-FITC and remains constant as the formation of the complex progresses further. This result and the lack of an interaction between aldolase and free fluorescein indicate that the formation of a complex between the two enzymes is unlikely to be mediated by FITC.

Tu-Pos263 TRANSIENT ELECTRIC BIREFRINCENCE OF MYOSIN ROD AND LMM

James F. Curry, Sonja Krause,Department of Chemistry, Rensselaer Polytechnic Institute, Troy, NY 12180-3590

Transient electric birefringence measurements were made on rabbit striated muscle myosin rod and light meromyosin, LMM. The specific Kerr constant, K_{sp}, of LMM was measured in solutions of 2 mM pyrophosphate with 0 to 0.1 M added KCL. The observed decrease in K_{sp} with increasing salt concentration will be discussed. The rotational relaxation time, τ, for LMM in 2 mM pyrophosphate was measured in the temperature range 5-40°C. $\tau_{20,w}$, the τ values corrected to 20°C in water, was 5.5 μ seconds in this temperature range, indicating a rigid rod with no denaturation or change in flexibility up to 40°C. In studies on myosin rod, two relaxation times were found, 19 μ seconds and 33 μ seconds, for lyophilized rod dissolved in 2 mM pyrophosphate at 20°C. After 36 hours of dialysis against 2 mM pyrophosphate however, a single relaxation time, 25 μ seconds, was found. These results indicate that the flexibility of the rod changed after dialysis, and that the elution of a low molecular weight species from the dialysis is probably responsible. This indicates that the adsorption of a low molecular weight species is probably responsible for the variations in flexibility of intact myosin from different sources observed previously. [S. Krause and K. Thallam, Abstract. W-Pos-167, Biophys. J. 49(2, pt.2)500].

Tu-Pos264 EFFECT OF IONIC STRENGTH ON TOBACCO MOSAIC VIRUS TITRATIONS,

Ragaa A. Shalaby[1] and D.L.D. Caspar[2], [1]Point Park College, Pittsburgh, PA 15222 and [2]Rosenstiel Basic Medical Sciences Research Center, Brandeis University, Waltham, MA 02254.

Hydrogen ion titration experiments were performed on deionized tobacco mosaic virus in KCl and in $CaCl_2$ solutions at 20°C. This was done at a range of KCl concentration between 10^{-3} and 2×10^{-1} molar. For the titrations carried out in $CaCl_2$, the concentration of $CaCl_2$ covered the range from 10^{-3} to 10^{-1} M. H^+ ion binding was studied as a function of pH between pH 3.0 and pH 8.5. For data analysis, pH 4.0 was arbitrarily taken to represent zero hydrogen ion binding. The number of hydrogen ions bound per protein monomer (H^+/m) for different ionic strengths was calculated and a maximum difference of about 1.7 H^+/m between TMV in 10^{-1} M KCl and TMV in 10^{-3} M KCl was observed. This difference occurred at a pH value between 5.5 and 6.0 and decreased to about 1.2 H^+/m at pH 7.0 and stayed approximately constant until pH 8.5. A similar pattern was obtained in $CaCl_2$ solutions except that the maximum difference of 1.6 H^+/m occurred at about pH 5.0 and went down to about 0.8 H^+/m at pH 6.5 to pH 8.5. When the titration in KCl was compared with the titration in $CaCl_2$, a maximum difference of 1.8 H^+/m occurred between pH 6.0 and pH 7.0. This difference dropped down to about 0.2 H^+/m at pH 8.5. When titrations carried out on TMV in double distilled water were compared with titrations on deionized TMV in 0.01 M KCl, a difference in H^+/m that increased with increasing pH to a maximum value of about one was observed at pH 8.5. These data indicate that alteration in electrostatic interactions due to changes in the ionic environment may lead to large shifts in the pK of the H^+ ion binding groups in the virus particle. The data also show a competitive binding of H^+, K^+ and Ca^+ to the same sites on TMV.

Tu-Pos265 THE REVERSIBLE FOLDING OF AVIDIN AFTER DENATURATION WITH GUANIDINE THIOCYANATE.

Paul Horowitz, Gerry Gitlin, Edward A. Bayer and Meir Wilchek, Department of Biochemistry, The University of Texas Health Science Center, San Antonio, Texas 78284 and The Weizmann Institute of Science, Department of Biophysics, Rehovot, Israel

Avidin, the biotin binding protein from egg white, is a remarkably stable protein. The concentration of denaturant giving half denaturation, D(½), =4.7M for guanidine hydrochloride. The protein renatures but displays hysteresis at high protein concentrations, and the D(½) for renaturation =2M. Further, the avidin-biotin complex is not denatured by 6M guanidine hydrochloride at 25 C. Denaturation studies were performed using guanidine thiocyanate, GdnHSCN, and followed with fluorescence with low avidin concentrations (70 μg/ml). On denaturation, the apparent maximum of the intrinsic fluorescence shifted from about 332 nm to 352 nm. In the absence of biotin, the denaturation was found to be fully reversible and gave D(½)=0.5 M. Avidin denaturation showed strong hysteresis when the experiments were performed in the presence of the specific ligand, biotin. The avidin-biotin complex denatured with D(½)=3.5 M and renatured with D(½)=1.35 M. The apparent irreversibility at high protein concentrations may be due to association of intermediates that kinetically limit refolding. The avidin-biotin complex may represent a species that is kinetically more stable, which would be in keeping with suggestions placing the biotin binding site at the interface between two subunits. (Supported by NIH grant GM25177 and Welch grant AQ723 and the Erna and Jacob Michael Foundation at the Weizmann Institute, Rehovot, Israel.)

Tu-Pos266 GENERATION OF A SUBSTRUCTURE LIBRARY FOR DESCRIBING PROTEIN CONFORMATION, S.J. Prestrelski Mount Sinai School of Medicine, New York, N.Y., A.L. Williams, Jr., ImClone Systems, New York, N.Y., M.N. Liebman, AMOCO Technology Co., Naperville, IL 60566

Experimental observations from Fourier-transform infrared spectroscopy indicate the potential for the high-resolution observation of protein secondary structure from analysis of the Amide I, II and III transitions. The resolving capability reveals bands beyond those assigned to the traditional conformations, e.g. helices, sheets and turns, etc. To expand our ability to describe the secondary structure of a protein and to develop discreet assignments in FT-IR, we have used the dynamic programming method of Williams and Liebman, based on the Linear Distance Function (Liebman), to develop a library of the substructures which can be observed within the proteins whose three-dimensional structure has been observed by x-ray crystallography. The construction of this library has been achieved using a pattern recognition capability which functions independent of template-bias and has successfully shown that its members can describe more than 95% of all known protein conformation The algorithm utilizes the linear distance function and a backbone dihedral angle computation. The initial test set was based on an analysis of the serine proteases from both eukaryotic and prokaryotic sources, and was further extended to all known protein structures. It is anticipated that the library will prove of use in correlation of other spectral and physico-chemical properties which can be experimentally determined.

Tu-Pos267 PREDICTED THREE DIMENSIONAL STRUCTURES FOR THE BOVINE CASEINS.
T. F. Kumosinski, J. J. Moscow, E. M. Brown and H. M. Farrell, Jr., USDA, ARS, Eastern Regional Research Center, 600 East Mermaid Lane, Philadelphia, Pennsylvania 19118.

Three-dimensional (3-D) structures derived from X-ray crystallography are extremely important in elucidating structure-function relationships for many proteins. However, not all proteins can be crystallized. The caseins of bovine milk are one class of noncrystallizable proteins (α_{s1}-, κ-, and β-). The complete primary and partial secondary structures of these proteins are known, but homologous proteins of known crytallographic structure cannot be found. Therefore, sequence-based predictions of secondary structure were made and adjusted to conform with global secondary structures determined by Raman and FTIR spectroscopy. With this information 3-D structures for these caseins were constructed using the Sybyl-Mendyl molecular modeling programs. The κ-casein structure contained two stranded β-sheets and one unstranded β-sheet; all are predominantly hydrophobic and capable of forming quaternary structural interaction sites with α_{s1}-casein. The α_{s1}-casein structure contained a hydrophobic and a hydrophylic domain connected by a reverse β-turn as determined from electrostatic potential maps. The α_{s1}- and κ- structures were compact, unlike β-casein which yielded an open structure with a radius of gyration of 34.8 Å. All structures were refined using the Kollman Force Field Energy Minimization calculation. Refined and unrefined structures are compared using electrostatic potential maps and other modeling representations. Small-angle X-ray scattering theoretical curves were calculated for comparison with future experimental results. All unrefined structures showed good agreement with global biochemical and structural information concerning the caseins.

Tu-Pos268 PROTEIN STRUCTURE PREDICTION BY USING CONSTRAINED DYNAMIC PROGRAMMING ALGORITHM. Istvan P. Sugar, Sandor Vajda, Charles DeLisi
Department of Biomathematical Sciences, Mount Sinai Medical Center, New York 10029

We explored a combinatorial approach to find low-energy conformations of polypeptide chains or small proteins. By means of this new algorithm the prediction of polypeptide backbone structures is two orders of magnitude faster than with other minimization methods. Incorporation of constraints imposed by NMR data (e.g. NOE distances, vicinal spin-spin coupling) and the statistical analysis of the available protein structural data (e.g. empirical Ramachandran plots), further reduces the computational effort.
The method, based on a generalized discrete dynamic programming algorithm, can avoid trapping in local energy minima and the problem of atomic overlaps. The method of unconstrained dynamic programming has been used to determine low-energy structures of 6 to 20 residue long polypeptides, while the structure of the small 58 residue long protein, called Basic Pancreatic Trypsin Inhibitor, has been determined by the constrained dynamic programming algorithm.

Tu-Pos269 SECONDARY STRUCTURE PREFERENCES OF AMINO ACIDS IN PROTEINS AS ANALYTICAL FUNCTIONS OF LOCAL HYDROPHOBICITY IN THE PRIMARY STRUCTURE. Davor Juretic, Laboratory of Cell Biology, NHLBI, NIH, Bethesda, MD 20892 and Byung-kook Lee, Physical Sciences Laboratory, Division of Computer Research and Technology, NIH, Bethesda, MD 20892.

We express secondary structure preferences of amino acids in proteins as analytical functions of (i) solvent accessible surface area, (ii) area buried upon folding, and (iii) hydrophobicity of their primary structure neighbors. Although the 3 physico-chemical parameters considered here are all related to hydrophobicity, we find important differences among the three functional dependencies. Preference for α-helix structure increases for all amino acids whose primary sequence neighbors can bury more of their solvent accessible surface area during the protein folding process. Increased preference for α-helix conformation is generally not found in the presence of more hydrophobic neighbors. These results do not depend on the choice of proteins of known X-ray structure that are analyzed to find preferences. The implications for protein folding and for secondary structure prediction algorithms are discussed.

Tu-Pos270 TITLE: MOLECULAR TOPOLOGY OF MULTI-DISULFIDE POLYPEPTIDE CHAIN.

AUTHOR: Boryeu Mao, Computational Chemistry, The Upjohn Company, Kalamazoo, MI 49001.

ABSTRACT: Molecular topology of the polypeptide chain in a stable folded protein is characterized from analyzing the graph representation of molecular covalent structure and the embedding of such a graph. The subset of topologies which do not contain knotted structures is enumerated and classified for some graphs. It is also conjectured that topologies of the polypeptide chain in a folded protein can be represented by such a subset. Thus, for any polypeptide chain containing three or fewer disulfides, there is only one topology. For some four-disulfide and some five-disulfide chains, their covalent structure graphs are intrinsically non-planar (of genus 1), and several molecular topologies would be allowed in each case: two allowed topologies for a non-planar four-disulfide case, and two to six for a non-planar five-disulfide case. The allowed molecular topologies for non-planar polypeptides belong in two families, D and L. Only one of the allowed topologies will represent the stable folded tertiary structure of a protein; e.g., variant 3 toxin from North Americal scorpion Centruroides sculpturatus Ewing, a non-planar four-disulfide protein, has the D-topology. The existence of multiple possibilities for the molecular topology of non-planar polypeptide chains also indicates that the correct prediction of molecular topology must be a criterion for any scheme that predicts tertiary structure of these proteins.

Tu-Pos271 AB INITIO FORCE FIELDS OF GLYCINE AND ALANINE DIPEPTIDE IN C_5 AND C_7 CONFORMATIONS

T.C. Cheam and S. Krimm, Biophysics Research Division, University of Michigan, Ann Arbor, MI 48109

Valid force fields for peptides are important in calculating dependable vibrational frequencies and in developing reliable potential functions for molecular dynamics studies. We have done ab initio calculations of the quadratic force fields and dipole moment derivatives of the dipeptides $CH_3CONHCHRCONHCH_3$ (R=H, CH_3) in a total of five conformations. These conformations, which were optimized by Schafer and coworkers [J. Chem. Phys., 76, 1439 (1982); J. Am. Chem. Soc., 105, 3438 (1983)], are the C_5 and C_7 structures, respectively with five- and seven-membered intramolecular NH•••OC hydrogen bonds: C_5 and C_7^{ax} for Gly dipeptide; C_5, C_7^{eq}, and C_7^{ax} for Ala dipeptide. The split-valence 4-21 Gaussian basis set was used, and the force constants were scaled using scale factors derived by Fogarasi and Balázs [J. Mol. Struct., 133, 105 (1985)] for small amides, with minor changes. The differences in the force constants, harmonic frequencies, dipole derivatives, and infrared intensities among the conformations and within each conformation will be discussed and related, where possible, to differences in hydrogen bonding and structure. In particular, the NH and CO stretch and bend force constants and dipole derivatives show trends that can be correlated with the C_5 and C_7 hydrogen bonds. The force constants and dipole derivatives show that, of the three Ala dipeptide conformers, the C_7^{ax} hydrogen bond is the strongest, in agreement with the NH•••OC geometries, even though the SCF energy of this conformer is the highest. These studies also provide insights into the dependence of force field on conformation. This research was supported by NSF grants DMB-8517812 and DMR-8806975.

Tu-Pos272 DYNAMICS OF TRYPTOPHAN-47 IN VARIANT-3 SCORPION NEUROTOXIN.
Christopher Haydock, Salah S. Sedarous and Franklyn G. Prendergast. Department of Biochemistry and Molecular Biology, Mayo Foundation, Rochester Minnesota 55905.

The indole sidechain of variant-3 scorpion neurotoxin tryptophan-47 is on the solvent exposed side of an antiparallel beta sheet. Neighboring TRP-47 on this exposed surface are three aromatic residues, which are part of a conserved-hydrophobic band, and two glutamic acid side chains. Molecular dynamics calculations indicate that on a picosecond time scale these neighboring groups constrain TRP-47 to fairly small wobbling motions, but that on longer time scales they can participate in slow rotational motions of TRP-47. Starting from the crystallographic positions the neighbors can be sufficiently displaced to allow rotation of TRP-47 into a flipped conformation with a relative free energy of about 3 kcal/mole. The rotational motion of TRP-47 and concomitant displacements of neighbors occur on the nanosecond time scale and longer. We are currently developing a Brownian dynamics simulation, which includes both slow and fast time scale motions, to model both the anisotropy decay and multiple lifetimes of TRP-47 fluorescence in the scorpion neurotoxin. This work is supported by ONRNK 00014-86-K-0521 P00001.

Tu-Pos273 DISULFIDE BRIDGE CONFORMATION FROM RAMAN SS AND CS STRETCH FREQUENCIES CHARACTERIZED BY AB INITIO FORCE FIELD NORMAL MODE CALCULATIONS
W. Zhao, J. Bandekar, and S. Krimm, Biophysics Research Division, University of Michigan, Ann Arbor, MI 48109

Using a 3-21G* basis set, ab initio optimized geometries and force constants have been obtained for CH_3SSCH_3 (1), $CH_3SSC_2H_5$, and $C_2H_5SSC_2H_5$. By adjusting 11 force constant scale factors, 63 observed frequencies of these 3 molecules could be very well fitted in a normal mode refinement procedure. These results indicate that there is a much more complex dependence of ν(SS) and ν(SC) on χ(SS), χ(SC), and χ(CC) than had been predicted by previous studies. We also show how local symmetry of the disulfide bridge can be identified from the Raman spectrum. When combined with our empirical polypeptide force fields (2), it is possible to calculate the vibrational frequencies of disulfide bridges in peptides and proteins, thus enabling detailed analyses of their conformations from Raman spectra. We present an example of such a calculation for cyclic(Cys-Gly-Pro-Phe)$_2$ (3).
This research was supported by grants from Monsanto Co. and NSF (DMB-8517812).
1. W. Zhao, J. Bandekar, and S. Krimm, J. Am. Chem. Soc. 110, 6891 (1988).
2. S. Krimm and J. Bandekar, Adv. Protein Chem. 38, 181 (1986).
3. K.D. Kopple, Y.-S. Wang, A.G. Cheng, and K.K. Bhandary, J. Am. Chem. Soc. 110, 4168 (1988).

Tu-Pos274 DEMONSTRATION OF A CLASS OF STERICALLY RESTRICTED BINDING SITES FOR SATURATED SHORT-CHAIN FATTY ACID ANIONS ON HUMAN ALBUMIN BY DIFFERENTIAL SCANNING CALORIMETRY (DSC).
Andrew Shrake, FDA, Bethesda, MD 20892 and Frederick P. Schwarz, NBS, Gaithersburg, MD 20899

Stabilization of albumin monomer by fatty acids has been studied as a function of ligand chain length and concentration by DSC. Maximum increase in denaturation temperature (T_d) for each ligand relative to that for ligand-free protein (ΔT_d^{max}) increases monotonically from C_4 through C_9, which affords the greatest ΔT_d^{max}, 23 °C. With increase in chain length beyond C_9, ΔT_d^{max} decreases monotonically. This is due to the relative magnitudes of free energies of ligand binding to folded and unfolded protein forms and does not derive from any unique structural attributes of C_9; both free energies of binding become more negative with increasing chain length.

With decrease in chain length from C_4, ΔT_d^{max} increases with C_3 and with C_2 such that a local maximum occurs in ΔT_d^{max} with C_2. Enthalpy of denaturation vs. chain length shows similar behavior. Furthermore, number of ligand binding sites, determined from the dependence of T_d on ligand concentration (J. Biol. Chem. 258, 13193 (1983)), vs. chain length also shows a local maximum with C_2 thereby suggesting a class of sterically restricted binding sites for C_3 and shorter. Data in the presence of 30 mM C_8 with increasing levels of C_2 demonstrate that at >1.1 M C_2, T_d is greater than without C_2 and that at >1.6 M C_2, T_d is greater than T_d attained with any concentration of added C_8 alone. This increased stability with C_2 derives from the occupancy of binding sites that are inaccessible to C_8. A control experiment substituting C_5 for C_2 shows no stability increase.

Tu-Pos275 BINDING OF HYDROPHOBIC LIGANDS TO PEANUT AGGLUTININ, Eugene J. Zaluzec, Marianne Yung, Opinya A. Ekabo, Stephen F. Pavkovic, and Kenneth W. Olsen, (Intr. by Duarte Mota de Freitas) Department of Chemistry, Loyola University of Chicago, 6525 N. Sheridan Road, Chicago, IL 60626.

The binding of cytokinin analogs to legume lectins suggest their possible involvement as phytohormone regulators (Roberts, D.D., and Goldstein, I.J. (1983) J. Biol. Chem. 258, 13820-13824). The hydrophobic binding of benzylaminopurine (BAP), adenine (AD), and adenosine (ADO), to the plant lectin peanut agglutinin (PNA) was studied by fluorometric titrations. Scatchard analysis of ligand induced quenching of the protein fluorescence by BAP, AD, and ADO gave dissociation constants of 33.3, 88.8, and 70.8 micromolar, respectively. Affinity labeling of the adenine binding site for lima bean and kidney bean lectins has recently been done (Maliarik, M.J., and Goldstein, I.J. (1988) J. Biol. Chem. 263, 11274-11279). Using the coordinates for concanavalin A, molecular modeling of the labeled region suggests a site for the hormone-protein interaction. In order to more fully describe the binding of hydrophobic ligands to plant lectins, a crystallographic analysis of PNA has been begun. Native crystals of PNA with unit cell dimensions of a=130 A, b=127 A, and c=78 A, in the orthorhombic space group $P2_12_12$ have been grown in the absence of a hydrophobic ligand (Olsen, K.W., and Miller, R.L. (1982) FEBS Lett. 145, 303-306). Crystals of PNA grown under similar conditions but in the presence of BAP are found to be different. Preliminary crystallographic results for the BAP-PNA complex will be presented. (Supported by a Biomedical Research Support Grant from NIH.)

Tu-Pos276 EXPERIMENTS ON THE THERMAL DENATURATION OF ββ TROPOMYOSIN CROSS-LINKED SELECTIVELY AT C-36. Marilyn Emerson Holtzer, William Clay Bracken, and Alfred Holtzer, Department of Chemistry, Washington University, St. Louis, MO 63130.

Each polypeptide chain of ββ-tropomyosin, a two-chain, coiled-coil protein, has 284 residues and two cysteines: C36 and C190. Thus, three crosslinked coiled-coil species are possible: crosslinked at C36-only (β_β); crosslinked at C190-only (β⁻β); and crosslinked at both sites (β⁻_⁻β). Schemes for production of β⁻β and of β⁻_⁻β species have been described earlier and their thermal unfolding curves (fraction helix from CD vs. T) have been investigated. A new scheme is described for production of the third crosslinked species, β_β. The scheme begins with skeletal muscle tropomyosin a mixture of, predominantly, αα and αβ species. Each α-chain has only one cysteine at C190. The scheme involves reversible blocking of C36 of the β-chains by carbamylation of C190-crosslinked skeletal muscle tropomyosin, followed by reduction of the crosslink, then permanent blocking of all C190s by carboxyamidomethylation, then decarbamylation and crosslinking at C36 to form the desired β_β species. Thermal unfolding curves are reported for the β_β product and its DTT-reduced form. The latter unfold much like the parent ββ noncrosslinked species. The β_β crosslinked species unfolds in a monophasic, cooperative transition with a melting temperature between the pretransition and posttransition shown by its β⁻β counterpart. Comparison of unfolding of all three crosslinked species is made in the light of two extant physical models. The all-or-none-segments model is qualitatively in disagreement with the data. The continuum-of-states model is qualitatively in accord and the general features of the β_β transition were predicted in advance by a theory based on that model. The availability of the three individual species makes possible unequivocal assignment of their mobilities on SDS/PAGE. They are, in order: β⁻_⁻β (fastest), β_β, β⁻β. This assignment reveals the presence of β⁻_⁻β species in crosslinked rabbit skeletal muscle tropomyosin in amounts consistent with random association of the *in vivo* population in which α chains outnumber β by four to one. The latter conclusion is contrary to presently accepted ideas.

[Supported by Institute of General Medical Sciences, US PHS and by Muscular Dystrophy Association.]

Tu-Pos277 COMPARATIVE PHYSICAL CHARACTERIZATION OF OXIDIZED AND REDUCED FORMS OF *E. COLI* GLUTAREDOXIN AND THIOREDOXIN. V.A. Sandberg, B. Kren, J.A. Fuchs and C.K. Woodward, Department of Biochemistry, University of Minnesota, St. Paul, MN 55108

E. coli glutaredoxin is a small (9700 dalton) redox active protein that appears to be important to basic cellular metabolism. It was discovered as a functional analog of the enzyme thioredoxin (11500 dalton) and may have similar three-dimensional structure although the two share no appreciable sequence homology outside the active site. Both contain an active site disulfide comprised of the only two cysteines in the molecule, separated by two amino acid residues. While both exhibit nearly identical isoelectric points, we find a difference in their electrophoretic mobilities on native gels at high pH which reflects a charge difference that may be mechanistically important. Despite their functional and apparent structural similarities, glutaredoxin is a much less stable protein. The temperature-induced unfolding/folding thermodynamics of glutaredoxin was monitored at various pH's by circular dichroism. At neutral pH oxidized glutaredoxin (with the active site disulfide intact) and reduced glutaredoxin (with the active site cys residues in the SH form) are equally stable. In contrast, oxidized thioredoxin is much more stable than reduced thioredoxin. For glutaredoxin, the temperature at the midpoint of the unfolding, T_m, is significantly below that of even reduced thioredoxin. Chemical denaturation of glutaredoxin was also investigated, using urea gradient gels. In urea denaturation reduced glutaredoxin is less stable than oxidized glutaredoxin. To facilitate these studies we developed an overexpression system capable of producing gram quantities of glutaredoxin from 20 liters of cells, and have refined the purification process to produce homogeneous glutaredoxin.

Tu-Pos278 DIFFERENCES IN THERMAL STABILITY BETWEEN REDUCED AND OXIDIZED CYTOCHROME b_{562}. Mark T. Fisher (Intr. by Earl R. Stadtman), Laboratory of Biochemistry, National Heart, Lung, and Blood Institute, National Institutes of Health, Bethesda, MD 20892.

The thermal stability of ferric and ferrous forms of cytochrome b_{562} were examined. Thermally induced changes in the heme environment and tyrosine residues (2) located in close proximity to the heme binding site were followed by absorption and second derivative spectroscopies, respectively. All observed thermal transitions were independent of scan rate (0.5 to 2°C/min) and the denatured protein exhibited partial reversibility upon return to ambient temperature. Since slow decomposition of the protein structure as evidenced by aggregation is only observed above the transition temperature (T_m) for oxidized and reduced species, the thermal transitions are assumed to be reversible and equilibrium thermodynamics were applied. All thermally induced spectral changes fit a simple two-state model. Examination of the thermal transition for the ferrous form of the cytochrome yielded Tm and the van't Hoff enthalpy (ΔH_{vH}) values of 82°C and 250 kcal/mole, respectively. In contrast, T_m and ΔH_{vH} values obtained for the oxidized form of the protein were 68°C and 118 kcal/mole. The enhanced thermal stability of the ferrous form of this cytochrome suggests that there are substantial protein structural changes accompanying reduction of the heme moiety.

Tu-Pos279 STABILITY AND ASSEMBLY OF YEAST CYTOCHROME *c* OXIDASE. P. Morin, D. Diggs, D. Montgomery, C. Gabel, and E. Freire. Department of Biology, The Johns Hopkins University, Baltimore, Maryland 21218.

The formation of functionally active integral membrane protein assemblies involves membrane insertion, folding and subunit association. The details and thermodynamic basis of these events are still not completely understood. We have started the investigation of the assembly process of the mitochondrial enzyme, cytochrome *c* oxidase from yeast. Cytochrome *c* oxidase is a multisubunit protein composed of mitochondrially (I-III) and cytoplasmically (IV-VII) synthesized subunits. The yeast enzyme has been purified and reconstituted into phospholipid vesicles in active form. These preparations have been used to assess the temperature dependence of the stability and the electron transfer activity of the enzyme. High sensitivity differential scanning calorimetry in conjunction with differential solubility thermal gel analysis of the membrane reconstituted cytochrome *c* oxidase are being used to characterize the energetics of unfolding and to identify the subunits involved at each stage of the overall process. The calorimetric unfolding profile of the DEPC reconstituted enzyme is characterized by a complex peak with a maximum centered at 60.7 at 45°C/h and a broad shoulder on the low temperature side of the transition. The transition is composed of a minimum of three major components (A, B, C) preliminarily identified as originating from subunits III (A), IV and VI (B), and subunits I and II (C). Except for subunits IV and VI, the unfolding of the enzyme is irreversible. At 70°C the passage of the unfolded enzyme to the irreversible state is characterized by a relaxation time of ~5 sec as determined by the rate of irreversible enzymatic inactivation. Subunits IV and VI of yeast cytochrome *c* oxidase can be dissociated from the enzyme complex by incubation at or above the transition temperature of the enzyme. Upon dissociation, subunits IV and VI partition into the aqueous medium indicating that these subunits have a significant degree of water solubility and that they are most likely peripherally associated to the enzyme complex and/or only partially inserted into the membrane. Preliminary data indicates that after dissociation, subunits IV and VI exhibit both temperature induced denaturation as well as isothermal solvent induced denaturation in aqueous solution. These experiments suggest that the folding of these subunits does not require prior attachment to the rest of the enzyme or to the membrane. (Supported by NIH grant GM-37911.)

Tu-Pos280 INFLUENCE OF α-HELICAL STRUCTURE ON DEAMIDATION OF ASPARAGINE RESIDUES. Cynthia L. Stevenson, Mark C. Manning, and Ronald T. Borchardt, Department of Pharmaceutical Chemistry, University of Kansas, Lawrence, KS 66045.

Chemical degradation of protein drugs is of major concern in the pharmaceutical industry. Deamidation of asparagine is one such degradation process, yielding aspartate (Asp) or its β-carboxy-linked isomer, isoaspartate (i-Asp), as the products. Peptide models are being developed to evaulate the role of secondary structure in modulating this reaction. In order to ascertain the influence of an α helix upon deamidation, we have prepared the hexadecapeptide, Glu-Leu-Thr-Ala-Ala-Asn-Ala_7-Thr-Ala-Arg, **1**. This sequence corresponds to the C-terminal portion of the antifreeze protein from Antarctic winter flounder. X-ray crystallographic studies have shown this protein to be entirely α-helical[1]. The hexadecapeptide, **1**, has been characterized by circular dichroism and ^1H NMR spectroscopy. Conformational energy calculations predict that while **1** and the Asp-containing product should retain helical structure, the i-Asp product and the succinimide intermediate should greatly disrupt the α helix. Results on the conformation and stability of **1** will be presented.

1. Yang, D.S.C. et al. *Nature* **1988**, 333, 232-237.

Tu-Pos281 SOLUTION AND LIPID-BINDING PROPERTIES OF SHORT α-HELICAL PEPTIDES. Larry R. McLean, Karen A. Hagaman, Thomas J. Owen, and John L. Krstenansky. Merrell Dow Research Institute, Cincinnati, OH 45215

Secondary structure is not typically observed for small peptides in solution. A series of model amphipathic α-helical peptides (MAPs) with primary structures that utilize all known factors important for α-helical stabilization were synthesized. The peptides are based on the repeating eleven amino acid sequence, Glu-Leu-Leu-Glu-Lys-Leu-Leu-Glu-Lys-Leu-Lys, referred to as MAP_{1-11}. The circular dichroic (CD) spectra of these peptides in aqueous buffers gives evidence for more α-helical content than has been reported for any peptide < 18-residues. This α-helical tendency does not require the presence of lipid or reduced temperature. For instance, Suc-[Trp^9]-MAP_{9-3},,amide, a 17-residue peptide, has 100% and 80% α-helical contents at 0.17 mM and 0.017 mM, respectively; Suc-[Trp^9]-MAP_{2-11}amide, a 10-residue peptide, has 51% α-helical content at a concentration of 0.17 mM in 0.1 M phosphate buffer at room temperature. The latter peptide effectively disrupts liposomes of dimyristoylphosphatidylcholine (DMPC) at 24°C, forming clear micelles. The single tryptophan residues on the MAP peptides were used to monitor the kinetics of association of the peptides with lipid. For peptides of 10-residues or greater, the rate of disruption of liposomes was inversely related to the α-helical content of the peptides in solution.

Tu-Pos282 STABILIZATION OF α-HELICITY IN BOVINE GROWTH HORMONE FRAGMENTS. Jody L. Tuls, S. Russ Lehrman, and Marilyn Lund (Intro. by H.A.Havel)
Control Division, The Upjohn Company, Kalamazoo, Michigan 49001

Porcine growth hormone, an antiparallel four helix bundle protein, is 91% homologous with bovine growth hormone (bGH), suggesting that the latter protein has a similar tertiary structure (1). We are interested in determining if peptide fragments of bGH which span helical regions of the intact protein retain helicity in the absence of long-range, stabilizing interactions. It has previously been shown that [96-133]-bGH (corresponding to helix 3 of the intact protein) forms a stable α-helix in aqueous solution. In this study we report that peptides comprised primarily of helices 1, 2, and 4 of bGH do not form stable α-helices in aqueous solution. However, upon addition of small amounts of trifluoroethanol, [12-34]-bGH and [164-Ser-153-180]-bGH undergo a strong, cooperative transition to helical conformation. Weaker propensities for helix formation are observed for peptides which correspond to helix 2 and non-helical portions of the protein. The amount of α-helix in these peptides has been studied as a function of trifluoroethanol, peptide concentration, sodium chloride, denaturant, and pH. Our results suggest that portions of bGH which are helical in the intact protein have a higher propensity for α-helix formation than other regions of the protein, and therefore could adopt their secondary structure as an early step in the folding process.

(1) Abdel-Meguid, S.S., Shieh, H.-S., Smith, W.W., Dayringer, H.E., Violand, B.N., and Bentle, L.A. (1987) Proc. Natl. Acad. Sci. USA 84, 6434-6437.

(2) Brems, D.N., Plaisted, S.M., Kauffman, E.W., Lund, M., and Lehrman, S.R. (1987) Biochemistry 26, 7774-7778.

Tu-Pos283 SECONDARY STRUCTURE OF HUMAN APOLIPOPROTEIN[a]

J. Guevara, Jr., M. Soma, J.W. Gaubatz, R.D. Knapp, and J.D. Morrisett. Departments of Medicine and Biochemistry, Baylor College of Medicine, Houston, TX 77030.

Plasma concentrations of lipoprotein[a], Lp[a], are highly correlative with cardiovascular disease in man. Apo[a] is an apolipoprotein unique to Lp[a] and may be responsible for its apparent atherogenicity. Apo[a] exists in >9 polymorphic forms with apparent M_r's of 400-900 kD. This polymorphism may be due to differences in the levels of glycosylation and/or size of the polypeptide chains. The sequence of a 503 kD polymorph (4548 amino acids) has been determined by McLean et al. (Nature 330:132, 1987). We have used this primary structure data to predict the secondary structure. Apo[a] appears to contain 2 structural domains: the first 75% of the sequence contains 11 types of repeating structural units (kringles) which, except for two units, consist of 114 residues; and, each unit contains 6 CYS that form 3 intra-kringle disulfides (1-6,2-4,3-5). (Kringles are also abundant in proteins involved in blood coagulation and fibrinolysis). These kringles have very low level α-helical and β-sheet as determined from predictive algorithms. The last 25% of the sequence is predicted to contain short stretches of α-helix and β-sheet. This domain contains a CYS not predicted to be involved in an intra-kringle disulfide and therefore, may be part of the inter-molecular disulfide that links one mole of apo[a] to apoB in Lp[a]. It also contains a potential proteolytic active site. (Supported in part by HL-32971)

Tu-Pos284 GRAND CANONICAL MONTE CARLO CALCULATIONS OF THERMODYNAMIC COEFFICIENTS AND RADIAL DISTRIBUTIONS OF COUNTERIONS FOR DNA OLIGOMER-SALT SOLUTIONS. M. C. Olmsted, C.F. Anderson and M. Thomas Record, Jr., Departments of Chemistry and Biochemistry, University of Wisconsin, Madison, Wisconsin, 53706.

Monte Carlo simulations based on the grand canonical ensemble are used to calculate thermodynamic coefficients and small ion radial distributions for a cell model representation containing a NaDNA oligomer (N-mer) and NaCl. The N-mer is represented as an impenetrable cylinder with N axial point charges uniformly spaced 0.17 nm apart. The goal of this work is to describe at both thermodynamic and molecular levels the approach to the polyelectrolyte limit ($N\to\infty$) and the approach to the Debye-Hückel behavior of an isolated charge. Electrolyte-oligomer interactions are described thermodynamically using the preferential interaction coefficient, Γ, which may be interpreted in terms of the number of Na^+ ions thermodynamically bound per phosphate $(1+2\Gamma)$. Γ has been calculated as a function of salt concentration over the range of oligomer chain lengths $8\leq N\leq\infty$. For $N>16$, we find that Γ is a linear function of $1/N$ at each salt concentration. The crossover in these plots near N=22 divides the regions of approach to simple electrolyte and to polyelectrolyte behavior. The linearity of Γ vs. $1/N$ indicates the utility of a two state model in which each terminal region (of length ~4 charges) has little thermo-dynamic counterion binding and where the interior region behaves thermodynamically like an infinite polyelectrolyte. In addition the local counterion concentration at the surface of the N-mer exhibits a linear dependence on distance from the end of a long N-mer and approaches the local concentration characteristic of the infinite polyelectrolyte at a distance of ~20 charges from each end. Thus the counterion radial distribution function also can be described by a two-state model. (Supported by NIH Grant GM 34351.)

Tu-Pos285 GENERAL PURPOSE NUMERICAL METHOD FOR ANALYZING COMPLEX MULTI-COMPONENT PROTEIN-LIGAND ASSEMBLIES. Catherine A. Royer and Joseph M. Beechem, Dept. of Physics, Laboratory for Fluorescence Dynamics, Univ. of Illinois at Urbana-Champaign, 1110 W. Green St., Urbana, IL 61801.

Allosteric oligomeric proteins are primarily responsible for the regulation of biological activity. Various generalized "Adair-type" equations have been used to analyze the observed ligation processes. We propose here a numerical method which directly solves for the concentrations of all the possible equilibrium species of such multicomponent systems. To perform this analysis, all of the possible subunit and ligand binding equilibria are utilized, each equilibrium having a particular Gibbs free energy. Given this set of simultaneous non-linear Gibbs free energy equations, we use a modified iterative Monte-Carlo algorithm to solve for the concentrations of all the microscopic equlibrium states, and thus all of the various individual and complex binding site isotherms. This technique was first used to examine a monomer-dimer equlibrium system, with one ligand bound per monomer. Very accurate solutions (errors 0.03 Kcal/free energy) can be obtained for these systems in less than 5 mins on an IBM AT type microcomputer. The algorithm has now been expanded to solve the multicomponent equilibria of a monomer/dimer/tetramer system binding four total ligands, with errors less than 0.3 Kcal/free energy. Examination of all the microspecies as a function of ligation state, protein concentration, temperature and pressure, completely characterizes the thermodynamic behavior of these complex systems. Such overdeterminations should aid in unravelling the physical mechanisms of allosteric regulation in multi-subunit macromolecular assemblies. This Monte-Carlo method is being incorporated into a general purpose non-linear analysis program designed to fit various types of spectroscopic data, which vary both ligand and protein concentrations as well as temperature and pressure.(CR: GM39969, JB: Lucille Markey Scholar)

Tu-Pos286 **THE ORIGIN OF THE SUPERPOSITION PRINCIPLE FOR CIRCULAR INTENSITY DIFFERENTIAL SCATTERING BY HIERARCHICAL CHIRAL STRUCTURES**
Laura Ulibarri and *Carlos Bustamante*, Department of Chemistry, University of New Mexico, Albuquerque, NM 87131.

The superposition principle states that the angle-dependent difference in scattering intensities for right and left circularly polarized light is the sum of the contributions from each level taken separately. Analytic expressions describing this superposition are obtained for oriented and rotationally averaged hierarchical chiral structures. It is shown that the superposition principle holds only when the coiling levels in the chiral structure are disparate. In particular, for a structure composed of two chiral levels, the lower order structure must be much smaller than both the wavelength of light and the higher order structure. Numerical calculations using these expressions are carried out for superhelices of varying dimensions. It is shown that the periodicity of each chiral level can be obtained directly from a fourier analysis of the differential scattering patterns.

Tu-Pos287 ANALYSIS OF DYNAMIC LIGHT SCATTERING BY FLEXIBLE MACROMOLECULES

Robert F. Goldstein and Albert S. Benight***

**Computer Center and **Department of Chemistry, University of Illinois at Chicago, Chicago IL 60680.*

We analyze the diffusional motion of flexible macromolecules with an increasingly realistic Rouse-Zimm model, i.e. by modelling the molecule as an arbitrary set of spheres and harmonic springs. Features include 1) nearly arbitrary arrangements of spheres, 2) arbitrary arrangements of translational and torsional springs, and 3) inclusion of torsional damping and various hydrodynamic cross-coupling effects with no additional fitted parameters. The calculation has three phases: 1) compute the inter-sphere diffusion matrix (hydrodynamic interactions), 2) find the Green's function for the appropriate diffusion equation, and 3) compute the appropriate correlation functions to analyze a specific experiment.

The hydrodynamic interactions(1) contain no adjustable parameters other than the radii and positions of the spheres, temperature and viscosity. If two spheres do not overlap, their positions and radii are otherwise unrestricted; if they overlap, they must have equal radii. Rigid body diffusion can be accurately calculated with the same hydrodynamics.

Given the positions, radii, and spring constant matrix, we calculate a full set of three-dimensional diffusional modes, including exact effects of vibrational-translational cross-coupling (i.e. motion along a vibrational coordinate may give rise to a translational force, and vice versa). We treat another form of coupling arising from the dependence of the inter-sphere diffusion matrix upon the internal coordinates of the molecule. This coupling is treated with a controlled approximation to a) improve the accuracy of the calculation, and b) assess the internal consistency of our results.

The diffusional modes are used to construct the Green's function for the diffusion equation and thereby describe general hydrodynamic behavior; we specifically analyze dynamic light scattering and present a comparison with simpler Rouse-Zimm models and with experimental results on dilute solutions of DNA.

(1) R.F. Goldstein *J. Chem. Phys.* **83:** 2390-2397 (1985)

Tu-Pos288 Dynamics of the atoms of polar side chains in the active site of proteins by Brownian dynamics simulations

Koh Yoshinada* and Takeshi Satoh**
* Research Center of Ion Beam Technology, Hosei University, Kajinocho, Koganei, Tokyo 184, Japan
** School of Hygienic Sciences, Kitasato University, Sagamihara, Kanagawa 228, Japan

We are concerned with local motion of the polar groups of side chains, lysine, histidine, and arginine, in the active site of Ribonuclease A and Lysozyme.

Analysis is made based on the harmonic oscillator approximation. The oscillator strength ω_o and the friction cofficient γ are involved as Langevin parameters. The former represents the restoring force constant in the potential of mean force as written by $V(x) = \frac{1}{2}m\omega_o^2(x)^2$. Assignment of the γ value to the positively charged groups of side chains must reflect precisely the degree of exposure of the protein matrix environment to the solvent.[1]

To yield agreement with the simulation results a superposition of two independent modes with different ω_o values is shown to be important.[2] In relation to this implication stabilization is promoted through the formation of hydrogen bonds with the water molecules and possibility of crosslinking between two close-by residues is suggested in some cases.[3]

1) Venable, R. M. and Pastor, R. W. (1988) Biopolymers, 27, 1001-1014.
2) Nadler, W., Brünger, A. T., Schulten, K., and Karplus, M. (1987) Proc. Natl. Acad. Sci. USA, 84, 7933-7937.
3) Brünger, A. T., Brooks III, C. L., and Karplus, M. (1985) Proc. Natl. Acad. Sci. USA, 82, 8458-8462.

Tu-Pos289 **Different ligands stretch the same springs: A quasi-harmonic model of allostery in glycogen phosporylase.** S. Skourtis,* S. R. Sprang,** R. J. Fletterick,*** and W. Bialek* **Departments of Physics and Biophysics, University of California, Berkeley, CA 94720. **Department of Biochemistry and Biophysics, University of Texas, Southwestern Medical School, Dallas TX 75235, ***Department of Biochemistry and Biophysics, University of California, San Francisco, CA 95143.*

The structure of glycogen phosphorylase in its several liganded states is known from X-ray crystallography. Since this is an allosteric enzyme one might have expected effector and substrate molecules to trigger a transition between discrete conformational states such as 'R' and 'T.' Instead the binding of each different ligand changes the conformation of the enzyme in a different way, as if the molecule were continuously deformable; most of the thousands of atoms in the protein move upon ligation. A qualitative examination of these data suggests that every binding event induces a structural change which either reinforces or weakens the changes brought about by other binding events.

A model in which every ligand couples to the same collective vibrational mode of the protein can account for this unusual pattern of structural changes. Quantitatively, we imagine that binding of different ligands applies different forces to the same collective mode, so that the structural changes we observe are in proportion to these forces and correspond to different equilibrium positions along the collective coordinate. Since the different ligands strech the same springs, the contribution of the elastic energy to the binding affinity is cooperative: The forces add but the energies do not. We present quantitative tests of this model through an analysis of the X-ray data. The extent to which a single collective mode fits the pattern of displacements is remarkable — ligand binding events separated by more than 30Å induce structural changes throughout the protein which are correlated at the 70% level. We try to estimate the energies which these simple collective effects can contribute to allosteric interactions, and we compare our picture to previous models for the molecular basis of allostery.

This work supported in part by the National Science Foundation and the National Institutes of Health.

Tu-Pos290 TEMPERATURE DEPENDENCE OF FLUORESCENCE DECAY PARAMETERS OF TRYPTOPHAN IN AQUEOUS SOLVENTS AND IN PROTEINS. Norberto Silva*, Enrico Gratton*, Nicola Rosato#, and Alessandro Finazzi-Agro#. *Department of Physics, Laboratory for Fluorescence Dynamics, University of Illinois at Urbana-Champaign, Urbana, IL 61801. #Department of Biochemistry, University of Rome "Tor Vergata," Rome, Italy.

The temperature dependence of the lifetime of N-acetyl-tryptophan amide and tryptophan shows a simple Arrehenius behavior in aqueous solvent. The values of the activation energy for the process of thermal quenching and the values of the pre-exponential factors have been determined using a global analysis approach over the temperature range from 0°C to 40°C. The same study for a series of single tryptophan proteins over a similar temperature range shows that the decay cannot be analyzed using a single or double exponential decay. The analysis using distribution of lifetime values can provide the temperature behavior of the mean lifetime values as measured by center of the distribution and the spread of lifetime values which characterizes the distribution width. For the proteins studied, the average lifetime value does not follow a simple Arrehenius relationship. Also, the lifetime distributions width shows a signmoidal temperature behavior. Experiments have also been performed at lower temperature using glycerol and ethylene glycol as cosolvents. In this case also, tryptophan and NATA have an Arrehenius behavior while most of the proteins investigated show a complex temperature behavior. These results are discussed in terms of a model for the protein interior which allow for a very large number of substates. Supported by NIH RR03155.

Tu-Pos291 **COMPARISON OF HYDROGEN EXCHANGE BEHAVIOR WITH SUBNANOSECOND DYNAMICS IN THE PROTEIN UBIQUITIN.** **Diane M. Schneider, Martin J. Dellwo and A. Joshua Wand, Institute for Cancer Research, Philadelphia, PA 19111.**

Ubiquitin, a 76 residue protein found in all eukaryotic cells examined to date, is a crucial component of the ATP-dependent proteolytic mechanism. In a complex series of enzymatic events, proteins are targeted for destruction through covalent conjugation to the C-terminus of ubiquitin. The molecular nature of this signalling system is not understood. As part of a comprehensive study of the structure, dynamics and energetics of this protein and its conjugates we are evaluating the relationship between the hydrogen exchange behavior of the exchangeable protons in ubiquitin and the subnanosecond dynamics at these sites. Hydrogen exchange measurements reflect the structural, energetic and dynamical properties of the hydrogen bonds in the ubiquitin molecule. In order to evaluate the dynamical component in this data, we are measuring the relaxation parameters in an ^{15}N-enriched ubiquitin sample. The results from these experiments are interpreted in terms of the model independent theory of Lipari and Szabo. This theory allows us to determine a generalized order parameter and an effective correlation time for each site investigated. The generalized order parameters, which reflect the amplitude of high frequency motion, can be compared with hydrogen exchange rates to determine the extent to which exchange at a particular atomic position is influenced by small amplitude fluctuations. Hydrogen exchange rates for 25 amide protons have been measured at 2 pH values in a series of 2D COSY experiments. These amides map primarily to the 5-strand β-sheet and the α-helix as expected and the rate constants range from minutes to days. Spin-lattice relaxation times and steady-state nuclear Overhauser enhancements for ^{15}N are measured at 2 fields. The internal motions giving rise to the relaxation occur on the subnanosecond timescale.

Tu-Pos292 **A HIGH RESOLUTION ^{13}C and ^{31}P NMR STUDY OF BOVINE CASEIN IN SOLUTION.** **L. T. Kakalis, T. F. Kumosinski and H. M. Farrell, Jr., USDA, ARS Eastern Regional Research Center, 600 E. Mermaid Lane, Philadelphia, PA 19118.**

High-resolution natural abundance $^{13}C\{^1H\}$ (100.4 MHz) and $^{31}P\{^1H\}$ (161.7 MHz) NMR spectroscopy was used to investigate in solution whole casein from milks with different genetic type for the major component ($\alpha_{s1}A$ and $\alpha_{s1}B$). This mutation results in dramatically different physical-chemical properties. In 0.125M KCl casein is in the form of submicelles (MW ~ 10^5KD) whereas in the presence of 15mM Ca^{+2} at 0.125M ionic strength, submicelles self-associate to micelles (MW >1x10^6 KD). The presence of numerous, well-resolved peaks in the tentatively assigned $^{13}C\{^1H\}$ NMR spectra, particularly in the case of submicelles, suggest considerable segmental motion (ns time scale). Micelle formation is manifested as a slight broadening of aliphatic and aromatic carbon peaks, indicating fast motion still exists in these large colloidal particles. This is in agreement with previous SAXS and water ^2H NMR results. Upon Ca^{2+} addition a change in the side-chain carbonyl peak envelope is observed and the Ser βCH_2 peak (66 ppm vs. DSS) is broadened almost beyond detection, indicating possible interaction sites. The $^{31}P\{^1H\}$ NMR spectra are partly resolved, each spectra consisting of 3-6 peaks. The peak pattern varies with the casein form present (submicelle vs. micelle) and the genetic variant. A general downfield chemical shift of ^{31}P resonances is observed upon the addition of Ca^{2+}. Data are consistent with a loose and mobile casein structure with Ser phosphoesters and possibly side-chain carbonyls being the putative sites for calcium binding.

Tu-Pos293 **MOLECULAR DYNAMICS SIMULATION OF SICKLE CELL HEMOGLOBIN - A PRELIMINARY REPORT**

M. Prabhakaran and Michael E. Johnson. Department of Medicinal Chemistry and Pharmacognosy, University of Illinois at Chicago, Chicago, IL, 60680.

A molecular dynamics (MD) simulation has been carried out on the crystal structure of the deoxy sickle cell hemoglobin double strand available from the Brookhaven Protein data bank. MD simulations for 22.5 ps have been carried out on the following systems: a) Human deoxy hemoglobin tetramer to serve as control and for comparison, b) sickle cell hemoglobin tetramer, c) the β chains of the double strand with the lateral contact involving Val 6 responsible for sickle cell anemia, and d) axial contact regions involving (α_1, β_1) of the first tetrameric unit with the (α_2, β_2) of the second tetramer in the same strand. The CHARMM MD algorithm was used to simulate the dynamics with a time step of 0.005 ps. In the trajectory analysis of the last 10 ps simulation, the radius of gyration and anisotropic factor were calculated to find the large scale oscillations of the system under thermal perturbation. The root mean square amplitudes of atomic motions were calculated to locate the flexible interior regions and to understand the dynamics of the contact and axial regions. The time course analysis of hydrogen bonding and hydrophobic bondings (in terms of solvent accessibility) may provide factors responsible for the general stability of hemoglobins and the strength of interactions in the axial and contact regions of sickle cell hemoglobin.

(Supported in part by NIH grant HL23697 and a Chicago Heart Association senior fellowship.)

Tu-Pos294 STRUCTURE AND DYNAMICS OF CHOLINERGIC LIGANDS IN SOLUTION, K.A. McGroddy, G.L. Millhauser* and R.E.Oswald, Department of Pharmacology, NYSCVM, Cornell University, Ithaca, NY 14853 and *Department of Chemistry, University of California at Santa Cruz, Santa Cruz, CA 95064.

Nuclear Magnetic Resonance spectroscopy (NMR) is being used to study the structural elements of an agonist as related to the binding to and activation of the nicotinic acetylcholine receptor (AChR). The importance of various structural features of agonist molecules can be elucidated from single channel recording experiments, but these give no information as to the actual molecular interaction between the AChR and its effectors once they enter the binding site. The use of nuclear Overhauser spectroscopy (nOe and NOESY) allows the determination of the folded conformation of a molecule in solution. This has been used to study the differences in conformation of the molecule in the presence and absence of the AChR. We are applying this technique to analyze the different conformations of molecules with very different agonist behavior in order to determine how changes in the structure of an agonist molecule affect its folding and its interaction with the receptor.

In addition, we have observed interesting internal dynamics in these compounds due to hindered rotation about an internal imide bond. This is analogous to what is observed in the folding of small proteins containing X-Proline imide bonds, and can be studied with variable temperature ^{1}H NMR. Analysis of the lineshapes gives rate constants for the rotation which are then entered into the Arrhenius equation to extract an energy of activation for the process. Studies of these compounds in solvents with very different properties have shown that the rates and the energies of activation for this rotation vary dramatically depending upon the presence or absence of nearby charges, the ability of the solvent to hydrogen bond and also with different concentrations of the molecule being studied.

These studies of cholinergic ligands have the potential to greatly increase our understanding of the preferred conformation of a cholinergic ligand in solution and in the ACh binding site, as well as to provide new ideas about important elements involved in the folding of small proteins.

Tu-Pos295 BROWNIAN DYNAMICS SIMULATION OF THE GLUCAGON SELF-ASSOCIATION PROCESS Huan Xiang Zhou* and Frank Ferrone, Department of Physics and Atmospheric Science, Drexel University, Philadelphia, Pa 19104

The process of glucagon monomer-dimer association is simulated by a two-stage Brownian Dynamics method. With the algorithm of S. H. Northrup et al (1984, J. Chem. Phys., 80:4448), rate constants are calculated. For the glucagon self-association system, the only pertinent direct force is provided by hydrophobic interactions. With short range hydrophobic interactions, the rate constant is found to be 3.6×10^7 $M^{-1}s^{-1}$. This is an order of magnitude smaller than the rate constant deduced from NMR measurments (M. E. Wagman, 1981, Ph. D. Thesis, Harvard University), 3.2×10^8 $M^{-1}s^{-1}$. F. Franks (1975, in *"Water, a Comprehensive Treatise"*, 4:1-94) has proposed a long range hydrophobic interaction model. Recently J. N. Israelachivili et al (1988, Science, 241:795) experimentally confirmed that hydrophobic interactions are indeed long-ranged, decaying exponentially with distance, with a characteristic distance of about 10Å. Using the empirical parameters determined by Israelachivili et al, the rate constant found in this simulation rises to 2.6×10^8 $M^{-1}s^{-1}$, and is in excellent agreement with Wagman's experimental results.

* Present Address: Laboratory of Chemical Physics, NIH, Bethesda, MD 20892

Tu-Pos296 CRYSTAL AND MOLECULAR STRUCTURE OF PERPHENAZINE: CONFORMATIONAL VARIABILITIES OF THE PHENOTHIAZINE RING. T. Srikrishnan, Center for Crystallographic Research, Roswell Park Memorial Institute, 666 Elm Street, Buffalo, New York 14263.

Perphenazine (2-chloro-10-(3-[4-(2-hydroxyethyl)piperazin-1-yl]propyl) phenothiazine (P) is a tranquilizer used primarily in the treatment of psychotics. It is antiemetic and is used as an anesthetic in veterinary medicine. It is a more potent neuroleptic drug than chloropromerzine but has less sedative and adrenolytic properties. Crystal structure of P has been undertaken to study the conformation of the molecule in the solid state and to compare the conformation of the phenothiazine ring in this structure with several other drugs having the phenothiazine moiety. Crystals of P (water/propanol) are triclinic, space group, P1, with a = 8.149(2), b = 11.879(2), c = 12.093(2)Å, α = 60.49(1), β = 89.54(2), γ = 89.98(2), V = 1018.9Å^3, Z = 2, D_o = 1.32 g/c.c., D_c = 1.317 g/c.c. The structure was solved with CAD-4 data (4287 reflections, 2267 $\geq 3\sigma$) using the SHELX-86 programs and refined to a final R value of 0.059. There are two independent molecules in the asymmetric unit, each with slightly different conformations. The dihedral angle between the planes of the butterfly tricyclic system is 142° and 138° in the two molecules whereas it is 141° in the published monoclinic form of P. The C-S-C angle in the tricyclic groups are 97° and 100°, and the C-S distances are 1.707 and 1.738Å. The piperazine has the chair conformation. An analysis of the phenothiazine conformation in the different structures solved to date shows a conformational variability in the dihedral angle between the tricyclic systems (134 to 155°). Work supported by ACS-IN54W8, New York State Dept. of Health and in part NIH-GM24864.

Tu-Pos297 THERMALLY INDUCED HELIX-COIL TRANSITION OF IRRADIATED POLY [d(A-T)·d(A-T)] AND POLY [d(A)·d(T)]. A. Surowiec and K.T. Wheeler, Dept. of Radiology, Bowman Gray School of Medicine, Winston-Salem, NC 27103

Two DNA models, the copolymer poly[d(A-T)·d(A-T)] and the homopolymer poly [d(A)·d(T)] were γ-irradiated in solution under oxic (O_2) and anoxic (N_2) conditions. In solution, these polymers assume a B and B' structure, respectively. The melting curves of the unirradiated polymers obtained by monitoring the UV absorbance vs temperature exhibited normal transition patterns. The melting curves for the irradiated polymers exhibited asymmetrical sigmoidal shapes. The T_m values decreased with increasing dose for the homopolymer irradiated under both O_2 and N_2 and for the copolymer irradiated under N_2. However, the T_m values remained constant for the copolymer irradiated under O_2 with doses up to 500 Gy. The transition widths, ΔTm, increased with dose for all samples; the order at 500 Gy was poly[d(A-T)]/N_2 > poly [dA·dT]/O_2 > poly [dA·dT]/N_2 > poly [d(A-T)]/O_2. With the exception of the copolymer irradiated under O_2, the differential melting curves at the higher doses showed a marked thermal destabilization of the polymers prior to their transitions. The formation and accumulation of specific base damage products (e.g. α-deoxyadenosine) in the copolymer probably causes a marked inhibition of base stacking interactions that leads to this thermal destabilization. In addition, the nonlinear behavior of T_m for the copolymer irradiated under N_2 is probably related to the large number of bases released and/or the large number of single strand breaks produced at doses > 250 Gy. An unchanging thermal stability of the copolymer irradiated under O_2 may result from intra- or interstrand crosslinking that restabilizes the stacking forces. (This work was supported by a grant, DE-FG05-86ER60464, from the Department of Energy).

Tu-Pos298 EFFECT OF SALT ON THE BENDING AND TWISTING RIGIDITY OF A RESTRICTION FRAGMENT. B. S. Fujimoto, U. S. Kim, J. M. Schurr, and P. G. Wu, Department of Chemistry, University of Washington, Seattle, WA 98195.

At high salt concentrations, native DNAs exhibit a large decrease in circular dicroism, but little if any change in intrinsic twist. Here we report changes in twisting and bending rigidity of restriction fragments drived from pBR322 as a function of NaCl concentration up to 4.3 M. These fragments are studied by dynamic light scattering (DLS), circular dichroism (CD), and time-resolved fluorescence polarization anisotropy (FPA). DLS yields the translational diffusion coefficient of the center-of-mass (D_0) and apparent diffusion coefficient at large scattering vector (D_{plat}). Relative changes in the persistence length, or bending rigidity, are obtained from D_0 using the theory of Fujii and Yamakawa. Static light scattering measurements also provide a rough indication of changes in radius of gyration. Flourescence measurements yield the torsional rigidity of the DNA and the relative amounts of bound and free dye. The bending rigidity remains constant from 0.1 to 1.0 M NaCl. Between 1.0 and 4.3 M NaCl, the bending rigidity monotonically decreases by 2-fold, the torsion constant decreases by the factor 0.75-0.80, D_{plat} increases monotonically by the factor 1.1, and the bound-to-free dye ratio increases slowly from a minimum near 1.0 M. Neither the changes in DLS or in CD are appreciably altered by the addition of 1 ethidium dye per 200 bp in 4.3 M NaCl. Evidently, both the bending and twisting rigidity of DNA are significantly reduced in the form that prevails at high salt.

Tu-Pos299 LONG RANGE EFFECT OF A $(GC)_8$ INSERT ON THE RIGIDITY, SECONDARY STRUCTURE, AND SALT-INDUCED TRANSITION OF AN 1100 BP RESTRICTiON FRAGMENT. U. S. Kim, B. S. Fujimoto, and J. M. Schurr, Department of Chemistry, University of Washington, Seattle, WA 98195.

Available evidence indicates that sequence-specific alterations of secondary structure in linear DNAs do not extend more than a few base-pairs beyond those specific sequences. Here we report evidence for much longer range effects. A 1096 bp restriction fragment containing the $(GC)_8$ insert near its center, and control fragments containing 1.4 and 1.1 kbp are prepared by standard molecular biology techniques. These fragments are studied by dynamic light scattering (DLS), circular dichroism (CD), and time-resolved fluorescence polarization anisotropy (FPA) of intercalated ethidium dye. DLS yields the diffusion coefficient of the center-of-mass (D_o) and the apparent diffusion coefficient at large scattering vector (D^{plat}). Fluorescence measurements yield the torsion constant of the DNA and the bound-to-free dye ratio. In 0.1 M NaCl, the insert fragment differs from the control fragments by a factor of 1.35 in CD, 0.55 in bound-to-free dye ratio, and 0.75 in torsion constant. With increasing salt concentration, the insert fragment undergoes a sigmoidal transition to a state with significantly lower D_0 from which a 2.5-fold increase in the effective bending rigidity of the entire filament is deduced, a significantly lower D_{plat}, and a significant bump in the salt profile of its CD. In contrast, the control fragment exhibits non-sigmoidal changes of D_0 and D_{plat} in the opposite direction and a rather different CD profile. Such an increase in rigidity of the insert fragment cannot result from any change confined to the 16 bp $(GC)_8$ insert, but must reflect a long range transition extending over a large DNA domain. One ethidium dye per 200 bp in 4.3 M NaCl completely reverses the transition exhibited by the insert fragment, but has no effect on the the control fragments.

Tu-Pos300 THE CONFORMATIONS OF $d(T_6A_6)$ AND $d(A_6T_6)$: RAMAN SPECTROSCOPY STUDY OF BENDING AND NON-BENDING DNA SEQUENCES. G. S. Tan, H. DeGrazia, and R. M. Wartell, School of Physics, Georgia Institute of Technology, Atlanta, GA 30332.

Previous studies have shown that repeating runs of $d(GA_4T_4C)$ show characteristics of bent DNA, whereas runs of $d(GT_4A_4C)$ do not (Hagerman, NATURE 321, 449, 1986, Burkoff & Tullius, NATURE 331, 4555, 1988). In order to study the structural basis of this difference, Raman spectroscopy was employed to examine the DNA oligomers $d(T_6A_6)$ and $d(A_6T_6)$. DNA solutions were at a concentration of about 30 mg/ml. Each contained 0.1 M Na^+. Spectra of the two oligomers were similar to each other. Both closely resemble the Raman spectrum of poly(dA) poly (dT). A direct comparison of the spectra show that many bands overlap. However small differences are observed in several regions of the spectra. A subtraction of the two spectra was made using the 1091 cm^{-1} dioxyphosphate band as an internal standard. Intensity differences are noted for bands at 655 and 815 cm^{-1}, and in the regions from 750-800 cm^{-1} and 1300-1370 cm^{-1}. Some of the changes are due to frequency shifts in the Raman bands. The band centered at 816 cm^{-1} is characteristic of C3'-endo family sugar pucker. The $d(A_6T_6)$ oligomer has a slightly greater intensity in this region than $d(T_6A_6)$. The intensities of the C2'-endo family bands at 841 cm^{-1} were the same. This result suggest that the $d(A_6T_6)$ sequence has a larger fraction of sugar rings with C3'-endo character than the $d(T_6A_6)$ duplex.

We thank W. D. Wilson and J. Zon for providing the DNA oligomers.

Tu-Pos301 CONFORMATIONAL STUDIES OF SELECTED DNA AND RNA's USING VIBRATIONAL CIRCULAR DICHROISM. L. Yang, A. Annamalai, A.S. Benight, T.A. Keiderling, Department of Chemistry, University of Illinois at Chicago, Box 4348, Chicago, IL 60680

Vibrational circular dichroism (VCD) offers the conformational sensitivity of CD coupled with the spectral detail of infrared spectroscopy. Thus it has the potential of yielding more structural detail in studies of nucleic acid conformation in solution. Natural DNA's and RNA's have been shown to exhibit very different melting curves as studied with VCD, with DNA having a sharp transition and RNA being gradual. On the other hand, the VCD of the heat-induced melting of the synthetic poly(A)·poly(U) double-stranded RNA in the 1750-1550 cm^{-1} region clearly indicates the occurrence of two steps in its denaturization process. Spectrally these correlate to stepwise changes in the hydrogen-bonding at the two C=O groups in uracil.

Salt-induced changes have also been studied. In particular, poly(dGdC) and various DNA oligomers have been shown to have major VCD sign reversals on undergoing a B to Z type transition at high salt conditions. Efforts have additionally been made to characterize hairpin-like structures via VCD studies of such B-Z transition measurements.

Tu-Pos302 FRAP AND FCS STUDIES OF SELF AND MUTUAL DIFFUSION IN ENTANGLED DNA SOLUTIONS. Bethe A. Scalettar (1), John E. Hearst (1, 2), and Melvin P. Klein (1), (1) Chemical Biodynamics Division, Lawrence Berkeley Laboratory, 1 Cyclotron Road, Berkeley, CA, 94720, and (2) Department of Chemistry, University of California, Berkeley, CA, 94720.

We have used two fluorescence techniques, fluorescence recovery after photobleaching and fluorescence correlation spectroscopy, to monitor, respectively, self and mutual diffusion in entangled phage λ DNA solutions. Ethidium monoazide, which binds covalently to the DNA, and ethidium bromide, a noncovalently bound intercalator, were used as fluorescent reporter molecules. For the DNA concentration regime examined, 17 $\mu g/ml \leq c \leq 305$ $\mu g/ml$, we find that the mutual-diffusion coefficient *increases* markedly with concentration. The self-diffusion coefficient, on the other hand, appears to be quite insensitive to variation in the DNA concentration; we find that the self-diffusion coefficient *decreases* by about 50% as the DNA concentration is *increased* from 40 to 300 $\mu g/ml$. Our data are in qualitative agreement with results obtained in recent light scattering studies of self and mutual diffusion in interacting DNA solutions. Our FCS data also support Phillies's prediction (G.D.J. Phillies, Biopolymers **14** 499 (1975)) that a mutual-diffusion coefficient is extracted from an FCS experiment if essentially all the macromolecules in the system are fluorescently labeled.

This work was funded in part by NIH grant GM30781, DOE contract DE AC03-76SF00098, and the Alexander Hollaender Distinguished Postdoctoral Fellowship Program.

Tu-Pos303 THE HELICAL REPEAT OF RNA IN SOLUTION David E. Draper, Roderick Tang, and Peter Kebbekus, Department of Chemistry, Johns Hopkins University, Baltimore, MD 21218

We have devised a method for measuring the helical twist of any RNA segment in solution. Using *in vitro* transcription of DNA by T7 RNA polymerase, we prepare two complementary RNA strands separately, and then anneal to form a duplex. If extra nucleotides are included in one strand, forming a bulge in the duplex, the electrophoretic mobility of the duplex in polyacrylamide gels is reduced. If two bulges are introduced into the helix, the gel mobility becomes a sine function of the number of base pairs separating the two bulges. Our best results have been obtained with bulges of five U residues, which gives a factor of two variation in gel mobility as the bulges vary in phasing. The results with 21 - 40 base pairs of random sequence RNA indicate a helical repeat of 12±0.3 base pairs/turn; further measurements should reduce the error to ±0.1.

We have also prepared duplex RNAs with an internal loop in the middle. The sequence reproduces the highly conserved loop E from 5S rRNA, which is thought to contain non-canonical purine-purine pairing. Under appropriate conditions (low temperature and 2 mM magnesium ion) the duplex migrates identically to fully Watson-Crick base paired helices in gels, while other internal loop sequences significantly retard the helix under all conditions. The helical repeat of this internal loop sequence is also being measured.

Tu-Pos304 TRIPLE-STRANDED HELICES OF OLIGODEOXYRIBONUCLEOTIDES. L. Kan, D. Callahan, P. Miller, T. Trapane, K. Blake, and P. Ts'o, Div. Biophysics, Johns Hopkins Univ. Baltimore, MD 21205

Recognition of nucleic acid base-pairs by a third strand in a triple-stranded helix deserves a rigorous investigation. Triple-stranded complex has been observed in slightly acidic solutions of poly[d(CT)·d(AG)] (Lee, et al., Nucleic Acids Res. (1979) 6, 3073). However, the detailed conformation of the triplet in solution is not yet known. We have synthesized the oligomers $d(CT)_8$ (I) and $d(AG)_8$ (II) and studied the duplex & triplet formation by circular dichroism (CD), ethidium bromide (EB) fluorescence assays and uv mixing curves at pH 7.0 or 5.5 at room temperature (10 mM phosphate buffer, 0.1 M NaCl and 10^{-5} M EDTA). The extinction coefficients of I and II were determined. CD spectra of a 2:1 mixture of I to II at pH 5.5 were very similar to the CD spectra reported for poly[d(C^+T)·d(AG)·d(CT)]. CD spectra of the same 2:1 ratio at pH 7.0 were merely the weighted average of double-stranded I·II and single-stranded I CD spectra. E. Coli DNA and an 1:1 mixture of I and II at pH 7.0 both produced an equivalent amount of EB fluorescence enhancement indicative of EB intercalation in the duplex. However, while the EB fluorescence enhancement of E. Coli DNA at pH 5.5 remained very close to that observed at pH 7.0, the enhancement produced by a 2:1 mixture of I and II at pH 5.5 was seen to decrease by approximately 70%, indicating triplet formation. Similar observations have been made in the case of poly[d(CT)·d(AG)]. Uv mixing curves were also constructed. At pH 5.5 an endpoint was observed at the 2:1 ratio of I to II. The nmr study of the triplet hydrogen-bonding scheme, sugar puckering mode, stacking mode of bases, and helical conformation will be reported. (Supported by NIH)

Tu-Pos305 SEQUENCE DEPENDENCE OF CONFORMATIONAL FLEXIBILITY OF DNA. A. Sarai, J. Mazur*, R. Nussinov† and R.L. Jernigan, Lab. Math. Biol., NCI, NIH, Bethesda, MD 20892 USA *Advanced Scientific Computing Lab. PRI, NCI-FCRF, Frederick, MD 21701 USA, †and Sackler Institute of Molecular Medicine, Sackler Faculty of Medicine, Tel-Aviv University, Ramat Aviv, 69978 Israel.

DNA shows a sequence-dependent conformational flexibility. that can be anisotropic in nature. Such a sequence-dependent property, together with the conformational polymorphism of DNA, could play important role in the sequence recognition by proteins. By conformational analyses, we have investigated the flexibility and its anisotropy along various conformational coordinates of DNA. We find that AT base step is most flexible along twist coordinate, while GG step is most rigid, and TA step is most flexible for rolling motion, while CT step is least flexible. The flexibility of rolls is quite anisotropic; the ratio of fluctuations toward major groove and minor groove is the largest for GG/GC steps and the smallest for AA/AT steps. These features generally agree with various experimental observations, including nucleosome structures, protein-DNA binding, and measurement of sequence-dependent flexibility. We discuss the effect of electrostatic parameters, relationship to available experimental results, and biological relevance of these results.

Tu-Pos306 **MELTING STUDIES OF SHORT DNA HAIRPINS WITH DIFFERENT LOOP AND STEM SEQUENCES.** T.M. Paner, M. Amaratunga, M.J. Doktycz and A.S. Benight. Department of Chemistry, University of Illinois at Chicago, Chicago, Illinois 60680.

We have measured thermal melting curves of the core DNA duplex sequence d(CGCGCCG) linked on one end by T_4, A_4, C_4 and G_4 single strand hairpin loops (set 1). Melting curves of d(GCGCGC), d(C*GC*GC*G) where C* is 5-methyl cytosine, and d(GGATAC) with a T_4 hairpin loop were also measured (set 2). A solvent of 100 mM NaCl was employed. All oligomers except the A_4 loop of d(CGCGCG) display a monophasic transition. The numerically exact theory of helix-coil transitions in DNA was modified to include effects of nearest-neighbor sequence and hairpin loops on the melting transition. Melting experiments were analyzed in terms of the theory. Model parameters of loop formation were evaluated by fitting calculated melting curves to experimental curves in set 1. The hairpin loop closure parameter, $f_{end}(n)$, for forming an n base single strand loop, was the single adjustable parameter used in the fitting. Effects of nearest neighbor duplex sequence on the stability of the T_4 hairpin loop were investigated from analysis of the melting curves in set 2. Nearly exact fits to the experiments were obtained for all the DNAs examined. The best fit theory curves for set 1 then provide an evaluation of the free-energy of loop closure as a function of hairpin loop sequence of these DNAs. Results indicate for this core duplex, the order of stability is $G_4 > C_4 > T_4 > A_4$.

Tu-Pos307 **STRUCTURE AND DYNAMICS OF M13mp19 CIRCULAR SINGLE STRAND DNA: EFFECTS OF IONIC STRENGTH.** D.H. Wilson[1], H.L. Price[1], S. Hanlon[2], J. Henderson[2] and A.S. Benight[1]. Departments of Chemistry[1] and Biological Chemistry[2], University of Illinois at Chicago, Chicago, Illinois, 60680.

We have conducted dynamic light scattering (DLS), circular dichroism (CD) and optical melting experiments to investigate the solution structure and dynamic properties of M13mp19 viral circular single strand DNA as a function of NaCl concentration. Over the 10,000 fold range in concentration from 100 μM to 1.0 M NaCl the melting curves and CD spectra indicate an increase in base stacking and stability of stacked regions with increased salt concentration. Analysis of DLS measurements as a function of K^2 from 1.56 to 20 x 10^{10} cm^{-2} indicates the collected autocorrelation functions are bi-exponential, thus revealing the presence of two decaying components corresponding to (1) translational motions of the molecular center of mass and (2) motions of the internal molecular subunits. From the relaxation rates of these components, the center of mass diffusion coefficient, D_o, and diffusion coefficient of the internal molecular subunits, D_{plat}, were determined. D_o decreases by 9% from 100 μM to 1.0 M NaCl. D_{plat} decreases by nearly 22% over this range in NaCl concentration. These results indicate the changes in M13mp19 single strand DNA structure and dynamics, that occur from 100 μM to 1.0 M NaCl, are predominantly associated with local structural rearrangements of the scattering elements and these local structural changes apparently do not appreciably perturb the overall global DNA tertiary conformation.

Tu-Pos308 STRUCTURAL STUDIES OF OLIGONUCLEOTIDES WHICH MODEL A FRAMESHIFT MUTATION.
Bonnie Gunn, Karol Maskos, Marty Beasley, Kathleen Morden
Dept. of Biochemistry, Louisiana State University, Baton Rouge, LA 70803

Frameshift mutagens are known to bind to DNA and cause deletions or additions upon replication. The previously proposed mechanism for this action is the stabilization of unpaired bases or base bulges. This proposal is being tested using synthetic oligonucleotide duplexes. The structural features of the following oligonucleotide duplexes were investigated using nuclear magnetic resonance, $dCGCT_4$ CGC + $dGCGA_2CA_2GCG$, containing an unpaired cytosine residue, $dCGCT_4CGC$ + $dGCGA_2TA_2GCG$, containing an unpaired thymidine residue and $dCGCT_4$ CGC + $dGCGA_4GCG$, the fully complimentary or parent duplex. For each of these duplexes, the resonances from the non-exchangeable aromatic protons were assigned using both two-dimensional correlated spectroscopy (COSY) and two-dimensional nuclear Overhauser effect spectroscopy (NOESY). The NOESY spectra also provide information on the structure in the local region of the unpaired bases. The resonances from the base pairing imino protons were assigned using one-dimensional NOEs with a water suppression pulse sequence for observation. The temperature dependence of the chemical shift for the imino and the aromatic protons was determined to aid in understanding the effects of the unpaired cytosine and thymidine on the helix to coil transition. Thermodynamic parameters for the helix to coil transition were also determined for these duplexes by measuring the UV absorption at 260 nm as a function of temperature, concentration, and ionic strength. The impact of the pyrimidine unpaired bases on duplex formation and local helix geometry will be discussed.

Supported by N.I.H. Grant GM38137 and Louisiana Education Quality Support Fund LEQSF(86-89)-RD-A-12.

Tu-Pos309 SEQUENCE SPECIFICITY OF COVALENT DNA BINDING BY ACTINOMYCIN D AZIDE. Glenn Marsch and Randolph Rill, Department of Chemistry and Institute of Molecular Biophysics, The Florida State University, Tallahassee, Florida, USA 32306.

DNA chemical sequencing techniques were used to determine the specificity of photo-induced covalent DNA binding by the 7-azido derivative of actinomycin D. 7-Azido actinomycin D binds covalently to DNA after exposure to visible light. Some fraction of these adducts are labile in hot piperidine. Sites of such adducts were determined on nearly 800 bp of DNA from restriction fragments. The relative intensities of bands reflects both base chemistry, ie., the efficiency of formation of alkali-labile adducts, and sequence specificity. The relative efficiencies of formation of alkali-labile adducts according to base type were G>>C>T, A. Cleavages due to adducts of a particular base type are expected to reflect predominantly non-covalent binding affinities of the azido actinomycin D at a specific site encompassing the reacted base. A strong preference was observed for G and C residues in GC doublets, as expected from previous studies of actinomycin D binding. However, the reactivities of GC doublets were strongly dependent on flanking sequences. We observed a strong preference for a 5'-flanking pyrimidine, ie., TGC and CGC triplets were strongly preferred. Some longer range sequence effects were noted. Reactions of the PYGC triplet were suppressed by a 3'-flanking C, in the sequence PYGCC. Of particular interest is the observation of a highly preferential reaction of the central G in GGG triplets flanked on the 5'-side by T and the 3'-side by a pyrimidine (TGGGPY). Such a specificity has not been noted previously for actinomycin D. Supported by a grant from the Dept. of Energy.

Tu-Pos310 INVERTED REPEAT SEQUENCES INFLUENCE THE MELTING TRANSITIONS OF LINEAR DNAS. R. M. Wartell and C. R. McCampbell. School of Physics, Georgia Institute of Technology, Atlanta, Georgia 30332

The influence of inverted repeat sequences on the melting transitions of linear DNAs was examined. Derivative melting curves (DMC) of a 514 bp DNA, seven subfragments of this DNA, and four other DNAs were compared to predictions of DNA melting theory. The 514 bp DNA contains three inverted repeat sequences which can form cruciform or hairpin structures. Previous work showed that the DMC of this DNA, unlike a number of other DNAs, is not accurately predicted by DNA melting theory. Since the theoretical model does not include hairpin structures, it was suggested that hairpin or cruciform formation may be responsible for this discrepancy. Our results support this hypothesis. Predicted DMCs were in good agreement with DNAs with no inverted repeats. Differences between the theoretical and experimental T_m's were < 0.3°C. DNA molecules which contained one or more inverted repeat were not as accurately predicted. Experimental T_m values were lower than predicted values by 0.7 to 3.8°C. It is concluded that structures formed by inverted repeat sequences occur during the melting of linear DNAs, and lower their stability. DNAs without inverted repeats were employed to evaluate nearest neighbor stacking interactions.

Tu-Pos311 DNA STRUCTURAL ANOMALY AT THE CAC/GTG TRIPLET — POSSIBLE FIXED BENDING OR ANISOTROPIC HINGING. P. T. McNamara, E. Charney, and R. E. Harrington, University of Nevada Reno, Dept of Biochemistry and LCP, NIADDK, National Institutes of Health, Bethesda, MD.

Conformational properties of both cloned naturally occuring and synthetic DNA fragments containing CAC/GTG trinucleotides were studied. Transient electric birefringence data from pBR322 restriction fragments and an upstream sequence from the mouse B-globin gene indicate shorter effective molecular lengths than expected. These fragments contain CAC/GTG triplets in various arrangements, with some repeats in near helical phase. Control fragments give normal relaxation times. We have also synthesized a number of DNA fragments which possess helical repeats of the triplets both with themselves and with poly-A_6 tracts. Gel retardation analysis shows that certain CAC/A_6 helical repeat fragments which contain AT rich intervening regions are retarded less in polyacrylamide gels than expected from the A_6 tract effect alone. A similar effect is observed at half helical repeat with fragments containing GC rich intervening regions. Circularization and electro-optical experiments using polymers of these and similar sequences further support the concept of a conformational anomaly at the CAC/GTG trinucleotide, which may be influenced by neighboring base pairs and which may be a site of anisotropic hinging or fixed bending, possibly with a different directionality from that of the poly-A_6 tract.

Tu-Pos312 THE DOUBLE STRANDED RNA POLYMER POLY[r(G-U)]· POLY [r(A-C)] CAN ASSUME A Z-RNA CONFORMATION.

P. Cruz, and L. M. Scott, Department of Biochemistry, Wright State University, Dayton, Ohio 45435.

In concentrated ammonium fluoride solutions the alternating purine-pyrimidine RNA sequence poly[r(G-U)]· poly[r(A-C)] undergoes a transition from A- to Z-RNA, as monitored spectroscopically. The circular dichroism (CD) spectra indicate a structure similar to that of alternating G-C sequences in concentrated sodium bromide, or alternating A-U sequences in ammonium fluoride. Unlike the A-Z transition with poly[r(G-C)], elevated temperatures do not promote Z-RNA formation. If the temperature of the solution is raised above room temperature, aggregation of the RNA occurs as indicated both by CD and visual inspection.

Nuclear magnetic resonance (NMR) spectra of the various Z-RNA forming sequences will be compared, and the kinetics of the the A to Z transition will be presented. These data indicate that Z-RNA forming sites are not limited to alternating G-C, and that other naturally occurring alternating purine-pyrimidine sequences may potentially assume a Z-form.

Tu-Pos313 HAIRPIN FORMATION OF d(CGCG-TA-CGCG), d(CGCG-TG-CGCG) AND THEIR CYTOSINE METHYLATED ANALOGS.

Fu-Ming Chen, Department of Chemistry, Tennessee State University, Nashville, Tennessee 37209-1561.

Hairpin formations of decamers d(CGCG-TA-CGCG), d(CGCG-TG-CGCG), and their m^5dC analogs are evidenced by the existence of biphasic absorbance melting profiles in which the lower transition temperature increases with increasing oligomer concentration, whereas the higher melting temperature is concentration independent. The corresponding temperature dependent CD intensity at 285 nm exhibits a maximum around 50 °C. These observations are consistent with the interpretation that the lower temperature transition corresponds to the duplex to hairpin transformation while the melting of hairpins into single strands constitutes the higher temperature transition. The CD spectrum of the hairpin conformation appears to be characterized by a couplet with nearly equal positive and negative intensities at 285 and 255 nm, respectively, while a significantly smaller intensity at 285 nm is apparent for the duplex form. The hairpin conformation is suspected to contain a two-nucleotide loop. Titrations with NaCl further suggest that, in contrast to the TA sequence, the TG sequence with wobble base pairing favors Z formation under high salt conditions. (Supported by NIH Grant CA-42682 and in part by a subproject of MBRS Grant S06RR0892)

Tu-Pos314 DYNAMICS OF SHORT DNAs MONITORED BY A SITE SPECIFIC SPIN PROBE

Andreas Spaltenstein, Paul B. Hopkins, Eric J. Hustedt, and Bruce H. Robinson,*
Dept. of Chemistry, University of Washington, Seattle, WA 98195.

Recent work has suggested that there are differences in the dynamics of duplex DNA as a function of base sequence or composition. The resolution of this issue has been confounded by the problem of determining to what extent the dynamics are due to local independent motions of the base or to the collective modes. Progress in these areas has been impeded by the lack of an experimental method to place a dynamics probe at a specific place and test for components of the dynamics which are local, global or base pair dependent.

To address these problems we have prepared an EPR active spin-labeled analogue of thymidine that can be site specifically incorporated into DNA via automated deoxyoligonucleotide synthesis. We have prepared deoxyoliognucleotides of 12, 24, 48 and 96 bases which exist as duplex DNA under standard buffered conditions. Analysis of the ESR data as a function of length and temperature enables us to separate the more rapidly moving, length independent components from the length dependent components of the dynamics (of which the uniform modes scale according to the dynamics of a right circular cylinder). Length dependent differences in the dynamics are seen for the entire series of duplex DNAs studied thus far. Placement of the spin probe at different distances from the center enables us to estimate the extent of end effects associated with internal flexibility and coupled modes.

Tu-Pos315 MEASUREMENT OF DEOXYRIBOSE ^1H-^1H COUPLING CONSTANTS IN DNA FRAGMENTS BY 2D NMR

Ad Bax and Laura Lerner*, Laboratory of Chemical Physics, NIDDK, NIH, Bethesda MD 20892. *current address, Department of Chemistry, University of Wisconsin-Madison

^1H-^1H scalar coupling constants can provide information about deoxyribose ring conformation in DNA fragments. A slightly modified version of the PE-COSY experiment (1) is ideally suited for measuring couplings to the H2' and H2" protons in DNA. In addition, the coupling between H3' and H4' can be measured from a cross section through the H3'-H4' cross peak in a COSY spectrum that incorporates F_1 decoupling of the H3' interaction with the H2'/H2" protons. Simple guidelines will be presented that permit estimating the accuracy of couplings measured from partially resolved antiphase doublets, as encountered for the H3'-H4' cross peaks. The experiments are used to determine the pseudorotation angles for the dodecamer d(CGCGAATTCGCG)$_2$.

(1) L. Mueller, J. Magn. Reson. 72, 191 (1987)

Tu-Pos316 THE DUPLEX-HAIRPIN CONFORMATIONAL TRANSITION OF THE DODECAMER d(CGCGAATTCGCG): A NUCLEAR MAGNETIC RESONANCE INVESTIGATION. Irina M. Russu, Danuta Tracz and Sandia Wang, Department of Molecular Biology and Biochemistry, Wesleyan University, Middletown, Connecticut 06457

Nuclear magnetic resonance (NMR) spectroscopy has been used to investigate a thermally-induced structural transition in the dodecamer d(CGCGAATTCGCG) which contains the EcoRI recognition site. An alternate conformation of the dodecamer is observed in equilibrium with the duplex form at low counterion concentrations (≤ 0.02 M Na+). The fraction of the DNA in this conformation is enhanced by raising the temperature (from 10 to 55°C) and/or by lowering the DNA concentration (from 1.2 to 0.1mM in single strands). These results, and a preliminary structural characterization based on proton and phosphorus NMR data, suggest that the alternate conformation assumed by the dodecamer under these conditions corresponds to an unimolecular hairpin structure. A hairpin conformation for the same dodecamer at low salt and low oligomer concentrations has been previously proposed by L. A. Marky, K. S. Blumenfeld, S. Kozlowski, and K. J. Breslauer (Biopolymers 22, 1247, 1983) on the basis of differential scanning calorimetry, UV-absorption and circular dichroism data. The relevance of the present results for the recognition of the dodecamer d(CGCGAATTCGCG) by EcoRI endonuclease will be discussed. (Supported by NIH grant GM 33862).

Tu-Pos317 SOLUTION STRUCTURE OF DEOXYOLIGONUCLEOTIDE STUDIED BY HIGH RESOLUTION NMR. G-J. Huang, T. R. Krugh, Department of Chemistry, University of Rochester, Rochester, NY 14627, S. S. Wang, P. N. Borer, G. C. Levy, Department of Chemistry, Syracuse University, Syracuse, NY 13244.

A deoxyoligonucleotide, [d(CACACGCACACA)·d(TGTGTGCGTGTG)], has been studied by solution NMR in preparation for determining the structure of the covalent adduct with the carcinogen, acetylaminofluorene. The nonexchangeable protons have been assigned. A series of NOESY spectra at five different mixing times (25, 50, 75, 150 and 600 ms) have been used for inter-proton distance determination. A semi-automated procedure has been developed and used to determine the crosspeak volumes, the NOE buildup rates, and the distances. The inter-proton distances are being used for model building, and progress toward a refined 3D-structure will be reported.

Tu-Pos318 **THREE DIMENSIONAL STRUCTURAL FEATURES OF [d(TAGCGCTA)] IN SOLUTION REVEALED BY ^{1}H AND ^{13}C NMR.** K. D. Bishop*, S. S. Wang & P. N. Borer, Chemistry Department & NIH Resource for NMR & Data Processing, Syracuse University, Syracuse, NY 13244.

A crude three-dimensional solution structure of $[d(TAGCGCTA)]_2$ has been determined, and is being refined. NOESY spectra at 15, 30, 60, 90, 150, 300 and 600ms mixing times were collected and, together with the incorporation of deoxyribofuranose conformational constraints, are being used for refinement. The average sugar conformations have been obtained by measuring the coupling constants between the H1′ and H2′, H2′′ protons and fitting the sums of the coupling constants to the model developed by Rinkel and Altona [J. Biomol. Struct. Dyn., 4, 621 (1987)]. The average %S conformation varies from 61 to 88%, with an unusually low value at C6, where the NOESY constraints identify a structural anomaly. The deoxyribofuranose ^{13}C chemical shift versus temperature profiles correlate strongly with the average sugar conformation. It is seen that the sugar carbons on most purine residues have very little temperature dependence of chemical shift, while the pyrimidine residues exhibit a much larger temperature dependence. [Supported by NIH grants GM35069 & RR01317.]

Tu-Pos319 CONFORMATIONAL AND STRUCTURAL ANALYSIS OF NUCLEIC ACID PHOTOPRODUCTS BY MOLECULAR MODELLING, MOLECULAR MECHANICS, AND NMR. J.-K. Kim, R. M. Wollman, S. D. Soni, and J. L. Alderfer. Roswell Park Memorial Institute, Biophysics Department, Buffalo, NY 14263.

Sensitized UV-B irradiation (sunlamps) of the dinucleoside monophosphate, d-TpF (F=fluorouracil), produces the usual cyclobutane-type photodimer and an unexpected 5-5 photoadduct, d-T5p5U. In d-T5p5U, the original T C5=C6 bonding is modified such that the T C5 bonds with the U C5 (where the fluorine had been) and the T C6 acquires an OH group. On the basis of 2D-NOE data, the chiralities of the C5 and C6 atoms were proposed as 5R and 6S. Molecular mechanics calculations (CHARMM) were performed to aid in further defining and in refining the NMR determined conformation and structure. Starting from the NMR observed conformations [furanose: $^{3}T_2$ (d-T5p), $_{1}E$ (p5U); backbone: ϵ,β,γ = t,t,g^{+}], forced T(C5)-U(C5) bonding, and a 5R,6S configuration at T(C5 and C6), the structure of d-T5p5U was energy-minimized explicitly including all hydrogens, with complete geometry optimization. The calculated minimum-energy form is a structure in which the T C5 and C6 are 5R and 6S, and with the C5-uracil and C6-OH trans axial, and the C5-methyl pseudo-equatorial. Backbone dihedral angles (ϵ,β,γ) and qualtitative hydrogen-hydrogen distances obtained after refinement were similar to those observed by NMR. However, there are differences in the calculated sugar puckers: d-T5p is ^{3}E and p5U is ^{2}E. In the case of performing the calculation starting with T C5 constrained in a 5S configuration, the energy-minimized form was T 5S and 6S, with the C5-uracil equatorial. This structural form has furanose conformations similar to the 5R,6S form but has markedly different backbone dihedral angles, and predicts certain hydrogen-hydrogen distances which are not observed by the NOE experiments. (Supported in part by NIH CA39027.)

Tu-Pos320 **PREDICTION OF THREE DIMENSIONAL STRUCTURES OF RIBONUCLEIC ACIDS: FROM tRNA TO 16S RIBOSOMAL RNA.** Arun Malhotra, Robert K.Z. Tan and Stephen C. Harvey, Department of Biochemistry, University of Alabama at Birmingham, Birmingham, AL 35294

We describe a computer-assisted procedure for folding an RNA chain into three dimensional conformations consistent with its secondary structure. Additional constraints, such as helix stacking and contacts determined by cross-linking or other experimental methods can be incorporated to further restrict the range of acceptable models. These contacts may be intramolecular or between the RNA and other molecules. The method provides many conformations for each case, so the range of models that are consistent with the data is determined. A test run with tRNA is shown here, with the following successive stages of refinement: (1) a random chain; (2) secondary structure only; (3) correct stem stacking; (4) required contact between D and T loops. Studies on the structure of the ribosome are underway, and progress on them will be described if there is any.

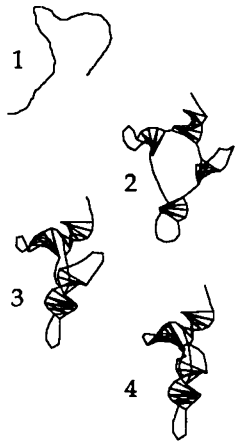

Tu-Pos321 SECONDARY STRUCTURE ANALYSIS OF SUPERCOILED, LINEARIZED AND SINGLE-STRANDED ØX174 DNA BY LASER RAMAN SPECTROSCOPY. James M. Benevides, Nino Incardona and George J. Thomas, Jr., Division of Cell Biology and Biophysics, School of Basic Life Sciences, University of Missouri-Kansas City, Kansas City, MO 64110.

Raman spectroscopy is a valuable probe for the elucidation of nucleic acid structure and is particularly advantageous for the study of backbone geometry of aqueous DNA. In order to assess the extent to which DNA local backbone geometry may be perturbed by supercoiling, we have compared Raman spectra of ØX174 DNA as a covalently closed single strand (ss), covalently closed and supercoiled double strand (sds), and linearized (nicked) double strand (ds). The Raman spectra show no evidence of glycosyl torsions in the syn range for any of the DNAs, which rules out left-handed Z-DNA in the sds form. Further, the Raman spectra of all three forms indicate that nucleoside sugar conformations are consistently C2′-endo. The ssDNA clearly exhibits backbone characteristics similar to those of base paired dsDNA, which may be attributed to extensive hairpin formation. However, clear-cut differences exist among the spectra of ss, sds and ds forms. The ss form is characterized by enhanced intensity at 1240 cm^{-1}, which we attribute to specific nucleoside base orientations. The ss form also exhibits increased intensity in the C=O stretching region which results from non-paired T residues. This intensity difference may be exploited for estimating the extent of base pairing in the ss form. It appears that the different conformations of ØXDNA are achieved by small alterations in the C-O-P-O-C torsion angles (α,ζ), and possibly by changes in related torsion angles (β,γ) which are reflected in the Raman spectra. (Supported by NIH.)

Tu-Pos322 INTERACTIONS OF AMSACRINE ANALOGS WITH DNA. Randy M. Wadkins and David E. Graves. Department of Chemistry, University of Mississippi, University, Mississippi 38677.

Structural analogs of m-AMSA are used to probe the biophysical properties associated with the interaction of this potent antitumor agent with nucleic acids. Earlier studies from this laboratory reveal that at low bound drug concentrations, m-AMSA binds DNA in a highly cooperative manner. In an effort to characterize the biophysical properties associated with this interaction with nucleic acids, the thermodynamic profiles of m-AMSA and several structurally related analogs are examined. Structural derivatives of m-AMSA and related acridine compounds were synthesized and their interactions with calf-thymus DNA studied over a wide range of temperatures and salt concentrations and bound drug concentrations. van't Hoff analyses are used to correlate the thermodynamic binding profiles of these analogs with DNA to the corresponding chemical modifications of the analog structure. These studies reveal that the addition of the phenyl group to the N9 position of 9-aminoacridine results in a substantial decrease in the enthalpy of binding to DNA. Addition of the methanesulfon-amide to the 1' position of the ring results in a large negative increase in the binding enthalpy, relative to the parent m-AMSA. In contrast, the addition of the methoxy moiety at either the ortho or meta positions on the phenyl ring results in a decrease in the enthalpy of binding of this analog to DNA. From these studies a direct link between chemical substituent modification and DNA binding thermodynamics can be resolved, thus providing insight into improved drug design and development. Supported by a grant from the National Cancer Institute CA-41474.

Tu-Pos323 INHIBITION OF THE "B" TO "Z" TRANSITION OF POLY(dGdC)·POLY(dGdC) BY COVALENT ATTACHMENT OF ETHIDIUM. Pam Gilbert and David E. Graves, Department of Chemistry, University of Mississippi, University, Mississippi 38677.

The effects of covalent modification of poly(dGdC)·poly(dGdC) by ethidium monoazide (a photoreactive analog of ethidium) on the salt induced "B" to "Z" transition are examined. Earlier studies have shown ethidium monoazide to bind DNA (in the absence of light) in a manner identical to that of the parent ethidium bromide. However, photolysis of the ethidium azide-DNA complex with visible light results in the covalent attachment of the photoreactive analog to the DNA. This capacity to form a covalent adduct was utilized as a probe for examining the salt induced "B" to "Z" transition of the poly(dGdC)·poly(dGdC) structure. In the absence of drug, the salt induced transition from the "B" to "Z" structure is highly cooperative. In contrast, this cooperativity is diminished as the concentration of covalently attached drug is increased. The degree of inhibition of the "B" to "Z" transition is quantitated as a function of the concentration of covalently attached drug. At a concentration of a drug bound per four base pairs, total inhibition of this transition is achieved. Lower concentrations of bound drug were effective in a partial inhibition of this transition and can be used to quantitate an overall size of the junction region between the two DNA structures. Supported by a grant from the National Cancer Institute CA-41474.

Tu-Pos324 **IMAGING OF THE MOTIONS AND CONFORMATIONAL TRANSITIONS OF SINGLE DNA MOLECULES USING FLUORESCENCE MICROSCOPY**

T. W. Houseal and C. Bustamante , Department of Chemistry, University of New Mexico, Albuquerque, NM 87131; *M. F. Maestre,* Lawrence Berkley Laboratory, Berkley, CA 94720; and *R. F. Stump,* UNM School of Medicine, Albuquerque, NM 87131.

A modification of the fluorescence staining methods developed by Morikawa and Yanagida (J. Biochem. 89:693-696, 1981) has allowed to us to obtain fluorescence images of single DNA molecules in solution. Motions of individual molecules were recorded on video tape using a fluorescence microscope equipped with a super intensified camera system, housed in the Department of Chemistry at the University of New Mexico. Single DNA molecules in solution fluctuated rapidly between a thin, extended filament and a condensed sphere. In some cases, molecules fully extended in solution condensed into a compact particle. We have also observed the breaking of DNA molecules attached to the coverslip. Upon breaking, the fragments retracted towards the points of attachment, exhibiting elastic behavior. In addition, bundles of DNA molecules underwent various conformational transitions including supercoiling and condensation. Using this technique we have also followed the electrophoretic motion of single DNA molecules migrating through thin gels. We have observed trapping of molecules, formation of microscopic electrophoretic bands, and the creation of microscopic channels in the gel. The potential applications of this technique to molecular biology and polymer dynamics are discussed.

Tu-Pos325 TRIPLET ANISOTROPY DECAY ANALYSIS OF SHORT DNA FRAGMENTS. S. A. Allison (1), R. H. Austin (2), M. E. Hogan (3), and A. Wierzbicki (1). (1) Dept. of Chemistry, Georgia State Univ., Atlanta, GA 30303; (2) Dept. of Physics, Princeton Univ., Princeton, NJ 08544; (3) Center for Biotechnology, Baylor College of Medicine, The Woodlands, TX 77381.

DNA flexibility has been established by numerous studies and this flexibility undoubtedly plays a significant role in controlling expression, replication, and packing. The technique of triplet anisotropy decay (TAD) is particularly useful in studying torsional and bending motions on the timescale of about 0.01 to 10 microseconds. TAD experiments have been carried out on monodisperse wild type and synthetic duplex DNA's in the size range of 200 to 450 base pairs. The results are analyzed by Brownian dynamics in terms of a "caterpillar" model with adjustable parameters for torsional rigidity, bending rigidity, and anisotropic bending. Provided the effective persistence length is held constant (along with the torsional rigidity), anisotropic and isotropic bending models predict similar TAD decays. Persistence lengths of about 100 nm or larger are estimated for most of the fragments analyzed. These values are significantly larger than estimates obtained by other methods.

Tu-Pos326 **THERMODYNAMIC CHARACTERIZATION OF BISBENZIMIDE BINDING TO DNA DUPLEX STRUCTURES** Renzhe Jin and Kenneth J. Breslauer, Department of Chemistry, Rutgers, The State University of New Jersey, New Brunswick, NJ 08903.

We have employed a combination of spectroscopic and calorimetric techniques to determine the first complete set of thermodynamic profiles for the binding of bisbenzimide (BB) to a series of DNA duplexes. As expected, based on the solution and crystal structures, BB binds most strongly to DNA duplexes with minor grooves that are not sterically blocked (e.g. polyd(AT)•polyd(AT), polyd(AU)•polyd(AU), and polyd(IC)•polyd(IC)). By contrast, BB binding to the polyd(GC)•polyd(GC) duplex is much reduced since the minor groove is blocked by exocyclic amino group of guanine. Our calorimetric measurements reveal that the nature of the thermodynamic driving forces for BB binding (ΔH°, ΔS°) depend on the host duplex. Specifically, BB binding to the polyd(GC)•polyd(GC) duplex is overwhelmingly enthalpy driven; BB binding to the polydA•polydT duplex is overwhelmingly entropy driven; BB binding to polyd(AT)•polyd(AT), polyd(AU)•polyd(AU), and polyd(IC)•polyd(IC) duplexes is both enthalpy and entropy driven. Surprisingly, the salt dependent studies ($\partial \log K/\partial \log[Na^+]$) reveal that BB binding to each duplex exhibits an electrostatic contribution characteristic of a monocation despite the formal tricationic structure of the ligand. This research was supported by National Institutes of Health grants GM-34469 and GM-23509.

Tu-Pos327 **A METHOD FOR DETERMINING LOW LIGAND-DNA BINDING CONSTANTS USING FLUORESCENCE SPECTROSCOPY**

Renzhe Jin and Kenneth J. Breslauer, Department of Chemistry, Rutgers, The State University of New Jersey, New Brunswick, NJ 08903.

We describe a method for analyzing fluorescence data that permits the determination of DNA binding constants, K, for ligands that exhibit low binding affinities. We show how this method has been used to determine K values for the low-affinity binding of bisbenzimide to the polyd(GC)•polyd(GC) duplex and bisbenzimide derivatives to the polyd(AT)•polyd(AT) duplex. This work was supported by National Institutes of Health grant GM-34469.

Tu-Pos328 **SOLVENT PERTURBATION STUDIES ON ETHIDIUM BROMIDE AND BISBENZIMIDE BINDING TO DNA DUPLEXES**

Renzhe Jin and Kenneth J. Breslauer, Department of Chemistry, Rutgers, The State University of New Jersey, New Brunswick, NJ 08903.

We have employed a combination of spectroscopic and calorimetric techniques to derive thermodynamic profiles for the binding of bisbenzimide, BB (a minor groove binding ligand) and ethidium bromide, EB (an intercalating ligand) to DNA duplexes in aqueous buffer, ethanol-water, and 1,4-dioxane-water mixed solvents. Our data reveal the following significant trends: (1) As the organic component in the mixed solvent systems is increased, the DNA binding affinity for the both drugs decreases, with BB showing a slightly greater dependence than EB. (2) The DNA binding free energies of both drugs exhibit a solvent dependence that correlates with the dielectric constant of the bulk solvent. (3) As the organic component in the mixed solvents is increased, the thermal stabilities of the drug-DNA complexes decrease more rapidly than the thermal stabilities of the drug-free DNA duplexes. (4) As the organic component in the mixed solvent systems is increased, $\Delta H°$ and $\Delta S°$ for drug binding exhibit the changes that depend on the nature of host duplex. However, none of the solvent induced changes convert a process from enthalpy to entropy driven, or vice versa. This work was supported by National Institutes of Health grant GM-34469.

Tu-Pos329 RNA-DRUG INTERACTIONS: IN VITRO ANTIVIRAL ACTIVITY OF POLY r(A-U) AND ELLIPTICINES.

Daniel G. Flowers, Keith Krabill, James M. Jamison and Chun-che Tsai, Department of Chemistry, Kent State University, Kent, Ohio 44242 and Department of Microbiology and Immunology, Northeastern Ohio Universities College of Medicine, Rootstown, Ohio 44272

The role of N^2-methyl-9-hydroxy ellipticinium acetate (NMHE) and N^2,N^6-dimethyl-9-hydroxy ellipticinium chloride (DMHE) in modulating the antiviral activity of poly r(A-U) was examined using the human foreskin fibroblast-vesicular stomatitis virus (HSF-VSV) bioassay. The concentration of poly r(A-U) was fixed at 0.05 mM or 0.2 mM while the NMHE or DMHE concentration was varied to produce variable NMHE (or DMHE)/ribonucleotide ratios ranging from 1:16 to 2:1. Poly r(A-U), NMHE and DMHE were not efficacious antiviral agents when they were tested individually at the concentrations employed in the NMHE (or DMHE)/poly r(A-U) combinations. However, when the poly r(A-U) was combined with the NMHE or DMHE, the antiviral activity of the poly r(A-U) was potentiated eleven- to fourteenfold at NMHE (or DMHE)/ribonucleotide ratios in the region of 1/4 to 1/6. Direct viral inactivation of the VSV by the NMHE, DMHE, poly r(A-U) or the NMHE (or DMHE)/poly r(A-U) combinations was not responsible for the potentiated antiviral activity. Additional experiments employing NIH sheep antiserum to human fibroblast interferon demonstrated that NMHE, DMHE and poly r(A-U) induce the production of β-interferon. The elevated antiviral activity of poly r(A-U) in the presence of NMHE or DMHE may be due to their ability to stabilize the formation of short, double-helical tracts of poly r(A-U) and subsequently protect these tracts from nuclease degradation.

Tu-Pos330 **^{23}NA NMR OF CONCENTRATED DNA SOLUTIONS.**

Teresa E. Strzelecka and Randolph L. Rill, Institute of Molecular Biophysics and Department of Chemistry, FSU, Tallahassee, Florida 32306.

Solutions of short DNA fragments (147 bp) with concentrations ranging from 10 to 300 mg/mL at ionic strengths of 0.01, 0.1 and 1.0 M Na^+ were studied by sodium-23 NMR spectroscopy. The T_1 relaxation time was measured at 20, 40 and 60 C for each set of samples. The magnitude of T_1 at all DNA concentrations and ionic strengths increased with increasing temperature, indicating a fast exchange between free and "bound" counterions. The relaxation time also decreased with increasing DNA concentration.

Estimates of the relaxation rate of bound ions ($R_{1,b} = 1/T_{1,b}$) were obtained from the T_1 relaxation data in terms of a two-state model of counterion binding. The magnitude of $R_{1,b}$ increased with increasing DNA concentration at a given ionic strength and temperature. For a given DNA concentration the relaxation rate of bound ions increased with increasing ionic strength.

At all ionic strengths the spectral line-shape of isotropic samples was Lorentzian. Spectra of anisotropic samples showed quadrupole splitting, the magnitude of which decreased with increasing DNA concentration for solutions with ionic strenghts of 0.01 and 0.1 M Na^+. Quadrupole splitting was almost concentration-independent in 1 M Na^+ samples. All anisotropic samples exhibited a change of sign of the quadrupole splitting upon increase in temperature. The T_1 relaxation and quadrupole splitting data were analysed in terms of the existing models of counterion-DNA interactions.

Tu-Pos331 FREQUENCY DEPENDENT CO-59 NMR RELAXATION STUDIES OF COBALT HEXAMMINE BINDING TO DOUBLE-HELICAL DNA. W. H. Braunlin, Department of Chemistry, Polytechnic University, 333 Jay Street, Brooklyn, NY 11201

For a sample of double-helical DNA containing 18.8 mM DNA phosphate and 2.1 mM $Co(NH_3)_6^{3+}$ at 21.4 °C, the Co-59 (I=7/2) NMR lineshape at 7.0 Tesla (71.6 MHz) is a single Lorentzian. Large differences between transverse (R_2) and longitudinal (R_1) relaxation rates are consistent with an effective correlation time of about 10 ns. Under conditions where all $Co(NH_3)_6^{3+}$ is bound, R_1, R_2 and the chemical shift all depend strongly on the binding density, consistent with multiple binding environments for $Co(NH_3)_6^{3+}$ on the DNA polyion. Under the same conditions, the lineshape at 2.1 Tesla is distinctly non-Lorentzian, and asymmetric. This asymmetry can be attributed to a dynamic frequency shift. I am presently 1) exploring the frequency dependent relaxation in more detail, in order to model the motions dominating the relaxation 2) studying base composition and structural effects on the apparent binding heterogeneity, and 3) using Co-59 chemical shift and relaxation parameters to monitor the state of $Co(NH_3)_6^{3+}$ over the B-Z transition.

Tu-Pos332 **Determining ΔG, ΔH and ΔS Using Quantitative Footprinting Methods.** Koren Kissinger, Jerry Goodisman and James C. Dabrowiak, Department of Chemistry, Syracuse University, Syracuse, New York 13244-1200.

The sequence specificity and thermodynamics of binding of a mono-cationic lexitropsin ligand have been studied using quantitative DNase I footprinting methods. Autoradiographic data from five footprinting experiments at 0°, 15°, 25°, 37° and 45° C in the presence of carrier DNA and one experiment at 37° C in the absence of carrier DNA were scanned using microdensitometry. The density data were corrected for gel loading errors. The data for four lexitropsin binding sites on the 139-mer, along with the analogous plots from sites where no drug binding was occurring, were analyzed (Biochemistry (1988) 27, 1198) to calculate binding constants for the lexitropsin toward its interaction sequences. The model considers ligand binding equilibria at each interaction sequence, as well as enhanced cutting by DNase I at non-ligand binding sites. For each binding site, a plot of the logarithm of the footprinting-derived binding constant versus the reciprocal of temperature, van't Hoff plots, is linear with a correlation coefficient >0.9. The observed values of ΔH for the four sites were: all 5′→3′ (kcal/mole), ACGCAG, -8.11; ACCGTG, -14.2; TCGTCA, -18.5; ACCGTC, -17.6. The work demonstrates that it is possible to obtain thermodynamic information as a function of sequence for drugs and other ligands bound to natural DNA molecules.

Tu-Pos333 STUDY OF THE MAMMALIAN cGMP-GATED CHANNEL IN EXCISED MEMBRANE PATCHES.
H.Lühring & U.B.Kaupp, Abteilung Biophysik, Universität Osnabrück, FRG

We studied the electrical properties of the cGMP-gated channel by measuring macroscopic cGMP-activated currents in excised membrane patches from bovine rod photoreceptors. Currents were cooperatively activated by cGMP (n = 2.3 and EC_{50} = 55 µM). In the absence of divalent cations, the I-V relation was only weakly rectifying and perfectly matched the I-V curve recorded from amphibian rod cells. Relative ion *permeabilities*, determined from the reversal potential under symmetrical biionic conditions (120 mM), were $NH_4^+ > Li^+ > Na^+ > K^+ > Rb^+ > Cs^+$ = 1.96:1.3:1:0.9:0.7:0.6. A different selectivity sequence was obtained for the relative *conductance* determined from the macroscopic membrane current at +60 mV: $NH_4^+ > Na^+ \geqslant K^+ > Rb^+ > Li^+ \geqslant Cs^+$ = 1.5:1:0.95:0.6:0.34:0.25. When Li^+ was present in the perfusion bath, Na^+ currents were blocked. We suggest that Li^+ and Na^+ compete for a common binding site within the channel pore. A similar mechanism could be responsible for the block of the cGMP-gated channel by divalent cations.
Present address:Institut für Biologische Informationsverarbeitung, KFA Jülich, POB 1913, D-5170 Jülich, FRG

Tu-Pos334 DIRECT ACTIVATION of cGMP-DEPENDENT CHANNELS OF RETINAL RODS BY THE cGMP PHOSPHODIESTERASE.
N. Bennett, M. Ildefonse, S. Crouzy, Y. Chapron & A. Clerc. Laboratoire de Biophysique Moléculaire et Cellulaire, Centre d'Etudes Nucléaires de Grenoble, 85X, 38041, Grenoble cedex, France.
"Intr. By Raymond Kado".

Vesicles from purified bovine retinal rods were incorporated into planar lipid bilayers in order to study the cationic conductances of the membranes. When the membranes are stripped of all peripheral proteins (G-protein and cGMP-phosphodiesterase involved in the mechanism of phototransduction), cationic fluxes are only observed in the presence of cGMP, suggesting that the only channels present in the membranes are the cGMP-dependent channels. Reconstitution experiments in which purified cGMP phosphodiesterase and/or G-protein are reassociated to the vesicles provide evidence for a direct interaction between the cGMP-dependent channel protein and the phosphodiesterase. This interaction is modulated by light :

i) in its inhibited state, the phosphodiesterase markedly stimulates the activity of the channels in the presence of cGMP (situation in the dark adapted rod), but is not capable of activating the channels in the absence of cGMP.
ii) in the absence of cGMP however, activation of the phosphodiesterase by G_{GTP} (equivalent to photoexcitation) induces the opening of cation channels which closely resemble the cGMP-dependent channels and have the same conductance for sodium ions (20-22 pS with two sublevels of about 7 pS and 13 pS).

Tu-Pos335 **RESONANCE RAMAN STUDIES OF HOOP MODES IN OCTOPUS VISUAL PIGMENT**
***P. Rath, *R.H. Callender, **Y. Koutalos, **T.G. Ebrey, +M. Tsuda and ++J. Lugtenberg.; *Physics Department of City College New York, New York; **Department of Physiology and Biophysics, Univ. of Illinois, Urbana, Illinois; +Saporo Medical College, Saporo, Japan and ++University of Leiden, Leiden, Netherlands.**

The isolated Hydrogen Out Of Plane (HOOP) bending modes along the polyene chain of the visual pigment chromophores have strong Raman intensities appearing in the 800-1000cm^{-1} region. Octopus bathorhodopsin spectrum shows more strong HOOP modes compared to its bovine counterpart which is suggestive of a more strained chromophore structure probably due to the difference in the protein-chromophore interaction [1]. Although there is reason to believe that octopus rhodopsin isomerises from 11-cis to all-trans in presence of light, the Raman spectra are quite different as compared to either that of bovine rhodopsin or of model protonated Schiff bases [1]. We have undertaken isotopically labelled chromophore studies to probe the origin of the HOOP modes in octopus rhodopsin and bathorhodopsin which will provide hints in to the chromophore structure and the protein-chromophore interaction at specific sites.

1. Pande C., Pande A., Yue, K.T., Callender R., Ebrey, T.G., Tsuda, M.; (1987) Biochemistry, 26, 4941-4947

Tu-Pos336 LIGHT INDUCED MEMBRANE PROTEIN PHOSPHORYLATION IN THE BOVINE ROD OUTER SEGMENT: A MAGIC ANGLE SPINNING P-13 NMR STUDY. Arlene D. Albert, James Frey* and Philip L. Yeagle. Department of Biochemistry, SUNY Buffalo, Buffalo, N.Y. 14214 and *Department of Chemistry, Colorado State University, Fort Collins, CO 80523.

Magic angle spinning P-13 nucular magnetic resonance spectra of bovine rod outer segments, unphosphorylated and phosphorylated were obtained. In the phosphorylated samples the spectra showed new resonances not assignable to phospholipids. These resonances were present only when stimulation of receptor phosphorylation occurred. These resonances were not due to exogenous, soluble phosphorus-containing compounds. Limited proteolysis to remove the carboxyl terminal region of the photoreceptor that contains the phosphorylation sites removed these resonances. The chemical shifts were in the usual range for serine phosphate and threonine phosphate. The pKa obtained from a pH titration of the P-31 chemical shift was typical of serine phosphate. Therefore, these P-31 NMR resonances were assigned to the phosphorylation sites on membrane proteins in the rod souter segment disk membranes. The extent of phosphorylation, as derived from the P resonance intensity, was proportional to the extent of receptor activation (% bleach). These data indicate that it is possible to study phosphorylation sites on membrane proteins using MAS P-31 NMR,allowing one to study regions of receptors crucial to receptor function.

Tu-Pos337 PHYSICAL STUDIES OF α-$\beta\gamma$ SUBUNIT INTERACTIONS OF THE ROD OUTER SEGMENT G PROTEIN, G_t: EFFECTS OF MONOCLONAL ANTIBODY BINDING. M.R. Mazzoni and H.E. Hamm, Dept. Physiol. Biophys., Univ Ill. Coll. Med. Chicago, Chicago, IL.

We recently reported that a monoclonal antibody (MAb 4A) against the α subunit of G_t interrupts the interaction of photolyzed rhodopsin (R*) with G_t (Hamm et al., J. Biol. Chem. 262:10831 (1987). It is known that α-$\beta\gamma$ subunit interaction is critical for the R*-G_t interaction. We have shown that MAb 4A immunoprecipitates holo-G_t and thus does not appear to interrupt α-$\beta\gamma$ interaction. To evaluate the effects of antibody binding on α-$\beta\gamma$ interaction with an independent method, the hydrodynamic properties of G_t in the presence and absence of various antibodied were studied.

The sedimentation coefficients of holo-G_t, purified subunits, antibodies 4A and 4H, and MAb-G_t complexes were determined using linear sucrose density gradients (5-20% sucrose run at 41,000 rpm for 15 h at 4°C). The following sedimentation coefficients ($s_{20,w}$) were obtained: G_t, 4.0 ± 0.07; α_t, 3.48 ± 0.34; $\beta\gamma_t$, 3.75 ± 0.13; MAb 4A, 5.7; MAb 4H, 4.6; G_t-Mab 4H, 6.8. Control IgG had no effect on the migration of G_t. MAb 4A-G_t complexes resulted in α_t and MAb 4A comigrating at 6.7 S; the $\beta\gamma$ subunit migrated with a peak at 3.8 S, and a tail migrating at higher densities.

The major MAb 4A epitope is the α_t carboxyl terminal; the amino terminal does not appear to be involved in MAb binding (Hamm et al., Sci. 241:832 (1988). The ability of MAb 4A binding to cause subunit dissociation during the course of sedimentation suggests that a) the carboxyl terminal of α make up a part of the $\beta\gamma$ binding site **or** b) binding of MAb to the carboxyl terminus sterically hinders $\beta\gamma$ binding to a neighboring region. The pattern of $\beta\gamma$ trailing in sucrose gradients suggests that MAb 4A causes subunit dissociation via a steric hindrance mechanism.

Tu-Pos338 THE BLUE VISUAL PIGMENT IN *BUFO MARINUS* CONTAINS AN UNPERTURBED RETINAL PROTONATED SCHIFF BASE CHROMOPHORE: A RAMAN MICROPROBE STUDY.

Glen R. Loppnow, Bridgette A. Barry#, and Richard A. Mathies, Chemistry Department, University of California, Berkeley, CA 94720. #Present Address: Department of Biochemistry, University of Minnesota, St. Paul, MN 55108.

Vertebrate visual pigments contain 11-*cis* retinal bound via a Schiff base linkage to a lysine of a 41,000 D apoprotein called opsin. These pigments exhibit absorption maxima that range from 440 to 580 nm. To examine the molecular mechanism of wavelength regulation in visual pigments, we have used a Raman microprobe to study the structure of the chromophore in the 440 nm pigment found in green rods of the toad, *Bufo marinus*. Resonance Raman vibrational spectra of the retinal prosthetic group were obtained by focusing the probe laser on individual photoreceptors on a 77 K cold stage designed especially for microscopy. Since retinal Schiff bases absorb at 370 nm and their protonated forms absorb at 440 nm, a 440 nm-absorbing pigment may contain an unprotonated Schiff base that has its absorption red-shifted by interactions with protein charges or it may simply contain an unperturbed protonated Schiff base. The 9-*cis* isorhodopsin form of the green rod pigment exhibits a 1662 cm^{-1} C=NH$^+$ Schiff base stretching mode which shifts to 1636 cm^{-1} in D_2O. This demonstrates that the Schiff base linkage to the protein is protonated. Protonation of the Schiff base in the green rod pigment is sufficient to explain the 440 nm absorption maximum of this pigment without invoking any additional protein-chromophore interactions. The absence of additional perturbations is supported by the observation that the ethylenic band and perturbation-sensitive C_{10}-C_{11} and C_{14}-C_{15} stretching modes at 1142 cm^{-1} and 1190 cm^{-1} have the same frequency as those of the 9-*cis* retinal protonated Schiff base.

Tu-Pos339 CHOLESTEROL HETEROGENIETY IN BOVINE ROD OUTER SEGMENT DISK MEMBRANES. Kathleen Battaglia and Arlene D. Albert. Department of Biochemistry, SUNY/Buffalo School of Medicine, Buffalo, N.Y. 14214

Rod cells are responsible for vision at low levels of light. The outer segments of these rods contain a large number of internal membrane sacs, known as disks. Freeze fracture studies using filipin have suggested that newly formed disks are richer in cholesterol than those at the apical tip of the ROS (Andrews & Cohen, 1979, J.Cell Biol.81, 215 and Cladwell & McLaughlin, 1985,J.Comp.Neurology 236, 523). Electrophysiological studies have also shown a difference in the amplitude of the single photon response at the tip versus the base of the ROS (Schnapf, 1983, J.Physiology 343 147). The work described here uses the detergent digitonin to separate ROS disk membranes based on their cholesterol content and hence their position in the ROS. Sub-solubolizing concentrations of digitonin interact with the cholesterol in the disk membrane resulting in an increase in membrane density. This allows their fractionation on a sucrose density gradient. Digitonin treated disks isolated from these sucrose density gradients range in cholesterol to phospholipid mole ratios from 0.30 to 0.05. The phospholipid to protein ratios of these disks is uniform; approximately 65 phospholipids per rhodopsin. The lipid composition of the isolated disks was analyzed as a function of cholesterol content. Data on both lipid headgroup composition and fatty acid composition were obtained. This work represents compositional heterogeneity in disk membranes which may affect function. (Supported by NEI grant RO1-03328.)

Tu-Pos340 ABSORPTION SPECTROSCOPY OF THE RHODOPSIN OF *CHLAMYDOMONAS REINHARDTII*. Dorine Starace and Kenneth W. Foster. Department of Physics, Syracuse University, Syracuse, NY 13244-1130.

A convenient system to study rhodopsin, both *in vivo* and *in vitro*, is a unicellular eukaryote, *Chlamydomonas reinhardtii*. Through spectral studies of *Chlamydomonas'* reaction to light of different wavelengths (action spectroscopy), it has been shown that the photoreceptor of *Chlamydomonas* is functionally similar to vertebrate rhodopsin. It is therefore of great interest to characterize, *in vitro*, the Chlamydomonas photoreceptor. By mechanically breaking *Chlamydomonas* cells and separating the lysate into its constituents on a density gradient, the eyespot membrane fragments of the cell, containing the photoreceptors, can be isolated. In order to do a spectral profile of the photoreceptor *in vitro* and determine the isomer of retinal used in this receptor, absorption spectra of eyespot fragments reconstituted with different isomers of retinal were measured. Absorption spectra were measured between 370-620 nm, before and after a 545.5±38 nm bleach of the fragments. The absorption spectrum of unreconstituted eyespot fragments absorbs maximally at 498 nm and this absorption decays upon bleaching. After bleaching, reconstitution with 5μM 11-*cis* retinal restores absorption after 10 minutes, maximal absorption is 498 nm, and it decays upon bleaching. Addition of 5μM 9-*cis* retinal also restores the absorption, but 45 minutes is required for reconstitution and only a small absorption change is observed. An absorption change upon 5μM all-*trans* retinal reconstitution has not been observed. From comparison with the *in vivo* action spectra data, these experiments suggest that 11-*cis* retinal is the native chromophore of the *Chlamydomonas* photoreceptor.

Tu-Pos341 USE OF PH-DEPENDENT ABSORPTION CHANGES OF OCTOPUS RHODOPSIN MEMBRANES FOR MEASURING SURFACE CHARGE DENSITY AND SCHIFF BASE PK.

Y. Koutalos and T.G. Ebrey, Department of Physiology and Biophysics, University of Illinois, Urbana, IL 61801 and B. Honig, Department of Biochemistry, Columbia University, New York, NY 10027.

The chromophore of octopus rhodopsin is 11-cis retinal, linked via a Schiff base to the protein backbone. Its stable photoproduct, metarhodopsin, has all-trans retinal as its chromophore. The Schiff base of acid metarhodopsin (λ_{max} = 510nm) is protonated while that of alkaline metarhodopsin (λ_{max} = 376nm) is unprotonated. Metarhodopsin containing photoreceptor membranes were titrated and the apparent Schiff base pK was measured at various ionic strengths. From these salt-dependent pKs, and by using the Gouy-Chapman-Stern equation, the surface charge density of octopus photoreceptor membranes and the intrinsic pK of the Schiff base of metarhodopsin were obtained. The apparent pK of octopus rhodopsin's Schiff base was also measured and compared to metarhodopsin's. The significance of the measured quantities (charge density and pKs) will be discussed with respect to current models of octopus rhodopsin structure and color regulation.

Tu-Pos342 META I/META II KINETICS AND EQUILIBRIUM IN THE PRESENCE OF VARIABLE LEVELS OF CHOLESTEROL. Drake C. Mitchell, Martin Straume, James L. Miller, and Burton J. Litman, Department of Biochemistry, University of Virginia, School of Medicine, Charlottesville, Virginia 22908.

The effect of cholesterol on the kinetic and equilibrium aspects of Meta I-Meta II conversion was studied in egg PC vesicles containing purified bovine rhodopsin and 0, 15, and 30 mol% cholesterol. Kinetic and equilibrium spectrophotometric data was acquired from 10 to 37 degrees. Equilibrium constants derived from deconvolution of spectra containing Meta I/Meta II equilibrium mixtures agreed within experimental error with those derived from analysis of the kinetic data. The derived equilibrium constants decreased with increasing cholesterol content and with decreasing temperature. At 10 degrees the values were 0.30 and 0.15 for 0 and 30 mol% cholesterol respectively, and at 37 degrees they were 0.94 and 0.54 for 0 and 30 mol% respectively. These results show a direct correlation with a fractional volume parameter derived from fluorescence depolarization measurements (Straume and Litman, Biochemistry, in press). This correlation implies a positive volume change in going from Meta I to Meta II. This conclusion is in good agreement with the pressure dependence of the MetaI/MetaII equilibrium (Lamola et al., Biochemistry 13:738, 1974). These results demonstrate a strong coupling between lipid composition and the ability of rhodopsin to undergo the conformational change associated with Meta I to Meta II conversion. This conformational change is believed to be required for the binding and subsequent activation of G-protein. (Supported by NIH grant EY00548 and NSF grant PCM8316858).

Tu-Pos343 LIGHT ADAPTATION IN GEKKO RODS MAY INVOLVE CHANGES IN BOTH THE INITIAL AND TERMINAL STAGES OF THE TRANSDUCTION CASCADE. G. Rispoli & P.B. Detwiler. Univ. of Washington, Dept. Physiol. & Biophys., Seattle, WA.

In whole-cell voltage clamp (V_H = -29 mV) detached rod outer segments dialyzed with a standard internal solution containing 5 mM ATP, 1 mM GTP-γ-S, and 0 added Ca & Mg (no chelators) support an inward dark current that is suppressed by light. Responses evoked by moderate to bright flashes (520 nm, 20 ms) recovered to a maintained plateau that is less than the dark current before the flash. The plateau represents a new baseline dark current that is consistent with a step increase in phosphodiesterase (PDE) activity due to permanent activation of transducin (T_α) by GTP-γ-S, a hydrolysis resistant GTP analog. The decrease in dark current during the plateau is similar to the decrease in dark current caused by steady background illumination because both may be presumed to be associated with an abrupt increase in T_α and persistent stimulation of PDE. They are different in that the former is in dark while the latter is in light which causes continuous activation of the early, as well as the latter stages of the transduction process. To evaluate the relative roles of the initial and terminal transduction stages in light adaptation we compared the properties of dim flash responses superimposed on a plateau with those superimposed on background illumination that suppressed a similar fraction of dark current. Responses on a plateau are desensitized, reach peak early, and recover slower than responses in the dark before the plateau. Responses on a background, with or without GTP-γ-S are desensitized, reach peak earlier, and recover faster than responses in the dark. In the presence of GTP-γ-S when the background light is turned off there is a negligible change in baseline dark current but the recovery of the dim flash response is slowed.

Our results show that steady light accelerates response recovery in a way that is not mimicked by a fall in dark current due to continuous activation of the terminal stages of the transduction cascade. While recovery kinetics are influenced by Ca-regulated guanyl cyclase, the strength of the Ca feedback signal and its effect on outer segment enzymology should be similar for similar reductions in dark current. Consequently, we conclude that either the Ca feedback pathway is affected by light or that a transduction event preceding T_α production is involved in light adaptation.

Tu-Pos344 A 15-15′-B-CAROTENE DIOXYGENASE IN *CHLAMYDOMONAS REINHARDTII*. Jureepan Saranak, Dorine Starace and Kenneth W. Foster, Department of Physics, Syracuse University 13244-1130.

We have identified an oxygen dependent enzyme that converts β-carotene into retinal in the single-celled eukaryotic alga, *Chlamydomonas reinhardtii*. The alga shows phototaxis swimming in response to light due to a rhodopsin pigment even in the absence of oxygen. The sensitivity of the phototaxis is linearly dependent on the amount of rhodopsin formed from the retinal chromophore and opsin. Using cells lacking retinal synthesis, but with normal opsin, it was possible to measure the relative amount of retinal synthesis for a known amount of exogenous β-carotene added at different oxygen concentrations. In addition to the oxygen requirement we noted that exogenous addition of β-carotene results in a phototaxis action spectrum identical to that obtained with addition of 11-*cis* or all-*trans* retinal. It is likely that the enzyme splits β-carotene to retinal at the 15,15′ position since incorporation of fragments of β-carotene of different chain length gave action spectra shifted from the retinal spectrum. Probably this enzyme is homologous with the hypothesized 15-15′-β-carotene dioxygenase of humans that is responsible for conversion of dietary carotenes into the essential retinal and hence vitamin A.

Tu-Pos345 11-CIS-LOCKED ANALOGS OF RETINAL RESTORE SENSITIVITY TO BLEACHED RODS FROM THE TIGER SALAMANDER. D.W. Corson,[1,2] M.C. Cornwall[3], E.F. MacNichol[3], J. Jin[3], F. Derguini[4], T. Zankel[4], P. Mazur[4], R. Johnson[4], R.K. Crouch[2] & K. Nakanishi[4]. Depts. of [1]Pathology & [2]Ophthalmology, Medical University of South Carolina & [3]Dept. of Physiology, Boston University School of Medicine [4]Dept. of Chemistry, Columbia University.

The 11,13-dicis & 11-cis isomers of an 11-cis ring-locked (cycloheptatrienylidene) analog of retinal were used together with membrane current recordings and microspectrophotometry to explore the role of isomerization in phototransduction in isolated rods from the tiger salamander, Ambystoma tigrinum. The isomers were synthesized as described previously (H. Akita et al., 1980) and the purity was confirmed by HPLC. The compounds were applied at ~100ug/ml of Ringer in lipid vesicles to cells which had been desensitized by 2.5 log units with a bleaching light. Four cells exposed to the 11,13-dicis isomer recovered 1.4 ± 0.2 log units of sensitivity out of 2.6 ± 0.2 log units within 1 hour. Comparable resensitization was found for the 11-cis ring-locked isomer (1.2 ± 0.4 log units out of 2.4 ± 0.4 within 1 hour, n=2). The isomers restored currents evoked by test flashes to their pre-bleached amplitude and time course but shifted the spectral sensitivity maximum to shorter wavelengths. A control experiment with all-trans retinal did not restore any sensitivity, confirming Cornwall et al., 1983. Microspectrophotometric measurements revealed photopigments which had characteristic absorption maxima near 495 nm but which were stable in the presence of repeated exposures to lights which completely bleach normal pigments. The restoration of sensitivity by the analogs suggests either that excitation can be initiated without full cis to trans isomerization or that occupation of the chromophore binding site alone is sufficient to turn off a stable component of adaptation initiated by opsin. Supported by NIH grants EYO-7543, 1157 & 4939 and GM-36564.

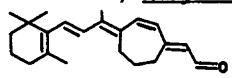

Tu-Pos346 LIGHT CONTROL OF ADAPTATION IN *PHYCOMYCES* PHOTOTROPISM. E. D. Lipson, P. Galland, M. Orejas, and L. M. Corrochano. Department of Physics, Syracuse University, Syracuse, NY, 13244-1130.

In the fungus *Phycomyces blakesleeanus*, phototropism and the related light-growth response operate over the intensity range from 10^{-9} to 10 W m^{-2}. Genetic and physiological experiments on *Phycomyces* have suggested previously that blue-light receptor pigments, probably flavoproteins, participate not only in in the light responses but also in the underlying adaptation phenomena that enable the organism to manage such large intensity ranges. In *Phycomyces*, the standard method for monitoring dark-adaptation kinetics is first to light-adapt the sporangiophore symmetrically, and then to change to unilateral light of lower intensity. The adaptation kinetics can be inferred from the dependence of the phototropic latency on the intensity of the unilateral light. In the present work, we have generalized this protocol by varying the conditions of the "subliminal" (i.e. subthreshold for phototropism), unilateral light applied during the latent period. We have found that the adaptation kinetics depend critically on these conditions. For subliminal light of wavelength 447 nm, the threshold for reducing the phototropic latency is about 10^{-11} W m^{-2}. Surprisingly, 575 nm light, which is generally ineffective for phototropism is about as effective as 447 nm light. Near-ultraviolet 347 nm light, which is very effective for phototropism, was, however, quite ineffective in reducing the phototropic latency. Our results suggest the presence of a novel green-light absorbing pigment in *Phycomyces*, that specifically regulates dark adaptation. (Supported by NIH grant GM29707)

Tu-Pos347 EDGE DETECTION AND NEURAL NETWORK IMPLEMENTATIONS USING ORIENTED FILMS OF BACTERIORHODOPSIN (BR). HIROYUKI TAKEI‡, ZHONGPING CHEN‡ AND AARON LEWIS*‡. ‡DEPT. OF APPLIED PHYSICS, CORNELL U., NEW YORK 14853 *DEPT. OF APPLIED PHYSICS, THE HEBREW U. OF JERUSALEM, ISRAEL.

We have exploited the unique optical and photoelectrical characteristics of BR in order to fabricate technologically useful devices that are based on the methodologies used in biological systems to perform computational tasks. We will demonstrate a scheme using oriented films of purple membrane for edge detection. Edge detection is an important step in retinal image processing where an edge can be located by calculating the zero in the second derivative of the image intensity. This is accomplished in nature by organizing the retina into receptive fields consisting of excitatory and inhibitory regions. The BR edge detector consists of dried purple membrane films in which BR is oriented along two opposite directions perpendicular to the membrane surface, one acting as an excitatory region and the other as an inhibitory region. We have shown that by appropriately designing the pattern of excitatory and inhibitory regions in the detector, we can effectively detect edges.

Neural network computation is another scheme that can use BR. Based on the biological evidence of how the brain functions, neural networks consist of a large number of highly interconnected neurons. BR can be used as a modifiable synapse in a neural network implementation that sandwiches BR films between two gratings oriented orthogonally to one another. In view of our development of purple membrane films in which images can readily be impressed and the known electro-optical characteristics of BR, it appears to have great potential as a high density reprogrammable neural network in addition to its use in a variety of other parallel computational schemes.

Tu-Pos348 4-OXORETINAL ANALOGUE PIGMENT OF BACTERIORHODOPSIN - CJ Beischel, V Mani, DR Knapp and RK Crouch Medical University of South Carolina, Charleston, SC 29425

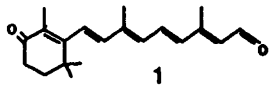

1

To further investigate the chromophore binding pocket of bacteriorhodopsin, the retinal analogue, all-trans 4-oxoretinal 1 was synthesized. Addition of 1 to bacterio-opsin generates a pigment with an absorption maximum of 524nm and a half-time of formation of 5 minutes. Addition of the native chromophore, all-trans retinal, to the apo-protein generates a pigment with an absorption maximum of 568nm and a half-time of formation <1minute that reversibly light and dark adapts. The blue shift in the absorption maximum from 568nm to 524nm in the pigment formed with 1 is readily explained by known protein-chromophore interactions. Irradiation of the analogue pigment with white light causes an irreversible 20nm blue shift and 30% decrease in the absorption maximum. This 20nm blue shift in response to white light is unusual in its magnitude, direction and permanence. The irradiated and non-irradiated pigments are stable to competition with all-trans-retinal and to hydroxylamine in the dark. Since the basis for this unusual shift is likely to be the state of the chromophore, the chromophores of both non-irradiated and irradiated 4-oxo pigments were extracted as oximes. The efficiencies of extraction and the absorption maxima are similar for the chromophore-oximes of these two pigments. HPLC analysis yields similar chromatograms for the all-trans 4-oxoretinaloxime in ethanol and that extracted from the non-irradiated pigment. HPLC analysis of the extracted chromophore-oximes from the irradiated pigment shows multiple peaks with retention times near those of 4-oxoretinaloximes. The nature of these extracted chromophores is being investigated using the enhanced gas chromatographic-mass spectrometric properties of the methoxime derivatives. (Supported by NIH-EY04939)

Tu-Pos349 PURIFICATION AND CHARACTERIZATION OF WILD-TYPE AND MUTANT FORMS OF BACTERIO-OPSIN EXPRESSED IN E. COLI. L. Miercke, R.F. Shand, M. Betlach, S. Fong, and R. Stroud. Dept. of Biochemistry and Biophysics, University of California, San Francisco, CA 94143.

Bacterio-opsin was expressed in E. coli at high levels as part of a fusion protein containing 13 heterologous residues at the amino-terminus. This "e-bO" was purified by size exclusion chromatography in the presence of SDS. Addition of CHAPSO, lipids, and retinal to purified e-bO resulted in 95-100% refolding to light-adapted bacteriorhodopsin (e-bR). Subsequently, lipids, SDS and excess retinal were removed by size exclusion chromatography in CHAPSO. The retinal regeneration, light absorption and proton pumping properties of the purified e-bR were identical to those observed for delipidated bacteriorhodopsin isolated and purified from the native halobacterial organism. Mutant forms of e-bO were generated using site-directed mutagenesis and expressed in E. coli in the same vector used for the wild-type. Analysis of the optical and functional properties of the purified proteins will be discussed.

Tu-Pos350 DETERMINATION OF THE ORIENTATION OF THE PROTONATED SCHIFF BASE GROUP IN LIGHT-ADAPTED BACTERIORHODOPSIN BY ABSORPTION LINEAR DICHROISM. Steven W. Lin and Richard A. Mathies, Department of Chemistry, University of California, Berkeley, CA 94720.

Knowledge of the orientation of the retinal Schiff base (C=NH) group in bacteriorhodopsin (BR) is essential for elucidating the proton-pumping mechanism. The plane of the chromophore is approximately perpendicular to the membrane plane in BR_{568} (Earnest et al., *Biochem.* 25:7793, 1986; Ikegami et al., *Springer Proc. of Physics* **20**:173, 1987). However, it is not known whether the N→H bond points toward the cytoplasm or the exterior. To address this question, we performed linear dichroism experiments on light-adapted purple membrane films containing native retinal (A_1) and its 3,4-dehydroretinal (A_2) analog. Calculations show that the angle between the transition moment and the long-axis of the polyene is 3.5° more for A_2 retinal than for A_1 retinal. Since the difference between the two transition moments is a vector which points along the C_3–C_4 bond, a comparison of the transition moment angles can be used to determine which way the ionone ring "points" in the membrane. Since the chromophore has an all-*trans* structure, this comparison will also enable us to specify the N→H orientation. The angles of the transition moments were found to be 72.3° ± 0.5 and 69.2° ± 0.4 from the membrane normal for A_1- and A_2- retinals, respectively, after correcting for mosaic spread. This shows that the N→H bond and the N→C_5 vector of the chromophore point toward the same membrane surface. Results from energy transfer experiments show that the center of the chromophore is 10 ± 3Å from the cytoplasmic membrane surface (Otomo et al., *Biophys. J.* 54:57, 1988) suggesting that the N→C_5 vector points toward the cytoplasm. Based on this assignment, we conclude that the N→H bond points toward the cytoplasm in BR_{568}. If Asp-212 is the counterion, this N→H orientation argues for a "backside" electrostatic interaction which is consistent with the weak hydrogen-bonding of the Schiff base.

Tu-Pos351 SURFACE POTENTIAL EFFECTS ON PROTON MOVEMENT IN PURPLE MEMBRANE

S. Y. Liu, R. Govindjee and T. G. Ebrey, Dept. of Physiology and Biophysics, University of Illinois, Urbana, IL 61801

When illuminated, purple membrane (PM) oriented in a polyacrylamide gel produces a photocurrent. The surface potential effects on the μs component (B2) of the photocurrent of the gel are studied. We found that in 100 mM KCl or 50 mM $CaCl_2$ the B2 component of the photocurrent correlates well with the L-M optical transition. This correlation holds up to pH 11 in the $CaCl_2$.

Upon decreasing the ionic strength (from 0.1 M to 0.1 mM), which should increase the surface potential, the B2 component becomes smaller and faster, however, the optical signal is not affected. The B2 component is smaller and faster in the monovalent cation solution than in divalent or trivalent cation solutions of the same concentration. Reducing the surface potential, either by removing the lipids with CHAPS or by neutralizing the carboxyl groups with glycine methyl ester makes the B2 component larger and slower. Reconstituted purple membrane with K^+ or Ca^{++} in the binding sites also shows different shapes of the B2 component although the L-M transition is not affected. All these experiments suggest that the B2 component represents a cation(s) moving away from the surface of PM and varying the surface potential affects this movement.

This cation(s) is probably a proton because the signal is affected by pH buffers. Measuring the pH change with a pH dye at different ionic strengths also shows that proton release by PM is reduced in low salt, but less than the B2 component is reduced. These experiments suggest that when the surface potential is increased, PM can still pump protons. However, the protons cannot leave the surface easily, and part of them may be trapped at the surface of PM.

Tu-Pos352 RETINAL ANALOG RECONSTITUTION OF BACTERIAL SENSORY RHODOPSIN I.

T. Takahashi[1], B. Yan[2], B. Rao[2], K. Nakanishi[2], J. L. Spudich[1], [1]Depts. Struct. Biol. Physiol. and Biophys., A. Einstein College of Medicine, Bronx, NY 10461; [2]Dept. Chemistry, Columbia University, New York, NY 10027.

Retinal analogs altered in their ring structure were introduced into the apoprotein of sensory rhodopsin I (SR-I) from Halobacterium halobium. The properties of the regenerated pigments in native membrane vesicles were studied by flash photolysis and photostationary state measurements, and SR-I analog-mediated phototaxis signaling studied by computerized cell tracking of swimming cells. Five analogs, in which ring components have been selectively removed (ring desmethyl or acyclic forms), share the common property of generating 2 photochemically reactive species of SR-I analog, distinguishable by their actinic wavelength dependence, kinetic constants, and absorption. In each case we observe a faster cycling species similar to native SR-I in its photocycling rate and absorption difference spectrum, and exhibiting lesser opsin shifts in absorption maximum than the native $SR\text{-}I_{587}$. Also in each case, we observe a slower cycling species with two absorption maxima (at ~420 nm and 530 -570 nm). The ratios of the fast to slow species range from 1:6 to 2:1. Since we observe a slight deviation from first order kinetics in the decay of the long-lived intermediate of native SR-I, it is possible all-trans retinal also produces two species of SR-I, but if so the major species as previously described (Spudich and Bogomolni, Annu. Rev. Biophys. Biophys. Chem. 1988. 17:193-215.) accounts for >90% of the flash-induced absorbance changes. Behavioral analysis indicates that the slow forms of the ring-altered analogs, though greatly perturbed from the native pigment spectroscopic properties, generate functional phototaxis signaling states of SR-I. We are conducting a similar analysis with other analogs, including locked isomeric forms.

Tu-Pos353 **SEQUENCE OF PROTON TRANSFERS BETWEEN BACTERIORHODOPSIN RESIDUES DEDUCED FROM FTIR SPECTRA OF SITE-DIRECTED MUTANTS**

M. S. Braiman†, T. Mogi, Th. Marti*, L. J. Stern*, H. G. Khorana*, and K. J. Rothschild†. From the *Departments of Chemistry and Biology, MIT, Cambridge, MA 02139 and the †Physics Department, Boston University, Boston, MA 02215.*

Bacteriorhodopsin (bR) mutants with single amino acid replacements at each of 4 Asp residues (Asp-85, 96, 115, and 212) were examined by means of low-temperature FTIR difference spectroscopy of the bR→K, bR→L, and bR→M photoreactions. Along with previously published spectra of bR containing isotope-labeled aspartic or glutamic acid, these data permit the assignment of FTIR difference peaks in the 1720-1760 cm^{-1} region to specific Asp residues in the bR sequence. Based on the spectral assignments, we conclude that Asp-96 is in the acid (COOH) form in bR and becomes deprotonated when L is formed and reprotonated when L decays to M. Asp-85 and Asp-212 appear to be deprotonated in bR; both gain protons during the L→M transition. Finally, Asp-115 appears to undergo hydrogen bonding changes while remaining un-ionized throughout the photocycle. Based on these results and existing models for bR folding in the membrane, a proton pumping mechanism is proposed in which the path of the proton is **Cytoplasm⇒Asp-96⇒Asp-212⇒Retinylidene Schiff's base⇒Asp-85⇒External medium.** *Supported by grants from the O.N.R., N.I.H., and N.S.F. M.S.B. is a Lucille P. Markey Scholar and this work was supported in part by a grant from the Lucille P. Markey Charitable Trust.*

Tu-Pos354 **EVIDENCE FOR THE INTERACTION OF TRYPTOPHAN-86 WITH THE RETINYLIDENE CHROMOPHORE IN BACTERIORHODOPSIN** *K.J. Rothschild, D. Gray, T. Mogi, Th. Marti, M.S. Braiman, L.J. Stern, and H.G. Khorana* **Dept. of Physics, Boston University, Boston, MA 02215 (KJR, DG and MSB) and Departments of Chemistry and Biology, MIT, Cambridge, MA 02139 (TM, ThM, LJS and HGK)**

Fourier transform infrared difference spectra have been obtained for the bR→K and bR→M photoreactions of bacteriorhodopsin mutants with Phe replacements for Trp residues 10, 12, 80, 86, 138, 182, and 189 and Cys replacements for Trp residues 137 and 138. None of the tryptophan mutations caused a significant shift in the retinylidene C=C or C-C stretching frequencies of the light-adapted bR_{570} state. Since these frequencies are known to be strongly correlated with the visible absorption maximum of the chromophore, it is concluded that tryptophans are not directly responsible for color regulation in bR. However, a 742-cm^{-1} negative peak attributed previously to the perturbation of a tryptophan residue during the bR→K photoreaction [P. Roepe *et al., J. Am. Chem. Soc.*, in press] was found to be absent in the bR→K and bR→M difference spectra of the the Trp-86 mutant. On this basis, we conclude that the structure or environment of Trp-86 is altered during the bR→K photoreaction. A model of bR is discussed in which Trp-86, Trp-137, Trp-182 and Trp-189 form part of a retinal binding pocket. One likely function of these tryptophan groups is to provide the structural constaints needed to prevent chromophore photoisomerization other than at the C_{13}-C_{14} double bond. *This work was supported by grants from the NSF (DMB-8509587) to KJR, NSF (PCM-8110992), NIH (GM28289-06) and ONR (N00014-82-K-0668) to HGK, and from the Lucille P. Markey Charitable Trust to MSB.*

Tu-Pos355 **^{15}N NMR EVIDENCE FOR A COMPLEX SCHIFF BASE COUNTERION IN BACTERIORHODOPSIN**

H.J.M. de Groot,[*-@] G.S. Harbison,[#] P.B. Rosenthal,[@&] A.C. Kolbert,[@] J. Herzfeld[*] and R.G. Griffin.[@]
* Dept. of Chemistry, Brandeis University, Waltham, MA 02254; @ Francis Bitter National Magnet Laboratory, MIT, Cambridge, MA 02139; - Gorlaeus Laboratoria der Rijksuniversiteit te Leiden, 2300 RA Leiden, The Netherlands; # Dept. of Chemistry, State University of New York, Stonybrook, NY 11974; & Committee on Higher Degrees in Biophysics, Harvard University, Cambridge, MA 02138.

High resolution solid state NMR techniques have been used to study the Schiff base nitrogen in bacteriorhodopsin (bR) and model compounds. Chemical shifts were measured for bR568 (light adapted), bR600 (blue) and bR565 (acid purple). The chemical shift of bR600 is remarkably low (about 130 ppm), while the chemical shift of bR565 (145 ppm) is close to that of bR568 (144 ppm). Thus, the chemical shift correlates with color, rather than with pH. Interestingly, the ^{15}N chemical shifts of N-all-*trans* retinylidene butylimine salts are linearly related to the frequency of maximal visible absorbance, with a slope indistinguishable from that for the bacteriorhodopsins. This slope represents the contribution of local electronic variations to the opsin shift, while the difference in the intercepts of the two lines must represent contributions to the opsin shift elsewhere in the chromophore. Of all the salts studied (including halides, carboxylates, phenolates and triflate), the most shielded nitrogen occurs in the tetrafluoroborate (150 ppm), which is still well downfield from bR568 and bR600. This suggests the presence of a complex counterion in bacteriorhodopsin. Tnis work was supported by the NIH (grants GM36810, GM22316, GM23289 and RR00995) and the ZWO.

Tu-Pos356 ASP85 AND ASP96 ARE INVOLVED IN DE-AND REPROTONATION OF THE SCHIFF BASE DURING THE CATALYTIC CYCLE OF *BACTERIORHODOPSIN* J. Tittor, J. Soppa, D. Oesterhelt, H.J. Butt* and E. Bamberg*, Max-Planck-Institute for Biochemistry, D-8033 Martinsried, *Max-Planck-Institute for Biophysics, D-6000 Frankfurt/Main, Kennedyallee 19, W-Germany

Phototroph negative mutants of *Halobacterium spec. GRB* were randomly produced by UV and x-ray mutagenesis and subsequently selected with the bromodeoxyuridine method. Two point mutations D85->E and D96->N were isolated and showed the following characteristics: The absorption maximum of D85->E was redshifted by about 40 nm to 610 nm with a pronounced shoulder at 550 nm. This species could be enriched by illumination of the original sample with red light (>610 nm) and by increasing pH. Also the action spectrum of stationary photocurrents of oriented purple membranes in polyacrylamide showed a maximum at 530 nm. The rise time of the M intermediate was found to be 5 us compared to 50 us in the wildtype. The mutant D96->N showed absorption characteristics like the wildtype but its M-decay was slowed down to 500 ms. Other time constants of the photocycle remained unaffected. The stationary and kinetic behaviour of light-induced pump currents were in good agreement with the spectroscopic data. It is concluded that Asp85 serves as the proton acceptor of the Schiff base whereas Asp96 catalyzes the reprotonation of the Schiff base and participates directly in the proton pumping pathway.

Tu-Pos357 DECOMPOSITION OF FTIR DIFFERENCE SPECTRA AND THE MICROENVIRONMENT OF THE CHROMOPHORE SCHIFF-BASE IN BACTERIORHODOPSIN

Shuo-Liang Lin, Department of Physics, University of Illinois at Urbana-Champaign

FTIR difference spectroscopy has shown that aspartic acids are responsible for the photoreaction-induced absorption changes for bacteriorhodopsin (bR) in the carboxyl stretching region [Eisenstein et al. 1987, *JACS* 109, 6860]. The very low noise level (near 10^{-5} O.D.) in the data enables us to fit the spectra in this region. The best fits for the K/LA, L/LA and the M/LA difference spectra contain three to five Gaussian components, which can be associated with three aspartic acids. Analysis of the fitting provides an insight into the environment of these residues. It is likely that interaction and proton exchange between them and the bR chromophore occur during the photoreaction.

The 3.9Å Schiff-base–counterion distance suggested by the point charge model [Spudich et al. 1986, *Biophys. J.* 49, 479] leads to the question of whether this simple ion pair is stable in an apolar environment if the counterion is a negatively charged residue. An energetically more plausible configuration is presented which places an aspartate, a tyrosinate and a speculated positive charge in the vicinity of the Schiff-base This quadrupole scheme can retain the main feature of the point charge model but does not allocate the role of counterion to a single residue Possible alteration of the quadrupole during the photocycle is found to be consistent with the FTIR data. [Supported by NIH Grant PHS R01 GM32455 and University of Illinois Graduate College Fellowship in Physics]

Tu-Pos358 ADDITION OF GLUCOSE TO PURPLE MEMBRANES USED IN ELECTRON DIFFRACTION STUDIES MAY CAUSE TILTING OF THE BACTERIORHODOPSIN HELICES. N.J. Gibson and J.Y. Cassim, Department of Microbiology, The Ohio State University, Columbus, Ohio 43210

The orientation of the transmembrane α-helical segments of the membrane protein bacteriorhodopsin (bR) in purple membrane (PM) is still the subject of debate. While electron diffraction studies suggest that a substantial degree of helix tilt exists[1], circular dichroism (CD) studies of oriented PM films indicate that the helices are essentially untilted[2]. Furthermore, while electron diffraction work indicates little change in helix orientation on formation of $M_{1:2}$[3], CD techniques suggest that the helices are tilted substantially in this state[4]. Dehydration of PM films by vacuum has been found to cause tilting of the helices and polyhydric alcohols have been found to facilitate this effect[5]. Because native PM films lose their periodic structure under the usual vacuum encountered in electron microscopic studies, they are routinely protected by the addition of small amounts of glucose. CD studies of PM films now suggest that glucose, like other polyhydric alcohols, does cause a tilting of the bR helices. Indeed, glucose is able to cause this tilting even at atmospheric pressure. It may be that the results of electron diffraction imaging studies of PM structure, obtained with glucose embedded native PM, are more representative of bR photocycle intermediates such as $M_{1:2}$.

(1) Henderson et al., 1986. Ultramicroscopy. 19:147-178. (2) Muccio & Cassim, 1979. Biophys. J. 26:427-440. (3) Glaeser et al., 1986. Biophys. J. 50:913-920. (4) Draheim & Cassim, 1985. Biophys. J. 47:497-507. (5) Draheim et al., 1988. Biophys. J. 54: (November).

Tu-Pos359 DEIONIZATION OF PURPLE MEMBRANE CAUSES TERTIARY STRUCTURAL CHANGES IN BACTERIORHODOPSIN. N.J.Gibson and J.Y.Cassim, Department of Microbiology, The Ohio State University, Columbus, Ohio 43210

The deionized (Ca^{++} and Mg^{++} depleted) form of purple membrane (PM), generally known as blue membrane because of its red-shifted λ_{max}, is unable to undergo the photocycle characteristic of native PM. A change in the structure of the sole protein, bacteriorhodopsin (bR), following deionization of the membrane seems likely due to the observation that cation removal affects the membrane surface[1], yet leads to absorption changes which are mediated by retinal-protein interactions in the deeper regions of the protein. Circular dichroism studies of blue membrane in oriented films now indicate that 1) blue membrane consists of two separate species (the existence of two retinal isomers in blue membrane has been previously determined with Raman spectroscopy[2]) and 2) blue membrane α-helices are tilted relative to the membrane normal, unlike the case for the native PM. Such tertiary structural changes for bR in the PM have previously been observed by this lab during the light-induced, hydroxylamine-mediated bleaching of the PM[3] and during the formation of the M_{412} photointermediate of PM[4]. This most recent finding implies a significant influence of membrane surface charge on the in situ protein structure and function.

(1) Szundi & Stoeckenius, 1987. Proc. Natl. Acad. Sci. USA 84:3681-3684. (2) Smith & Mathies, 1985. Biophys. J. 47:251-254. (3) Muccio & Cassim, 1979. Biophys. J. 26:427-440. (4) Draheim & Cassim, 1985. Biophys. J. 47:497-507.

Tu-Pos360 THE PURPLE-TO-BLUE TRANSITION OF BACTERIORHODOPSIN LEADS TO A LOSS OF THE HEXAGONAL LATTICE.

M.P. Heyn, H. Otto, C. Dudda and F. Seiff
Biophysics Group, Freie Universität Berlin, Arnimallee 14, D-1000 Berlin 33, FRG.

The X-ray diffraction pattern of the deionized blue membrane shows that the bacteriorhodopsin molecules are not organized in a surface lattice. Addition of 2 Ca^{++} per bacteriorhodopsin restores both the purple color and the normal (63 Å) hexagonal protein lattice. In the blue state the CD spectrum in the visible has the typical exciton features indicating that a trimer structure is retained. Time-resolved linear-dichroism measurements show that the blue patch rotates in aqueous suspension with a typical correlation time of 20 ms and provide no evidence for rotational mobility of bacteriorhodopsin within the membrane on the time scale from 1 µs to 10 ms. The CD spectra of the blue and the Ca^{++}-regenerated blue state in the far-UV are within experimental error identical indicating no difference in secondary structure. The thermal stability of the blue membrane is much smaller than of the purple membrane. At pH 4 irreversible denaturation of the blue form already sets in at 50°C. The photocycle of the blue membrane (λ_{ex}=580 nm) has an intermediate at 510 nm with a ms lifetime and has only a very small absorbance change at 410 nm. The purple to blue transition apparently involves a conformational change from a highly ordered and stabile hexagonal lattice to a disordered array of thermally more labile trimers.

Tu-Pos361 THE EFFECTS OF A CHANGE IN SURFACE POTENTIAL ON THE CONFORMATION OF BACTERIORHODOPSIN. N. A. Swords and B. A. Wallace, Department of Chemistry and Center for Biophysics, Rensselaer Polytechnic Institute, Troy, New York 12181.

The chromophore retinal is bound to bacteriorhodopsin via a protonated Schiff base linkage. The retinal binding site is reported to be buried in the transmembrane portion of the protein, far from the membrane surface. When bound to bacteriorhodopsin, the absorption maximum of the retinal is red shifted from 366 nm to 568 nm producing a purple color. This color persists across a wide pH range. However, when the pH is raised above 12.0, the protein becomes pink in color, while below a pH of 3.0, a blue color is produced. The blue color can also be obtained by treatment with chelating agents. In this study, bacteriorhodopsin was examined by circular dichroism (far UV) and absorption spectroscopy to determine the conformational changes associated with the color shifts. Although the retinal chromophore can be completely removed (by bleaching with hydroxylamine) with no significant influence on the secondary structure of the protein, a change in the surface charge of the protein appears to effect the retinal binding site and results in measurable conformational changes in the protein.

Tu-Pos362 CHLORIDE IONS AND THE LOW pH BLUE-TO-PURPLE TRANSITION OF BACTERIORHODOPSIN.
Robert Renthal, Ruben Regalado and Kevon Shuler, U. of Texas at San Antonio, San Antonio, TX 78285

Purple membrane (PM) turns blue when deionized or titrated to low pH. Blue membrane (BM) provides insight into both the origin of opsin shifts and the mechanism of the bacteriorhodopsin proton pump. Surprisingly, acid BM turns purple in the presence of chloride ion. We have now examined acid Cl^- PM by chemical modification, and UV-vis and FTIR spectroscopy. UV-vis: In 1 M H_2SO_4 (pH 0) PM is completely converted to acid BM. However, 1 M H_2SO_4 containing 1 M NaCl completely restores the purple chromophore. Titration with Cl^- shows hyperbolic curves for conversion of blue to purple, with an apparent K for chloride dissociation of 46 mM at pH 0, 0.67 M at pH 1 and 1.3 M at pH 2. Using a dansyl reporter group attached to Lys 41 as a pH indicator (pK=4.5) we find the surface pH of the cytoplasmic side of the membrane drops from 5.5 to < 3 upon conversion from neutral pH PM to deionized BM. However, conversion of acid BM to acid Cl^- PM is not accompanied by any detectable surface pH change. Chemical modification: The dansyl group on Lys 41 has no effect on apparent Cl^- binding, ruling out Lys 41 as a Cl^- binding site. Modification of surface carboxyl groups with water soluble carbodiimide, or arginines with cyclohexane dione, has no effect on apparent Cl^- binding. FTIR: An FTIR study of deionized BM by Gerwert et al. (FEBS Lett. 213:39,1987) showed > 10 surface carboxyl groups titrating, masking any specific changes due to formation of BM. Using acid Cl^- PM, we observe selective changes in carboxylic acid frequencies (at 1753 and 1731 cm^{-1}) due to the conversion from blue to purple pigment at essentially constant surface pH. (Supported by NIH GM 25483 and GM 07717, and the Welch Foundation)

Tu-Pos363 FAST PHOTOELECTRICAL SIGNALS FROM RECONSTITUTED HALORHODOPSIN MEMBRANES.
Sherie Michaile, Albert Duschl*, Janos Lanyi*, and Felix T. Hong, Department of Physiology, Wayne State University, Detroit, MI 48201 and *Department of Physiology and Biophysics, University of California, Irvine, CA 92717.

We report on studies of the fast photoelectric response of reconstituted halorhodopsin membranes. Halorhodopsin was incorporated into phospholipid vesicles. The halorhodopsin-containing vesicles were then deposited onto a thin Teflon film (6 micrometers), according to a method originally developed by Trissl and Montal (Nature Vol. 266, p. 655, 1977). Photocurrent responses to pulsed-light excitation of the pigmented membranes were measured using a tunable voltage clamp technique (Hong and Mauzerall, Proc. Natl. Acad. Sci. USA, Vol. 71, p. 1564, 1974). The fast photoelectric signals observed are compared to those observed in membranes that contain other retinal proteins. The chloride concentration of the bathing solution was found to have a dramatic effect on the time course of the photoelectrical signal. This effect is discussed in terms of halorhodopsin's known function as a light-driven chloride pump.
(Supported by ONR Contract No. N00014-87-K-0047 and DOE Contract No. DE-FG03-86-ER13525)

Tu-Pos364 RETINAL RECONSTITUTION STUDY OF TWO PHOTOTAXIS RECEPTOR MUTANTS OF HALOBACTERIUM HALOBIUM.
T. Takahashi, E. N. Spudich, J. L. Spudich, Depts. Struct. Biol. Physiol. and Biophysics., Albert Einstein College of Medicine, Bronx, NY 10461

Flx5R is a mutant which overproduces the apoprotein of sensory rhodopsin I (SR-I); Flx3b (T.Takahashi, S.Yorimitsu, K.Tsujimoto, N.Kamo, Y.Kobatake, submitted) is $SR\text{-}I^-$ and contains only the second sensory rhodopsin (called by various authors phoborhodopsin, P480, or SR-II). We have used retinal-deficient membranes of these strains to incorporate [^{3}H]retinal isomers purified by HPLC, to compare biochemical properties of the two sensory rhodopsins. The kinetics of reconstitution of SR-I with all-trans retinal fits well a simple bimolecular reaction scheme. 13-cis retinal forms an intermediate species (λ max 430 nm), which is slowly converted (half-time ~10 hours at room temperature) to a species with absorption spectrum indistinquishable from the native all-trans form $SR\text{-}I_{587}$. SR-II, unlike SR-I, incorporates 13-cis retinal rapidly to generate a pigment similar in absorption spectrum to the native form (λ_{max} 490 nm, ε 4.5±1 X 10^4 $M^{-1}\cdot cm^{-1}$, and shoulder at 465 nm). A methyl-accepting 94 kd M_r band, which is radiolabeled when [^{3}H]all-trans retinal is reductively linked onto the 25 kD M_r chromophoric polypeptide of SR-I (E.N. Spudich, C.A. Hasselbacher, J.L. Spudich, J.Bacteriol. 1988. 170:4280-4285.), is missing in Flx3b, confirming the assignment of this protein to SR-I.

Tu-Pos365 PROBING THE ABSOLUTE ORIENTATION OF THE BOUND RETINYLIDENE CHROMOPHORE IN PURPLE MEMBRANE AND LIGHT INDUCED DIPOLAR PROPERTIES BY SECOND HARMONIC GENERATION

Zhongping Chen*, Jung Y. Huang*, and Aaron Lewis‡* *Department of Applied Physics, Cornell University, Ithaca N.Y. 14853. ‡Department of Applied Physics, The Hebrew University of Jerusalem, Isarel.

Second harmonic generation has been used to measure the second-order nonlinear optical properties of bacteriorhodopsin (bR) and its chromophore direction in the membrane. The magnitudes and the phases of the second order molecular polarizability of bR in bR_{570} and M_{412} are obtained. The results are compared with data obtained from the free retinylidene chromophores spread at an air–water interface. From this comparison it is determined that upon electron excitation the dipole moment change of the retinylidene chromophore in bR_{570} appears larger than that of the free chromophore. Furthermore, using the optical second harmonic interference technique, the absolute direction of the retinylidene chromophore in bR_{570} is determined. Our data indicate that the β-ionone ring of the bound retinylidene chromophore points away from the cytoplasmic surface of the purple membrane fragment. Since this result is independent of the detailed trans-membrane structure of the α-helices of bR, our finding can be used as one of the objective criteria in the determination of the assignment of the helical segments of bR sequence to positions of helices in the structural map.

Tu-Pos366 AT LEAST SEVEN SITES APPEAR TO BE CLEAVED DURING PROCESSING OF THE BACTERIORHODOPSIN PRESEQUENCE. P.E. Ross, L.J.W. Miercke,* S.L. Helgerson and E.A. Dratz, Chem. Dept., Montana State Univ., Bozeman, MT 59717; *Dept. Biochem. & Biophys., UC, San Francisco, CA 94143.

Purified bacteriorhodopsin (bR) samples exhibit multiple isoelectric forms on immobilized pH gradient (IEF) gels. It has been reported that most purple membrane preparations contain three to four bR species with different apparent molecular weights. We have used high resolution two-dimensional (2D) electrophoretic gels (first dimension pH 4-7 immobiline IEF, second dimension 5-20% SDS-PAGE) to examine the relationship between the isoelectric and molecular weight forms. Mature bR has an isoelectric point (pI) of 5.20 and migrates with the lowest apparent molecular weight of 24.4 kDa together with isoelectric species at pI 5.50 and 5.60 which co-migrate on one-dimensional (1D) SDS-PAGE gels. All three species (pI = 5.20, 5.50 and 5.60) separate in the 2D pattern. The 2D pattern indicates that isoelectric species at pI 5.24, 5.28, and 5.52 co-migrate on 1D SDS-PAGE gels in a band at a slightly higher apparent molecular weight of 25.2 kDa. Finally, the 2D pattern reveals that isoelectric doublets at pI 4.90 and 5.07 co-migrate in a single band on 1D SDS-PAGE gels at an apparent molecular weight of 25.9 kDa. Based on sequence data, it has been proposed that the higher molecular weight species at 25.2 and 25.9 kDa on 1D SDS-PAGE are precursor forms of bR with N-terminal extensions. The 2D gel pattern, taken with papain cleavage experiments relating isoelectric shifts to protein charge, have led to a model of the sequences of the different isoelectric forms. These observations suggest that at least 7 different positions are cleaved in the 13 amino acid presequence of bR during in vivo processing. (Supported by ONR N00014-87-K-0278).

Tu-Pos367 A COMPUTER-CONTROLLED PATCH-CLAMP AMPLIFIER. F. J. Sigworth#, C. Koitz*, M. Pusch*, F. Würriehausen*, R. Penner* and H. Affolter#, #Dept. Cellular and Molecular Physiol., Yale School of Med., New Haven CT and *Dept. Membrane Biophys., Max Planck Inst. für Biophys. Chemie, Göttingen, FRG.

We have developed a patch clamp amplifier that has no front panel controls and only one internal trim adjustment; all of the usual controls and calibration adjustments are implemented through multiplying DACs and other digitally controlled devices. The controlling software (~4000 lines of Modula-2 code) provides automatic self-calibration, and allows access to the "front panel" controls as well as novel functions (e.g. automatic capacitance adjustment) at four different levels:

- o As Modula-2 procedures; e.g. PROCEDURE SetCFast(Farads : REAL);
- o As a menu that can be built into data acquisition programs, allowing settings to be made from the keyboard or by dragging a mouse;
- o As a program that simulates the "front panel", along with a stimulator and oscilloscope, in graphics on the screen of an Atari ST computer;
- o Through ASCII commands via a serial port from another computer.

The computer control of all patch-clamp functions allows complex protocols to be automated, and promises to simplify whole-cell and membrane-capacitance measurements.

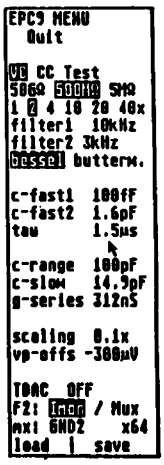

Tu-Pos368 A SWITCHED SINGLE ELECTRODE VOLTAGE CLAMP. APPLICATION OF CURRENT BOOSTING TO IMPROVE RESPONSE TIME. Alfred Strickholm, Physiology Section, Medical Sciences Program, Indiana University, Bloomington, IN 47405.

Sigworth (in: Single Channel Recording, (Plenum Press, N.Y., 1983), Sakmann and Neher, eds.) proposed a switching modification of the current to voltage convertor used in patch clamp amplifiers so that they could be used as a single electrode voltage clamp without series resistance compensation. The circuit proposed by Sigworth was modified by relocating the switching elements to provide minimum circuit delay times to optimize speed. In addition, current boosting was added to accelerate the settling time for membrane current and voltage. In this circuit design, a current to voltage convertor was modified so that when switched, the output voltage follows that of the amplifier input. Thus during the first half of the switching cycle, the output current becomes zero and the amplifier input voltage decays to the membrane potential with a time constant dependent on the microelectrode resistance and the input stray capacitance. The obtained membrane potential is sampled by a sample-hold amplifier, filtered, and compared with the command potential. The difference between the sampled membrane potential and command potential is amplified and used as the control voltage for the current to voltage patch clamp amplifier. In the second half of the switching cycle, the circuitry becomes an ordinary current to voltage convertor and the output current is sampled and held. Here, by repeated switching, the membrane potential is rapidly driven towards the command potential. Response time of the circuit, to 90% of command potential, with pipette resistance of 60 megohms, has been under 100 msec. This represents more than a ten fold improvement in response time over the ordinary current to voltage convertor.

Tu-Pos369 SINGLE CHANNEL RECORDING FROM CELLULAR ORGANELLES: IMPROVED TECHNIQUES

B.U. Keller[+], M. Criado[+], J. Kleineke[§], M.C. Sorgato[$], W. Stühmer[+]
[+]Max-Planck-Institut f. biophys. Chemie, 3400 Göttingen, [§]Universität Göttingen, 3400 Göttingen, F.R.G. and [$]Istituto di Chimica Biologica, I-35131 Padova, Italy.

Application of patch clamp techniques to intracellular membranes has been hampered by the small size of organelles. Using either osmotic swelling or the method of dehydration and rehydration, isolated organelles can be enlargened to form giant vesicles well suited for conventional patch clamp. Osmotic swelling was used to expand mitochondrial membranes from rat hepatocytes. Swollen mitochondria (mitoplasts) of 3-4µ in diameter were readily obtained without previous treatment with cuprizone (Keller et al. 1988, Biophys. J. 53, 31a). Patch clamp measurements revealed a voltage dependent anion channel (110pS in 150mM KCL) in the inner membrane of drug-free mitochondria. The method of careful dehydration (Criado and Keller, 1987, FEBS Lett. 224, No 1, 172-176) was used to enlargen endoplasmic reticulum (ER) membranes from the same source. Subsequent rehydration results in the formation of large membrane vesicles of 10-50µm in diameter. Single Cl^- channels (64pS in 50mM KCL) were observed in ER fractions isolated by Percoll gradient centrifugation. Osmotic swelling and the method of dehydration/rehydration promise to serve as valuable tools for future electrophysiological studies on intracellular membranes.

Tu-Pos370 **ON-LINE KINETIC ANALYSIS OF EXPERIMENTAL SIGNALS THAT BEHAVE LIKE MULTIEXPONENTIAL FUNCTIONS: APPLICATION TO CARDIAC ELECTROPHYSIOLOGY.**
Patrick Lechêne & Rodolphe Fischmeister. Laboratoire de Physiologie Cellulaire Cardiaque, INSERM U-241, Université de Paris-Sud, F-91405 Orsay, France.

A computer program, EXCALC, will be presented which performs a rapid kinetic analysis of multiexponential functions on an IBM-compatible personal computer (PC) under MS-DOS. The program, written in PASCAL language, is based on the powerful "Padé-Laplace" method (Yeramian & Claverie, Nature 326,169-174,1987) and on an earlier FORTRAN version (E. Yeramian, Doctoral Thesis, E.C.P., Chatenay-Malabry, 1986). When used on an Intel 80386/20 MHz-type PC with a mathematical coprocessor 80387, the complete calculation of the Padé approximants up to the order [9/10] of a signal f(t) containing 2000 regularly spaced samples requires 4-5 sec. The number of exponential components in the signal as well as the corresponding time constants and amplitudes must be extracted by the operator after scrutinizing the output table of Padé approximants and selecting the solution with the highest degree of stability. To increase further the performance of EXCALC an automated version has been written which 1) includes a logarithmically-variable sampling interval of f(t), 2) assumes f(t) constant between two consecutive samples (instead of using an integration procedure), and 3) searches automatically for stability within the output table of Padé approximants. Under these conditions, the complete kinetic analysis of a 2000 data points signal can be performed within 3-6 sec and the fit corresponding to the optimal multiexponential solution is drawn on to the screen on top of the original signal. These modifications allow EXCALC to be used on-line during an experiment, as will be demonstrated for the analysis of Ca current recorded from frog ventricular cells.

Tu-Pos371

DNANALYZE: A COMPREHENSIVE NUCLEOTIDE AND AMINO ACID SEQUENCE ANALYSIS SYSTEM EMPHASIZING SEQUENCE SIMILARITY COMPARISONS. **G.R. Wernke and R.L. Thompson. Intr. by Lois K. Lane. Department of Molecular Genetics, Biochemistry and Microbiology. University of Cincinnati.**

An all purpose nucleotide and amino acid sequence analysis package, called DNANALYZE, has been developed for the IBM PC type microcomputer, operating under the MS-DOS operating system (v3.0 or above). Because the most important aspect of any comprehensive sequence analysis package is the comparison routines of which it is comprised, DNANALYZE provides a number of comparison routines that are designed to provide an over-lapping, multiple level approach to sequence comparison problems. The comparative analysis routines contained within the DNANALYZE system are designed to facilitate this type of multiple level analysis approach. DNANALYZE can perform any type of comparison; from similarity scans of Genbank (Bilofsky et. al. 1986) and P.I.R. (George et. al. 1986) to comparisons of sequences to find common functional domains or sites. In general, the system's comparison routines operate on three "levels" of analysis. Level one consists of the data bank scanning routines. The level one nucleotide data base comparison routines are designed to interact effectively with the Genbank data base as issued by Intelligentics with only minor modifications. Level two allows the user to examine smaller groups of sequence at more sensitive match levels. The level two routines examine sequences found by the level one routines by using more efficient, though slower, comparison methods. Comparison level three provides very rigorous pair wise similarity comparison and optimal alignment comparison methods to the user. The capability of the routines comprising each level will overlap somewhat with other levels, yet each comparison routine in the system is fully independent of each other

Tu-Pos372 ELECTROCHEMICALLY DETERMINED MACROMOLECULAR REACTIONS OF N-OXIDIZED PROCAINAMIDE METABOLITES. JF Wheeler, WR Heineman, L Adams, R Govind, EV Hess; Intr. HB Halsall, College of Medicine and Depts. of Chemistry and Nuclear Engr., University of Cincinnati, Cincinnati, OH 45221.

The use of procainamide (PA) as an anti-arrhythmic drug has been linked to the onset of the autoimmune disorder Drug-Related Lupus (DRL) in a large percentage of those patients treated. While no mechanism has been established, recent emphasis has been placed on the N-oxidized metabolites PA hydroxylamine (PAHA) and nitroso PA (NOPA). It has been suggested that covalent binding of one or both of these metabolites to a specific macromolecule(s) may result in the production of autoantibodies, thereby eliciting the autoimmune response. To investigate this possibility, we are attempting to develop an appropriate animal model for monitoring immunomodulatory effects of PA in vivo. We have been successful in entrapping PA into liposomes for controlled drug delivery with minimal adsorption to membrane surfaces and no loss of activity following lysis. Recently, we described a controlled synthesis of NOPA utilizing a two electron electrochemical oxidation of PAHA, and demonstrated the greater stability of NOPA for in vivo studies. Subsequently, we have employed HPLC with electrochemical detection (LCEC) to determine the covalent and/or non-specific binding behavior of PAHA and NOPA with selected biomolecular species. Current decay is monitored as a function of time versus control to quantitate amounts of metabolite which have reacted. Our data suggest significant interaction of both PAHA and NOPA with mouse hemoglobin (>70% methemoglobin), which contrasts with the simple sulfhydryl redox behavior we observe for NOPA/glutathione incubations. Additional "binding" interactions are observed for incubations of these metabolites with selected calf-thymus histone subfractions. This is of particular significance since antibodies to histone serve as clinical markers for the diagnosis of patients as DRL positive. Results of these studies and their implications in the immunologic effects of PA will be discussed.

Tu-Pos373 TWO-DIMENSIONAL HIGH PERFORMANCE LIQUID CHROMATOGRAPHY, M. Molinaro, P.J. Baxter-Rahmoeller, and H. Mizukami. Division of Regulatory Biology and Biophysics, Department of Biological Sciences, Wayne State University, Detroit, Michigan, 48202.

High performance liquid chromatography is a widely used technique in industry as well as in the research laboratory. The technique allows for separations of complex mixtures into their components for collection and/or identification. With judicious choice of column and operating conditions, one may obtain spectra that clearly reflect the complexity of their sample as well as give information about the concentrations of the elements present. If one could then further separate a given fraction through use of a different column, even more conclusive information about the original sample could be obtained. Such an idea is already in use in 2-dimensional gel electrophoresis. We propose that a similar 2-dimensional approach to HPLC is feasible and desirable.

A size-exclusion column was used to perform the initial separation and the fractions were collected at regular time intervals. The fractions were then individually chromatographed through a second column, e.g. a cation-exchange column, and all the absorption spectra of the eluent collected and reduced to numerical, computer-compatible files. These files were then read by our 2-dimensional HPLC program which then reduced the data to three different representations. These representations included : (1) an output very similar to the appearance of a 2-dimensional gel, (2) one resembling the results that might be obtained from a topographical representation from a 2-D gel scanner, and (3) a standard 2-D representation of 3-D traces (output of peaks and valleys). We will present samples of each of these representations with several differing samples.(Supported partially by a grant from NIH HL 16008)

Tu-Pos374 CELLULAR RESPONSES TO BIOLOGICAL EFFECTOR MOLECULES MONITORED WITH A BIOSENSOR: A RAPID BIOASSAY FOR INTERLEUKIN-2 . Owicki, John C., Kercso, Karen M., and Parce, J. Wallace, Molecular Devices Corporation, 3180 Porter Drive, Palo Alto, CA 94304.

Proliferation of the CTLL cytotoxic T lymphocyte cell line requires Interleukin-2 (IL-2), and radiothymidine incorporation into CTLL cells is a widely used bioassay for IL-2. Using a biosensor based on the light-addressable potentiometric sensor [Hafeman et al. (1988) Science 240:1182] we have determined that the metabolic activity of CTLL cells is sensitive to the level of IL-2 and that changes in ambient IL-2 levels can thus be detected on the time scale of ~1 hour. The radiothymidine proliferative assay typically requires ~24 hours of cell culture before radioisotope counting. Our apparatus is a flow chamber in which a 100μm layer of medium flows across a $1cm^2$ region of cells. Non-adherent cells (such as CTLL) can be trapped in the chamber by a variety of gentle means, and adherent cells grow as a monolayer on a chamber surface. Signals are obtained from optically selectable ~$1mm^2$ regions within the flow chamber, corresponding to about 1,000 cells in 100 nL. When flow is temporarily interrupted, production of CO_2 by the cells slightly acidifies the medium, and the rate of this pH change is a measure of the overall metabolic activity of the cells. This process is detected by the sensor, which forms one surface of the chamber. Resumption of flow introduces fresh medium and resets the pH for subsequent measurements. At present the time resolution for metabolic measurements is tens of seconds. With normal culture medium, metabolic rates that are stable to within a few percent can be repetitively measured for hours. The measurements are non-destructive, so that repeated observations can be made on the identical population of cells. The device can be automated easily. We have observed the effects of a variety of hormones, irritants, and cytotoxic agents on the metabolic activity of several types of cells. With variations on this apparatus it should be possible to monitor redox potential or ion concentrations (e.g., K^+) instead of pH. Trans-eipthelial potentials can also be monitored. Supported in part by ARO contract DAALOO3-86-C-0009.

Tu-Pos375 GIGAHERTZ CROSS-CORRELATION PHASE FLUOROMETRY WITH SMALL SIDE-ON PHOTOMULTIPLIERS. Martin vandeVen and Enrico Gratton, Laboratory for Fluorescence Dynamics, Department of Physics, University of Illinois at Urbana-Champaign, 1110 W. Green, Urbana, IL 61801.

Multifrequency cross-correlation phase fluorometry is one of the techniques extensively used at present to study the dynamic behavior of proteins via the intrinsic fluorescent residues, Tryptophan and Tyrosine. A microchannel plate photomultiplier (MCP-PMT) light detector with external cross-correlation is one way to obtain a Gigahertz frequency response. Many phase instruments, however, are equipped with small and inexpensive Hamamatsu R-928 side-on photomultiplier tubes (PMT). By optimizing the electronic circuitry and redesigning the geometrical and optical layout, the frequency response of a R-928 PMT can be significantly increased to approximately one Gigahertz with either method of cross-correlation: internal or external. The influence of various parameters, e.g., PMT supply voltage, geometrical effects, and light intensity on the high frequency response, will be shown. An ultra-stable pico-second pulse train excitation light source is essential for this type of experiment. Supported by NIH grant RR03155.

Tu-Pos376 **BIOLOGICAL PHOTOCATHODES.** O. Hayes Griffith, Douglas L. Habliston, G. Bruce Birrell, Walter P. Skoczylas, and Karen K. Hedberg, Institute of Molecular Biology and Department of Chemistry, University of Oregon, Eugene, OR 97403.

Biological surfaces emit electrons when subjected to UV light. This emission is increased greatly after exposure to cesium vapor. Increases of from two to three orders of magnitude are observed, depending on the biochemicals present. Heme and chlorophyll exhibit unusually high photoemission currents. These changes in photoelectric properties are accompanied by pronounced changes in color. Photoemission from proteins and lipids is much less, but also can be increased by exposure to cesium. The formation of biological photocathodes with cesium greatly increases the practical magnifications attainable in photoelectron microscopy of organic and biological specimens. Photoelectron micrographs of light-harvesting chlorophyll complexes and of immunogold labeled cytoskeleton preparations of cultured epithelial cells at or above x100,000 demonstrate the improvement in magnification. Forming biological cathodes also opens up the possibility of the detection of chromophore binding proteins in membranes and the use of photoelectron labels for tagging specific sites on biological surfaces. (Supported by PHS National Cancer Institute Grant CA 11695.)

Tu-Pos377 A FIBER-OPTIC PHASE AND MODULATION LUMINOMETER, J. Ricardo Alcala, E. Shyamsunder (*), Beauford W. Atwater and Jennifer W. Parker. The BOC Group Technical Center, 100 Mountain Ave., Murray Hill, NJ 07974. (*) Physics Department Princeton University, Princeton, NJ 08544

A commercial instrument was modified to perform phase delay and modulation ratio measurements using single 100 micron graded index optical fibers. The excitation was provided by a mode-locked laser system. A bidirectional coupler was used to (i) conduct the excitation to the sample (ii) conduct the excitation to the reference detector and (iii) conduct the luminescent response to the sample detector. The use of optical fibers eliminates the need of optical tables in fluorescence and phosphorescence spectroscopy. As an application of the use of optical fibers in frequency domain spectroscopy the fluorescence and phosphorescence lifetimes of luminescent systems were determined. Details of the instrumentation and luminescent systems of interest will be discussed.

Tu-Pos378 NEAR INFRARED PHOSPHORESCENCE IMAGING USED TO DETERMINE OXYGEN DISTRIBUTIONS IN ISOLATED PERFUSED HEART AND LIVER. W. L. Rumsey, D. F. Wilson* & J. M. Vanderkooi*, Dept. of Biochemistry & Biophysics, University of Pennsylvania School of Medicine, Philadelphia PA 19104

An optical method to measure oxygen has been devised based upon a bimolecular reaction of oxygen with excited triplet states. Oxygen concentrations in solutions at room temperature can be determined from quenching of phosphorescence intensity and decrease in phosphorescence lifetime. This technique is now used to detect oxygen levels in cells and in the surface layers of tissues. Pd-coproporphyrin (1 uM), a dye which remains in the vasculature, was included in perfusion media for isolated rat liver and heart. The intensity of phosphorescence, detected by an infrared sensitive video camera, depends upon the perfusion rate. When flow was stopped, phosphorescence intensity increased several fold. Gradual reperfusion of the tissue with oxygenated buffer resulted in mottled patterns of phosphorescence intensity, indicating varying concentrations of oxygen. Heterogeneity of oxygen distribution in tissue reflects the varying patterns of flow and differences in metabolic rate within regions of tissue. Near infrared phosphorescence can be used to sensitively determine oxygen concentrations in a wide range of biological samples, including intact tissue (Supported by NIH grant GM 36393)

Tu-Pos379 SINGLE-CHANNEL CURRENT SIMULATION AND RECORDING USING A PHOTODIODE AS CURRENT GENERATOR. D. Bertrand, C-R. Bader, C. Distasi and I.C. Forster* Departement de Physiologie, CMU, Geneva and Physiologisches Institut, Uni. Zurich*, Switzerland.

Hardware based around a specially selected low noise, high speed photodiode has been developed to facilitate the tuning of patch clamp amplifiers and test the capabilities of post-acquisition software to extract kinetic parameters from single channel records. The photodiode connects directly to the input of the headstage and under zero bias conditions adequately simulates a gigaseal ($R > 10\ G\Omega$). By optically coupling the photodiode to an LED via a fibre optic link, ideal isolation is achieved and rectangular current pulses with rise-fall times < 500 ns in the pico-ampere range can be injected into the headstage. The overall transfer function is linear in the range 0-10 pA. The LED current is controlled by a PC driven DA converter which allows single and multiple channel simulations to be performed. This method provides a simple low cost solution to the problem of generating pico-ampere currents at the headstage input and obviates the need to use high value resistors having non-deal electrical characteristics.

The hardware and software aspects of this system will be discussed and examples of post acquisition analysis using single channel, multiple state models to generate data with known kinetic properties will be presented. Supported by Swiss NFG 3.594.0.87 and 3.143.0.85.

Tu-Pos380 **ALIGNMENT OF BIOLOGICAL ASSEMBLIES USING FERROFLUIDS.** Trewhella, J.*, Stubbs, G.+, Charles, S.x, Timmins, P.° *Life Sciences Division, Los Alamos National Laboratory, Los Alamos, NM 87545; +Dept. of Molecular Biology, Vanderbilt University, Nashville, TN 37235; xDept. of Physics, University College of North Wales Bangor, Gwynedd, UK LL5728W; °Institut Laue-Langevin, Grenoble 38042 Cedex France.

Scattering from isotropic solutions produces a 1-dimensional data set containing limited structural information due to spherical averaging. Scattering from oriented particles in solution produces a 2-dimensional data set that can provide more detailed information about molecular structure. We have been working with a ferrofluid system[1] that can be used to orient particles for neutron scattering studies. While orientation is achieved using a weak magnetic field, it does not depend on the intrinsic magnetic properties of the particle. Neutron scattering experiments have been completed on two rod-shaped viruses. Tobacco mosaic virus and tobacco rattle virus particles (with axial ratios of 16 and 8, respectively) were suspended in a deuterated ferrofluid in D_2O. The mean scattering density of the ferrofluid matched that of D_2O, thus, the neutron scattering data measured was dominated by that from the virus particles, and the ferrofluid particles were "invisible." The data showed that the particles could be oriented in the ferrofluid under conditions where even strong magnetic fields were not effective for orientation without ferrofluid. Furthermore, it was demonstrated that internal structure parameters such as the pitch of the helix formed by the viral coat protein subunits could be measured. We plan to apply this technique to biological systems that are less well characterized structurally, and to explore the potential for improving the orientation so higher resolution structural data can be obtained on the tobacco rattle virus.

[1]Hayter, J.B., Pynn, R., Charles, S., Skjeltorp, A.T., Trewhella, J., Timmins, P. "Ordered Macromolecular Structures in Ferrofluid Mixtures," submitted to Phys. Rev. Lett.

Tu-Pos381 IMAGING METHODS FOR NUCLEI WITH SHORT T_2 RELAXATION: APPLICATION TO ^{19}F AND ^{23}N IMAGING. C.B. Conboy, A.M. Wyrwicz*, and M. Nuss**, Department of Chemistry and *Department of Radiology, University of Illinois at Chicago, Chicago, IL, **Abbott Labs, Abbott Park, IL 60064

A modified spin-echo imaging sequence, which allows for a reduction of TE values, has been developed and applied to ^{19}F and ^{23}Na imaging. The sequence has been evaluated for image quality and signal-to-noise ratio and compared with spin-echo and gradient recalled imaging sequences. This version of the short TE sequence has been applied to ^{19}F imaging of halothane in rabbit brain. This technique allows for editing of the images and enhancement of the halothane signal from brain tissue. Due to the short T_2 component of ^{23}Na in tissue, a reduction of echo time is also advantageous to the imaging of this nucleus. The modified sequence has been used to monitor sodium levels in a rat kidney in vivo. Both systems have required novel coil designs for dual $^{19}F/^{1}H$ and $^{23}Na/^{1}H$ observation. A distributed capacitance solenoid coil has been used in the ^{19}F imaging experiments. This coil design provides excellent B_1 homogeneity and maximum sensitivity for the imaging experiments. A dual bird cage coil was implemented for the ^{23}Na imaging experiments. Both coil arrangements have produced good quality ^{1}H and multi-nuclear images. (Supported in part by UPHS grants GM29520, GM33415, and RCDA K04GM00503 to AMW).

Tu-Pos382 PROTEIN-WATER MAGNETIZATION TRANSFER IN VIVO. J. Eng, S.D. Wolff, B.A. Berkowitz and R.S. Balaban, LCE, NHLBI, Bethesda, MD 20892

We have developed an NMR method for detecting the exchange of magnetization between "free" water ^{1}H (H_f) and ^{1}H in regions of restricted motion (H_r) (i.e. proteins and "immobilized" water). This method is based on the saturation transfer technique. In these studies the H_r pool (broad line due to short T_2) was selectively saturated in vivo by irradiating (at ~1X10-6T) 5 to 10 kHz off of the H_f frequency. This caused a specific decrease in the magnetization and T_1 of the H_f pool which was not observed for fat and other metabolites in various biological tissues in vivo. The rate constant of exchange was determined from the ratio of H_f magnetization before and after irradiation (Mo/Ms) and the T_1 using standard methods. The rate constant for exchange from H_f to H_r was ~4 s^{-1} in the kidney and ~50 s^{-1} in skeletal muscle in vivo. The magnitude of these rate constants suggest that this process is a major mechanism of water proton relaxation in intact tissues. This exchange process was imaged in vivo using standard imaging techniques with irradiation of H_r during the sequence. Excellent contrast was generated in kidney, head, tumors and leg based on the decrease of magnetization or T_1, depending on the sequence used. The contrast generated by this technique is specific for this exchange process and independent of other T_1 or T_2 processes such as paramagnetic relaxation. Since the irradiation does not affect fat, cerebral-spinal fluid, urine or blood excellent contrast for structures containing these components were also obtained. This novel form of contrast may be useful in clinical characterization of tissue in vivo.

Tu-Pos383 TRANSIENT ENZYME KINETIC STUDIES USING STOPPED-FLOW CALORIMETRY

Millar,N.C[1], Howarth,J.V[1], Thorneley,R.N.F[2] and Gutfreund, H[3], The Marine Biological Association, Plymouth PL1 2PB, UK; Unit of Nitrogen Fixation, University of Sussex, Brighton BN1 9RQ, UK & Dept. of Biochemistry, University of Bristol, Bristol BS8 1TD, UK.

A new stopped-flow calorimeter has been used in enzyme kinetic studies (Howarth et al, 1987, Biochem.J. 248, 677). The instrument requires 100ul of reagent per push, has a sensitivity of <0.1m°C, and can resolve reaction rates <30s^{-1}. In addition to ΔH measurements, the technique can monitor spectroscopically silent events and can characterise ionisation steps by repeating the reaction in buffers with different heats of ionisation. An investigation of the myosin-S1 MgATPase has shown that the on-enzyme ATP cleavage step is endothermic (upper trace: 80uM S1 vs. 1mM ATP, 5°C, pH7, k_{obs}=7.1s^{-1} ΔH_{obs}=+32kJmol^{-1}), while the subsequent phosphate release is exothermic (Millar et al, 1987, Biochem.J. 248, 683). The acceleration of the phosphate release step by CaATP and by actin has been observed: ΔH is smaller in the presence of actin, indicating that actoS1 association is endothermic. ATP hydrolysis by the MoFe nitrogenase enzyme of Klebsiella Pneumoniae is similar to myosin (lower trace: 55uM nitrogenase vs. 5mM ATP, 5°C, pH7, k_{obs}=9.4s^{-1}, ΔH_{obs}=+36kJmol^{-1}). This technique should find useful application in a wide variety of chemical and biochemical investigations.

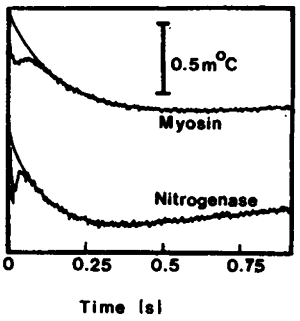

Tu-Pos384 **INFRARED SPECTROELECTROCHEMISTRY OF CYTOCHROME C.** D. Moss*, E. Nabedryk+, J. Breton+ and W. Mäntele*. *Institut für Biophysik und Strahlenbiologie der Universität Freiburg, D-7800 Freiburg, FRG. +Service de Biophysique, CEN Saclay, 91191 Gif/Yvette cedex, France.

We have developped a new technique for the study of redox-linked conformational changes in proteins, by the combination of two established techniques. Fourier transform infrared spectroscopy has been used together with direct electrochemistry of the protein at a bipyridyl-modified gold electrode surface. The resulting reduced-minus-oxidized difference spectra show changes in the frequencies and intensities of molecular vibrations. In contrast to the absolute infrared spectra of proteins, such difference spectra can be sufficiently straightforward to allow interpretation at the level of individual bonds. The technique has been applied to cytochrome c, because the availability of X-ray crystallographic structures of both redox states of the protein provides a reference against which our data can be compared. A number of the bands in the infrared difference spectra (Fig. 1) can be correlated with the reported redox-linked movements of specific amino acid and heme side chains. This band assignment was facilitated by comparisons of the difference spectra of cytochromes c from horse and tuna, and in H2O and D2O. The spectrum was rather insensitive to pH in the range 5.9 to 8.5 (Fig. 1a), but at pH values above 9.0 a number of new bands appear (Fig. 1b).

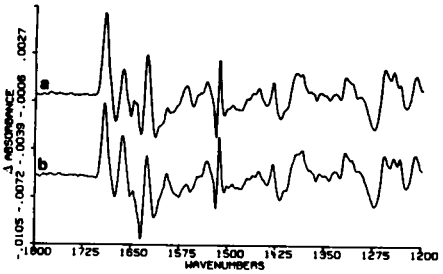

Fig. 1. Reduced-minus-oxidized infrared difference spectrum of cytochrome c, 10 mM horse heart cytochrome c, 2 mM dithiodipyridine, 250 mM KCl, 50 mM PO4; a) pH 6.75, b) pH 9.17.

Tu-Pos385 ASSOCIATION BETEEEN ICE NUCLEI AND FRACTURE INTERFACES IN SUCROSE:WATER GLASSES Robert J. Williams and David L. Carnahan, American Red Cross R&D Laboratories, Rockville, MD 20855

When samples of 65% to 70% Sucrose:water are cooled in the DSC to -130° C, a broad glass transition is seen between -80° and -70°C but no ice forms. This transition is seen during warming as well, followed by a large devitrification and melt. In fact, devitrification can be seen in samples cooled only to -40°C. Cryomicroscope observations reveal a different pattern. Ice nuclei, except for a few associated with microscopically visible particles, do not form in this material during cooling and warming and even these particles do not produce ice unless the temperature has been reduced below about -80°C. Homogeneous nucleation was not observed at temperatures down to -130°C. If during cooling the glass fractures (e.g., by quenching the sample in liquid Nitrogen), nuclei apparently do form on the fracture interfaces. During warming, ice is seen to grow from the cracks into the supersaturated glassy melt surrounding them. Prevention of cracking with plasticizing additives further inhibits massive ice formation. The disparity between these experiments results from differences in the samples. The glass in the cryomicroscope forms between two coverslips. That in the DSC sample pan is in contact with an air interface where ice nuclei could form, much as they had in the fractures. When we covered the DSC sample with 2-methyl butane, the glass was still seen but no ice formed even in samples warmed from -150° C. These results imply that cryopreservation by vitrification could be improved by the elimination of heterogeneous nuclei and the prevention of cracking.

Support by Grants GM 17959 and BSRG 2 507 RR05737 from NIH and the American Red Cross.

Tu-Pos386 STARK SPECTRA OF ANTENNA PREPARATIONS AND CHROMATOPHORS FROM RB. SPHAEROIDES RSP. RUBRUM AND R. VIRIDIS. H.P. Braun, M.E. Michel-Beyerle and J. Breton*, Institut für Physikalische und Theoretische Chemie, Technische Universität München, 8046 Garching, FRG and *Service de Biophysique, Departement de Biologie, CEN Saclay, 91191 Gif-sur-Yvette Cedex, France

The effect of an external electric field on the optical absorption spectra of the antenna preparation B800/850 from Rb. sphaeroides and chromatophors of Rsp. rubrum and R. viridis in films of polyvinylalcohol was recorded at 77 K. The calibration of the Stark spectrum of B800/850 to the Stark spectrum of reaction centers of Rb. sphaeroides, R-26, has been achieved by measuring both antenna and reaction center together and separately.

The essential results for the B800/850 preparation are: (i) a negligible Stark effect on the 800 nm absorption and (ii) a larger value for the change in the dipole moment for the 850 nm peak of about 4 Debye as compared to the value observed for monomer bacteriochlorophyll in reaction centers. Obviously, a significant charge-transfer contribution to the excited singlet state can also occur in dimers of bacteriochlorophyll, which are not functionally related to electron transfer. From the Stark effect on the long-wavelength transition of chromatophors of R. viridis a change in dipole moment of about 7-8 Debye is estimated, the respective value for chromatophors of Rsp. rubrum being slightly smaller.

Tu-Pos387

Reassigned to W-PM-E13

Tu-Pos388 QUALITATIVE ANALYSIS OF THE EFFECTS OF INELASTIC SCATTERING UPON CONTRAST IN ELECTRON MICROSCOPE IMAGES OF FROZEN-HYDRATED BIOLOGICAL MOLECULES. J.P. Langmore, K.V. Nolta, and M.F. Smith, Biophysics Research Division, The University of Michigan, Ann Arbor, MI 48109

Inelastic scattering seriously degrades the electron images of molecules in thick specimens by creating a large background of energy-loss electrons that increases statistical noise. One method to eliminate this background is to use the scanning transmission electron microscope. A second method is to employ an energy filter on a conventional electron microscope. We have used the energy-filtration system on the Zeiss EM902 to quantitate the phase and scattering contrast from TMV embedded in vitreous ice. A 40%-100% increase in both phase and scattering contrast is achieved by energy-filtration of images of molecules embedded in 50-300 nm of ice. Therefore, the electron dose required to achieve specific values of the signal-to-noise ratio is up to 10-fold lower in energy-filtered images. These experimental results are in quantitative agreement with multiple-scattering calculations based upon Hartree-Fock-Slater theoretical elastic scattering amplitudes and empirical inelastic scattering intensities for vitreous ice. These calculations can be extrapolated to thicker specimens and higher voltages to compare the characteristics of emergy-filtered images at 80KeV to unfiltered images at higher voltages.

Tu-Pos389 DRIED FIBERS OF MICROTUBULES. Stephen P. Edmondson, Anne L. Hitt, Robley C. Williams, Jr. and Gerald Stubbs
Dept. of Molecular Biology, Vanderbilt University, Nashville, TN 37235

Microtubules are filamentous cytoskeletal structures composed of the protein tubulin. Microtubules are not static structures but dynamically exchange subunits with free tubulin dimers. This has hindered the development of suitable microtubule specimens for X-ray fiber diffraction. The best specimens reported so far were slices from pellets obtained by centrifugation, in which the mean disorientation was about 10°. Oriented gels of microtubules, similar to those used for fiber diffraction from filamentous viruses, are unstable. Fibers prepared from solutions of microtubules are poorly oriented, and the microtubules tend to dissociate upon drying. However, stable fibers can be produced by controlled drying of tubulin solutions under conditions that promote self-association into microtubules. We present here the results of a systematic investigation into conditions for preparing specimens of microtubules for X-ray fiber diffraction. The effects of tubulin concentration, Mg^{++} concentration, and relative humidity are presented. Different techniques for making microtubule fibers are also discussed.

Supported by grants NSF/BBS-8717949 and NIH/GM25638.

Tu-Pos390 LOCALIZATION OF ABNORMAL CNS FUNCTIONS IN FETUS BRAIN USING MEG MEASUREMENTS WITH SQUID.
P.Diamantopoulos and P.A.Anninos Department of Medicine,University of Thrace, Alexandroupolis, Greece.

Although in the last decade with the use of computing Tomography and ultrasound techniques the diagnosis of the different brain pathologies was easier and the clinical picture of the fetuses was leading us more often in identifying a possible brain malfunction our knowledge for early prenatal diagnosis is still inadequate. For this purpose we examined 49 pregnant women with age between 17-35 years and pregnancy age between 36-41 weeks. In our research we use the Biomagnetometer SQUID by which we measured the magnetic activity emitted from the fetus brain activity.Our measurements consists of taking 32 consecutive records of one second duration each from the 32 equal spaced points chosen on the fetus skull around the T3,T4,P3,P4,F3 and F4 of the International 10-20 point system (depending on the chosen region on the skull). The sampling frequency was 256 Hz. Using Fourier statistical analysis for our data we construct a map which gives us the distribution on the scalp of the ISOspectral amplitudes of the magnetoencephalogram (MEG) power spectrum from each one of the measuring points and for a particular frequency band. With this method we were able to intentify for first time using the above noninvasive technique the normal and abnormal fetus brain function.

Tu-Pos391 THE INFLUENCE OF DIFFERENT TYPES OF MAGNETIC FIELDS ON BIOLOGICAL OBJECTS. A. Ottova, Institute of Biotechnology of SVST, 81237 Bratislava, Kollarovo, nam. 9, Czecholovakia

In the present paper are described the results as well as the explanations of the influence of the static and pulsed magnetic fields on biological objects. In both cases, the product of the induction B (in Tesla) and of exposure time t (in minutes), (B x t) on different biological objects has been investigated and seems to be of great importance. The explanation of results can be done by means of membrane biophysics. The investigated objects have been human red blood cells, hatchings of Japanese quail and chickens, as well as different kinds of seeds (flax, sunflowers, beans, etc.). It has been shown that the influence on the lipids in the membrane is of great importance. The pulsed magnetic fields in the induction range have been used for investigation of the adaptability of the biological objects in comparison with the static magnetic field (induction range - 0.05-0.5 T; time interval- 5-120 min.).

Tu-Pos392 **EFFECT OF HIGH ELECTRIC FIELDS ON THE PHOTO-ISOMERIZAION OF ALL-TRANS RETINAL** J. Taboada, F. Aldape and A.T.C. Tsin, USAF School of Aerospace Medicine, Brooks AFB, TX 78235 and Division of Life Sciences, The University of Texas at San Antonio, TX 78285. The visual chromophore 11-cis retinal when bound to opsin undergoes an absorption shift from the far blue to the red in the visible spectrum. Visual phototransduction is possible because of these shifts. A promising theory explaining this shift is the external point charge model of Honig, et al. in which point charges localized on the opsin bound chromophore account for the absorption band spectral shift. A simple calculation indicates electric fields of about 2 X 10^{10} volts/meter in the vicinity of the chromophore. To test the possible influence of an external field on the absorption properties of 11-cis retinal, an electric-field cell was constructed to expose all-trans retinal to fields on the order of 2 X 10^{7} volts/meter. The sensitive observable in this work to probe field effects is the resulting isomer distribution determined by HPLC. A solution of all-trans retinal in ethanol was placed in a thin (2mm) recess in teflon and light from an argon laser at 488 nm was channeled into the cell through an optical fiber simultaneously with the application of 20 KV across the thickness of the cell. The all-trans retinal samples in ethanol were dried down using nitrogen and resuspended in 6% diethyl ether/n-hexane (also the mobile phase), with a 1:10 dilution factor. The resultant isomers were quantitated by HPLC. Generally, the levels of cis isomers (13, 11, 9 & 7) were lower in samples exposed to high electric fields. Since the applied field was weak compared to the fields in the point charge theory, only a weak electric field effect in the retinal isomerization was anticipated and actually observed. Supported by AFOSR, Task 2312-W5.